

-Angle-Domain Attention and Rate-Distortion Retention for Memory-Bounded LLM Inference

Anay Chauhan^{*1} Gurucharan Marthi Krishna Kumar² Arion Das³ Amit Dhanda^{†4}
 Vinija Jain^{‡5} Aman Chadha^{§6} Amitava Das⁷

¹Synopsys, India ²McGill University, Canada ³IIIT Ranchi, India ⁴Amazon, USA
⁵Google, USA ⁶Google DeepMind, USA ⁷Pragya Lab, BITS Pilani Goa, India

Abstract

Motivation. Long-context decoding is increasingly limited not by FLOPs, but by **KV cache growth, High Bandwidth Memory (HBM) bandwidth, and peak memory**. As sequence length T scales, KV becomes the dominant resident state, shrinking feasible batch/context and forcing repeated **HBM streaming per token** that throttles throughput. Current mitigations—**windowing/sinks, heuristic eviction, and KV quantization/offload**—often move the bottleneck rather than remove it: they discard history uniformly, rely on brittle salience proxies, or compress KV yet pay an implicit **reconstruction tax** (unpack/dequantize/rebuild dense vectors) that breaks fusion and restores bandwidth pressure. The persistent gap is a frontier trade: **memory vs. quality vs. speed**.

Thesis. We frame KV memory as a **rate-distortion allocation** problem grounded in geometry: attention is primarily **directional** (query-key alignment) with magnitude as a scalar modulator. This yields two principles: (i) make **direction cheap** in the critical path, and (ii) allocate **bits and residency** only to states likely to **matter later**. We introduce **Spherical KV**, an inference primitive coupling **Angle-Domain Attention** with **Rate-Distortion KV Retention**.

Angle-Domain Attention (no reconstruction). Spherical KV stores keys in a **spherical parameterization**—a scalar **radius** plus compact **angle codes** for direction—and computes attention logits **directly from these codes** via an **angular recurrence**. This avoids dense-vector materialization in the hot loop, replacing bandwidth-heavy reads with compact streams that stay **paged, block-local, and fusion-friendly** for GPU kernels—directly targeting **HBM traffic**.

Rate-Distortion Retention (keep/drop + precision). Under a strict budget, the right decision is not only *which tokens to keep* but *at what precision*. A lightweight controller jointly chooses **retention** and **bitwidth tier** per token/head (optionally per layer), and emits a deployment-realistic write contract: tier-homogeneous pages, minimal headers, and coalesced reads.

$$\min_{\pi} \mathbb{E}[\mathcal{L}(\text{LLM}_{\text{SphKV}}(\pi))] \quad \text{s.t.} \quad \sum_i z_i \cdot \text{cost}(b_i) \leq B.$$

Results signature. At **matched quality** (single tolerance $\Delta=0.8$), Spherical KV consistently shifts the **memory-quality-throughput frontier**: across 8K/32K/128K, we observe **1.55×–1.72× higher tok/s** ($\approx 55\text{--}72\%$ faster) while simultaneously reducing **resident KV bytes/token by 24–42%** (and the corresponding **PeakKV** at long L). The gains strengthen in the **128K stress regime**, where paging/fragmentation are most punitive, yet the quality gap remains bounded by design. As a byproduct, per-head decisions expose an interpretable taxonomy of **long-horizon**

*Work does not relate to author’s position at Synopsys

†Work does not relate to author’s position at Amazon

‡Work does not relate to author’s position at Google, USA

§Work does not relate to author’s position at Google DeepMind, USA

memory vs. short-range processing and **direction-dominant vs. magnitude-sensitive heads**—linking deployable acceleration with mechanistic insight.

1 KV Cache and the Memory Bottleneck

KV growth is linear; HBM traffic is the killer. Autoregressive decoding caches per-layer **Keys** and **Values** to avoid recomputing attention over the full prefix. This convenience turns into the dominant systems bottleneck at long context: the cache grows **linearly** with context length T and multiplicatively with batch size B , layers L , and heads H . A useful footprint estimate is

$$\text{Mem}_{\text{KV}} \approx \underbrace{B}_{\text{batch}} \cdot \underbrace{L}_{\text{layers}} \cdot \underbrace{T}_{\text{context}} \cdot \underbrace{H}_{\text{heads}} \cdot \underbrace{(d_h^{(K)} + d_h^{(V)})}_{\text{per-head dims}} \cdot \text{bytes}.$$

During decoding, the dominant cost is often not FLOPs but **HBM bytes streamed per generated token**: each new token must attend over a large prefix, forcing repeated reads of KV pages. Past a few thousand tokens, decoding typically transitions from **compute-limited** to **memory-limited** in three distinct ways: **(i) capacity-limited** (KV does not fit), **(ii) bandwidth/latency-limited** (KV cannot be streamed fast enough), and **(iii) orchestration-limited** (paging/tiering/scheduling overhead dominates).

Operational premise. Long-context acceleration is therefore **not** primarily a FLOP reduction problem. It is the problem of improving the **memory-throughput-quality frontier**: reduce **KV bytes**, reduce **bytes moved**, and preserve **behavioral stability**. This is precisely why IO-aware attention kernels emphasize **data movement** and **fusion** rather than arithmetic alone (Dao et al., 2022; Dao, 2023).

1.1 Deployment substrate: paging + kernel reality

Paged KV is the baseline substrate (non-negotiable). In production, KV is rarely a contiguous tensor. Serving stacks use **paged / block-allocated KV** to reduce fragmentation, support dynamic batching, and enable preemption; **PagedAttention** effectively defines the baseline abstraction (Kwon et al., 2023a). As a result, any KV method that is not **block-local**, **allocator-friendly**, and compatible with **ragged/paged access patterns** is unlikely to translate into end-to-end serving wins.

Kernel realism: savings that cannot be fused do not count. Exact-attention kernels (FlashAttention-style dataflow) show that end-to-end performance is governed by **HBM reads/writes** and **kernel fusion**, not just tensor math (Dao et al., 2022; Dao, 2023). Modern serving libraries treat paged/ragged KV and multiple cache formats as first-class objects (e.g., FlashInfer’s serving-oriented attention engine) (Ye et al., 2025). Production stacks expose cache reuse and quantized-cache options (e.g., TensorRT-LLM KV cache reuse/quantization; Transformers quantized cache), with the same caution: speedups depend on **backend kernel paths**, not compression alone (NVIDIA, 2025a; Hugging Face, 2025). Consequently, representations that force **dense materialization**, **irregular gathers**, or heavy non-fusible (de)quantization can **erase their own theoretical gains**.

1.2 Existing Solutions: Three Levers for KV Efficiency

Three levers, and the deciding constraint. KV efficiency methods cluster into: **(I) store fewer tokens** (retention/eviction/admission), **(II) store fewer bits** (quantization/compression), and **(III) store elsewhere** (offload/reuse). In *deployed* serving, realized speedup is often decided by a **fourth constraint: kernel/serving compatibility**. If a method breaks **paged layouts**, requires **irregular gathers**, or introduces **non-fusible transforms**, its wall-clock gain can vanish despite reduced nominal KV bytes. This end-to-end view is explicit in KV-cache-centric analyses that separate **prefill**, **compression**, **retrieval**, and **loading** stages (Li et al., 2025).

What must improve simultaneously: capacity, IO, and behavior. Across all levers, the objective is not merely shrinking Mem_{KV} , but improving the joint frontier of: **(a) peak capacity** (GB of KV), **(b) decode IO** (**HBM traffic per generated token**), and **(c) behavioral stability** (**tokens generated**, termination, reasoning traces). Recent evaluations show that KV interventions can change *generation dynamics*; therefore robust protocols track **trace length** and **stability** alongside task metrics (Liu et al., 2025a,b).

1.2.1 Lever I: store fewer tokens (retention / eviction / admission)

Heuristics: windows, sinks, heavy hitters (training-free, but non-local). A **sliding window** is the simplest bounded-cache strategy, but fails when key evidence lies far in the prefix. StreamingLLM stabilizes windowed decoding by preserving a small set of **attention sink tokens** that anchor attention (Xiao et al., 2024). H₂O retains recent tokens plus **heavy hitters** (tokens with consistently high attention mass) under a fixed budget (Zhang et al., 2023). Scissorhands argues for **persistence-of-importance** and retains tokens whose salience remains stable over time (Liu et al., 2023c). These methods are attractive because they are often **training-free** and easy to integrate, but they expose the core difficulty: **future utility is non-local, task-dependent, and head-dependent**.

Prefill-time compression: one-shot selection with stable runtime. A pragmatic deployment pattern is to **compress after prefill** and keep the reduced cache fixed during decoding, avoiding per-step bookkeeping and runtime divergence. SnapKV selects prompt positions via an observation window and voting (Li et al., 2024). SAGE-KV performs one-time top-*k* selection at **token** and **head** levels after prefilling, yielding a reduced cache for subsequent decoding (Wang et al., 2025a). The appeal is operational: **predictable layouts, amortized decisions, bounded overhead**.

Depth-/head-aware budgets: one global rule is suboptimal. Cache utility is heterogeneous across layers and heads. PyramidKV varies budgets across layers to match depth sensitivity (Cai et al., 2024). CAKE frames eviction as layer-preference-aware allocation under strict constraints, achieving strong performance at tight budgets (Qin et al., 2025). The consistent message is structural: **KV allocation must be per-layer/per-head**, not a single global budget.

From eviction to admission: KV as a write-control problem. A recent shift treats KV caching as **write-control**: not only *what to evict*, but *what to write* at creation time. TRIM-KV learns intrinsic token importance via a lightweight gate and produces a retention score that decays with time (Bui et al., 2025). Write-Gated KV formalizes admission/selection/eviction and learns a **write filter** explicitly constrained by serving compatibility (Huang et al., 2025). Expected Attention provides a training-free estimator of future attention to rank/prune cached states (Devoto et al., 2025). KVPress standardizes evaluation under common stacks and budgets (NVIDIA, 2025b). Collectively, token-side KV is converging toward **explicit controllers over write/retain decisions** rather than ad-hoc heuristics.

1.2.2 Lever II: store fewer bits (quantization / compression)

Low-bit KV is effective only when paired with protection mechanisms. KIVI proposes asymmetric low-bit KV quantization (per-channel keys, per-token values) (Liu et al., 2024). KVQuant targets ultra-long contexts with sub-4-bit KV and layer-dependent formats (Hooper et al., 2024). ZipCache combines saliency identification with quantization (He et al., 2024), while GEAR uses low-rank/sparse residual correction to recover accuracy (Kang et al., 2024). At the extreme frontier, Kitty demonstrates accurate **2-bit KV** via **dynamic precision allocation** and page-centric layouts, emphasizing **kernel realism** and **paged coalescing** (Xia et al., 2025).

Outliers dominate error at extreme compression (non-optional to handle). A recurring empirical fact is that a small fraction of tokens/channels dominates quantization error. OTT protects **outlier tokens** by excluding them from quantization (Su et al., 2025a). RotateKV adds **outlier-aware rotation** and sink-aware protection to stabilize ultra-low-bit KV further (Su et al., 2025b). The general lesson is crisp: any method pushing below 4-bit must include **explicit protection of fragile mass** (outlier tokens, sink-like tokens, sensitive channels) or it will fail on long-context reasoning.

Kernel co-design: compression that is not compute-native often fails to speed up. Even when KV bytes shrink, naive dequantization can erase throughput gains. BitDecoding argues low-bit KV underperforms without Tensor-Core-centric execution paths and proposes kernels to realize decode speedups (Du et al., 2025). The emerging systems thesis is unambiguous: **the compressed representation must be the compute representation** to deliver wall-clock improvements.

Geometry-aware encodings: polar/spherical as direction-first coding. A parallel thread exploits that attention is driven by *relative similarity*; when keys are stabilized/normalized, **direction can dominate magnitude**. Polar/spherical parameterizations separate **angles** (direction) from **radius**

(magnitude), enabling precision to concentrate on angular fidelity where it most affects attention. Polar-coordinate methods explore angle/radius coding under different assumptions (Han et al., 2025; Wu et al., 2025). Spherical similarity primitives show dot products (cosine similarity) can be computed from angles via recurrences *without reconstructing Cartesian vectors* (Xiao, 2026), motivating **compressed-domain similarity compute**.

1.2.3 Lever III: store elsewhere (offload / reuse) and the orchestration tax

Offload reduces GPU footprint, but can become orchestration-limited. Tiering KV across GPU/CPU can unlock longer contexts and higher concurrency, but the benefit is bounded by transfer bandwidth and scheduling overhead. vLLM’s KV offloading connector targets CPU DRAM offload and optimizes host-device transfer throughput (Ozeri and Harnik, 2026). FlexiCache exploits **head-level temporal stability**: it keeps all pages for unstable heads on GPU, while offloading most pages for stable heads with periodic reranking/fetching (Takbir et al., 2025). The lesson is practical: tiering must be **policy-driven** and often **head-aware** to avoid thrashing.

Reuse across requests: KV as a first-class shared asset. Beyond per-request optimization, KV reuse across repeated prefixes (system prompts, scaffolds, shared retrieved context) yields multiplicative savings. LMCache operationalizes this as an external KV cache layer spanning GPU/CPU/storage/network (Cheng et al., 2025). This direction is complementary to compression: **reuse removes recomputation**, while token/bit methods reduce footprint and per-token traffic.

Serving stacks and kernel libraries are now part of the method. Modern stacks expose paged/ragged KV and multiple cache formats as first-class objects; performance is determined by whether the method maps onto efficient decode kernels. FlashInfer exemplifies this trajectory by providing serving-oriented attention kernels and APIs integrating into major serving frameworks (Ye et al., 2025). The most credible KV methods therefore **bundle** an algorithmic policy (retain/quantize/tier) with a **layout** (paged coalescing) and a **kernel path** (fused decode), and validate end-to-end under realistic paging, batching, and generation constraints.

1.3 Premise of Spherical KV

Core idea: geometry-first KV with angle-domain compute. Spherical KV starts from the task-relevant fact that attention depends on *relative similarity* between queries and keys. When keys are stabilized/normalized, **direction (angles)** can dominate **magnitude (radius)** in determining attention weights. A spherical/polar parameterization factors KV into **angular coordinates** plus a **radial term**, enabling a representation that spends bits where attention is most sensitive. Crucially, Spherical KV targets **angle-native similarity evaluation** (with a small radial correction), motivated by recurrence-style spherical similarity primitives (Xiao, 2026) and polar encodings that separate direction and magnitude (Han et al., 2025; Wu et al., 2025).

Not “just another quantizer”: two hard commitments. Spherical KV is premised on:

1. **Compressed-domain kernels.** Replace “decompress then dot-product” with **angle-domain compute** fused into IO-aware decoding kernels, reducing **HBM traffic per token** under FlashAttention-style dataflow constraints (Dao et al., 2022; Dao, 2023; Ye et al., 2025).
2. **Unified budgeting via rate-distortion control.** Unify **keep/drop** decisions (Bui et al., 2025; Huang et al., 2025) with **precision allocation** (Xia et al., 2025; Su et al., 2025a) by allocating a fixed budget per token/head/layer over (i) *retention* and (ii) *angular/radial bits*, optimizing an explicit distortion surrogate tied to downstream loss.

Evaluation requirements and deployment criteria. Spherical KV must satisfy two empirical requirements for its claims to be meaningful in practice.

(i) Kernel-realized efficiency. A spherical/polar representation that still follows a “decompress-then-dot-product” pipeline is functionally a quantizer and may lose wall-clock performance once dequantization, irregular gathers, and paging overheads are included (Hooper et al., 2024; Du et al., 2025). The method should therefore demonstrate an **angle-domain decode path** that is **fused, paged-KV compatible**, and reduces **HBM traffic per generated token**, translating these savings into measurable **end-to-end latency/throughput gains** under dynamic batching and realistic serving conditions.

(ii) **Long-horizon behavioral stability.** KV compression can perturb attention dynamics in ways that alter **trace length, termination,** and long-context **reasoning trajectories.** Evaluation should thus report not only task metrics but also **tokens generated,** stability across seeds, and failure modes on long-context reasoning suites (Liu et al., 2025a,b).

Finally, deployment relevance requires integration with **paged KV** memory managers and widely used inference stacks, rather than assuming bespoke contiguous layouts (Kwon et al., 2023a; NVIDIA, 2025a; Hugging Face, 2025; Ozeri and Harnik, 2026).

2 Spherical KV: Angle-Domain Attention and Rate-Distortion Retention

Section goal. Spherical KV is built from **two orthogonal ideas** plus a **servicing contract.** **Angle-Domain Attention (ADA)** is a *kernel primitive*: compute attention logits from *compact spherical key codes* without reconstructing dense keys in HBM. **Rate-Distortion Retention (RDR)** is a *controller*: allocate *residency* (keep/drop) and *precision* (tier/bitwidth) under a strict KV budget. Together they produce **paged, tier-homogeneous KV pages** compatible with ragged batching and streaming decode kernels, in the spirit of modern fused attention and paged serving stacks (Dao et al., 2022; Dao, 2023; Kwon et al., 2023b).

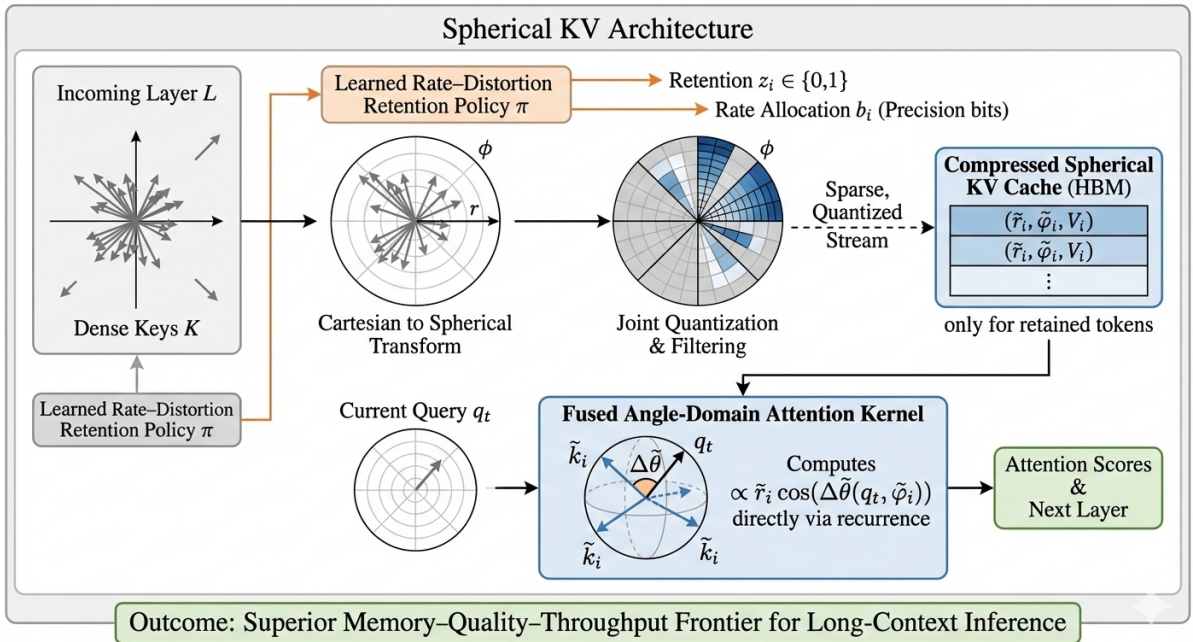


Figure 1: **Spherical KV Architecture.** Dense keys from the incoming layer are mapped to a spherical parameterization (radius r and angles ϕ). A learned rate-distortion retention policy π enforces a strict memory budget B by predicting (i) a keep/drop decision $z_i \in \{0, 1\}$ and (ii) a per-item precision (rate allocation) b_i . Joint quantization and filtering produce a sparse, quantized spherical stream that is stored in a compressed KV cache (HBM) for retained tokens only. During decoding, a fused angle-domain attention kernel consumes the quantized $(\tilde{r}_i, \tilde{\phi}_i)$ directly—avoiding dense Cartesian reconstruction in the critical path—to produce attention scores for the next layer. Overall, the pipeline targets a better memory-quality-throughput frontier for long-context inference.

2.1 Angle-Domain Attention

Directional factorization of attention logits. For a head with dimension d , standard attention uses

$$\ell(\mathbf{q}, \mathbf{k}) = \frac{\mathbf{q}^\top \mathbf{k}}{\sqrt{d}}.$$

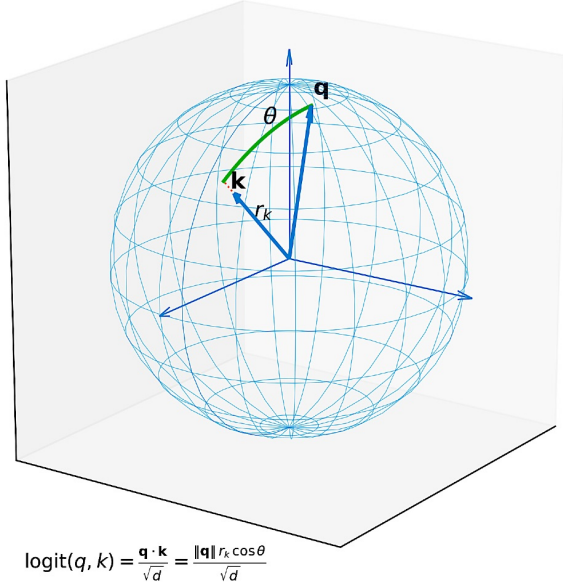
Write $\mathbf{q} = \|\mathbf{q}\| \hat{\mathbf{q}}$ and $\mathbf{k} = \|\mathbf{k}\| \hat{\mathbf{k}}$, where $\hat{\mathbf{q}}, \hat{\mathbf{k}} \in \mathbb{S}^{d-1}$. Then

$$\mathbf{q}^\top \mathbf{k} = \|\mathbf{q}\| \|\mathbf{k}\| \hat{\mathbf{q}}^\top \hat{\mathbf{k}} = \|\mathbf{q}\| \|\mathbf{k}\| \cos \theta, \quad \cos \theta \doteq \hat{\mathbf{q}}^\top \hat{\mathbf{k}}.$$

Hence the logit decomposes as

$$\ell(\mathbf{q}, \mathbf{k}) = \frac{\|\mathbf{q}\| \|\mathbf{k}\|}{\sqrt{d}} \cos \theta.$$

Angle-Domain Attention on a Sphere



Angle-Domain Attention in Practice (Paged-Realized; No Reconstruction)

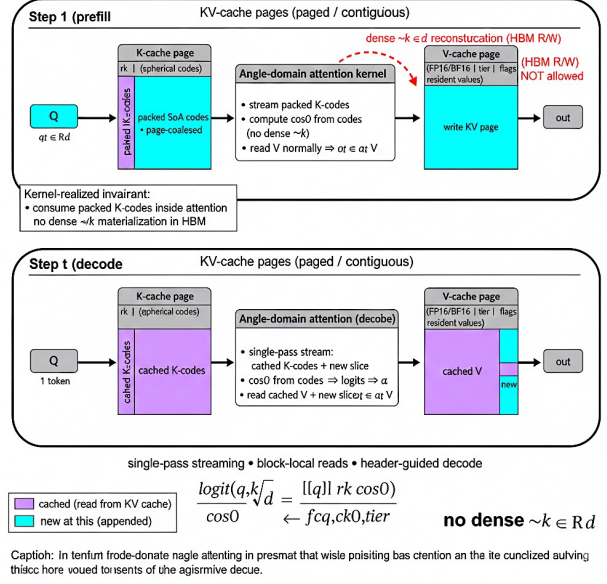


Figure 2: **Angle-Domain Attention in Practice (Paged KV; kernel-realized, no reconstruction)**. This diagram shows how **Angle-Domain Attention** fits into a standard paged KV-cache decode loop without paying a hidden densification tax. **Top (prefill)**: for each token, we write a **paged/contiguous K-cache page** that stores **compact spherical K-codes**—a scalar r_k (radius) and c_k^θ (packed angle codes), plus lightweight **tier/flags** metadata that makes the layout **header-guided** and kernel-friendly. In parallel, we write a standard **V-cache page** in FP16/BF16 (resident values), preserving deployable serving assumptions (paged KV, pointer tables, ragged batching). **Bottom (decode)**: at each step t , we **reuse cached pages** (shown as the large cached region) and **append a thin new slice** for the newly generated token, keeping the write path incremental and page-aligned. The **critical-path difference** is inside the attention kernel: instead of reconstructing a dense $\tilde{\mathbf{k}} \in \mathbb{R}^d$ (which would reintroduce HBM read/write traffic and extra passes), the kernel **consumes the packed K-codes directly** and computes the similarity via $\cos \theta$ from codes (hence $\mathbf{q} \cdot \mathbf{k} \propto \|\mathbf{q}\| r_k \cos \theta$). The resulting logits produce $\alpha_t = \text{softmax}(\cdot)$, and we then **read V normally** to form $o_t = \alpha_t V$; i.e., **K is compressed-domain consumed, V remains standard-domain read**. **Kernel-realized invariant (what makes the throughput gain “real”)**: the method forbids any dense-key reconstruction stage in the decode hot loop, ensuring a **single-pass, block-local stream** over packed K-codes and page-coalesced reads, so reductions in KV bytes translate into reduced bandwidth pressure and higher tok/s under paged serving.

This identity is exact and holds regardless of whether the model applies RMSNorm/LayerNorm upstream; in practice norms $\|\mathbf{q}\|$ and $\|\mathbf{k}\|$ remain well-behaved due to normalization and training dynamics, while $\cos \theta$ captures the *directional match* that dominates the ranking of keys.

Spherical key coding (what is cached). We represent each key by a **spherical tuple**

$$\mathbf{k} \mapsto (r_k, c_k^\theta; b, \text{flags}),$$

where $r_k \approx \|\mathbf{k}\|$ is a scalar radius, c_k^θ is a *packed angle/direction code* at tier $b \in \mathcal{B}$, and flags include protection/outlier/segment metadata used by the controller and kernel. The intent is **not to store** $\hat{\mathbf{k}} \in \mathbb{R}^d$ explicitly, but to store a compact representation from which the kernel can recover $\cos \theta$ directly.

Query-side coding (computed on the fly). At decode step t , the query is ephemeral and computed for the current token. We form

$$r_q \doteq \|\mathbf{q}\|, \quad \hat{\mathbf{q}} = \mathbf{q}/\|\mathbf{q}\|, \quad c_q^\theta \leftarrow \text{Encode}(\hat{\mathbf{q}}, b),$$

so the kernel receives r_q (or $\|\mathbf{q}\|$) and c_q^θ for the active tier b . The encoding is chosen to be **fast, branch-light**, and **GPU-friendly**.

Angle-domain similarity from codes. Define a compressed-domain similarity operator

$$\widehat{\cos \theta} \doteq f(c_q^\theta, c_k^\theta; b),$$

where f is the *angular recurrence* (or code-domain dot-product surrogate) implemented inside the attention kernel. Importantly, f operates on **packed code streams** (SoA layout) and is designed to run with **block-local, coalesced reads** consistent with fused attention kernels (Dao et al., 2022; Dao, 2023) and paged KV serving (Kwon et al., 2023b).

No-reconstruction invariant (kernel-realized). The central systems constraint is an explicit invariant:

No-reconstruction invariant. The decode kernel computes logits using $\widehat{\cos \theta} = f(c_q^\theta, c_k^\theta; b)$ and radius r_k , *without materializing* any dense $\tilde{\mathbf{k}} \in \mathbb{R}^d$ in HBM.

Accordingly, Spherical KV uses the **angle-domain logit**

$$\hat{\ell}(\mathbf{q}, \mathbf{k}) \doteq \frac{r_q r_k}{\sqrt{d}} \widehat{\cos \theta}, \quad r_q = \|\mathbf{q}\|.$$

Softmax and value mixing remain standard:

$$\alpha_i = \frac{\exp(\hat{\ell}_i)}{\sum_j \exp(\hat{\ell}_j)}, \quad \mathbf{o} = \sum_i \alpha_i \mathbf{v}_i,$$

where values \mathbf{v}_i are kept in FP16/BF16 (or another serving-native format) and read normally. Thus, ADA targets **HBM traffic** specifically in the $\mathbf{q}^\top \mathbf{k}$ path, where long-context decoding is bandwidth-bound.

Logit error propagation (distortion enters as angular error). Let the true cosine be $\cos \theta$ and the code-derived estimate be $\widehat{\cos \theta} = \cos \theta + \varepsilon_\theta$. Assume radii are either stored exactly or with small error $r_k = \|\mathbf{k}\| + \varepsilon_r$. Then the logit error is

$$\Delta \ell \doteq \hat{\ell} - \ell = \frac{r_q}{\sqrt{d}} \left[(\|\mathbf{k}\| + \varepsilon_r)(\cos \theta + \varepsilon_\theta) - \|\mathbf{k}\| \cos \theta \right],$$

so

$$|\Delta \ell| \leq \frac{r_q}{\sqrt{d}} \left(|\varepsilon_r| |\cos \theta| + \|\mathbf{k}\| |\varepsilon_\theta| + |\varepsilon_r| |\varepsilon_\theta| \right).$$

In typical regimes where $|\varepsilon_r| |\varepsilon_\theta|$ is negligible, the dominant term is

$$|\Delta \ell| \approx \frac{r_q \|\mathbf{k}\|}{\sqrt{d}} |\varepsilon_\theta|.$$

This clarifies the design target: **control angular error** $|\varepsilon_\theta|$ by choosing tier b and by protecting brittle states (Sec. 2.2).

From logit drift to attention drift. Softmax is Lipschitz in the logits in standard norms; a simple bound is obtained by noting that for any two logit vectors $\ell, \hat{\ell}$,

$$\|\text{softmax}(\ell) - \text{softmax}(\hat{\ell})\|_1 \leq 2 \|\ell - \hat{\ell}\|_\infty.$$

Thus, controlling $\|\Delta \ell\|_\infty$ (via tier selection and protection) directly controls attention-weight drift and downstream output drift. This is precisely why we treat **stability** as a first-class constraint rather than an afterthought: ADA supplies an explicit knob (b) that trades rate for distortion, and RDR chooses that knob under budget.

Why ADA is not “KV quantization as usual”. Many KV compression approaches reduce stored bytes but still *reconstruct dense vectors* (unpack/dequantize) for dot-products, paying a reconstruction tax that reintroduces bandwidth pressure and inhibits kernel fusion. ADA is explicitly designed around the **kernel consumption path**: *compressed-domain similarity* first, dense values later. This aligns with the philosophy of fused attention kernels (Dao et al., 2022; Dao, 2023) and serving stacks that emphasize paged locality (Kwon et al., 2023b).

2.2 Rate-Distortion Retention

KV control is joint keep/drop + precision. Under a strict memory budget, selecting a subset of tokens is insufficient: one must also choose the *precision tier* of the retained states. We index cache states by i (token \times head; optionally layer), and choose:

$$z_i \in \{0, 1\} \text{ (drop/keep), } \quad b_i \in \mathcal{B} \text{ (tier).}$$

Let $\text{cost}(b)$ be bytes-per-state under tier b (including headers/amortized metadata), and let $\mathcal{D}_i(b)$ denote the expected distortion incurred by coding state i at tier b . The controller solves

$$\min_{\{z_i, b_i\}} \mathbb{E}[\mathcal{L}(\text{Decode}_{\text{SphKV}}(\{z_i, b_i\}))] \quad \text{s.t.} \quad \sum_i z_i \text{cost}(b_i) \leq B,$$

which is a rate-distortion allocation problem in the classical sense (Shannon, 1948).

Rate-Distortion Retention: Joint Keep/Drop + Tiering Under a Strict KV Budget

Controller allocates residency and precision to high-impact states; emits tier-homogeneous KV pages consumed by streaming kernels.

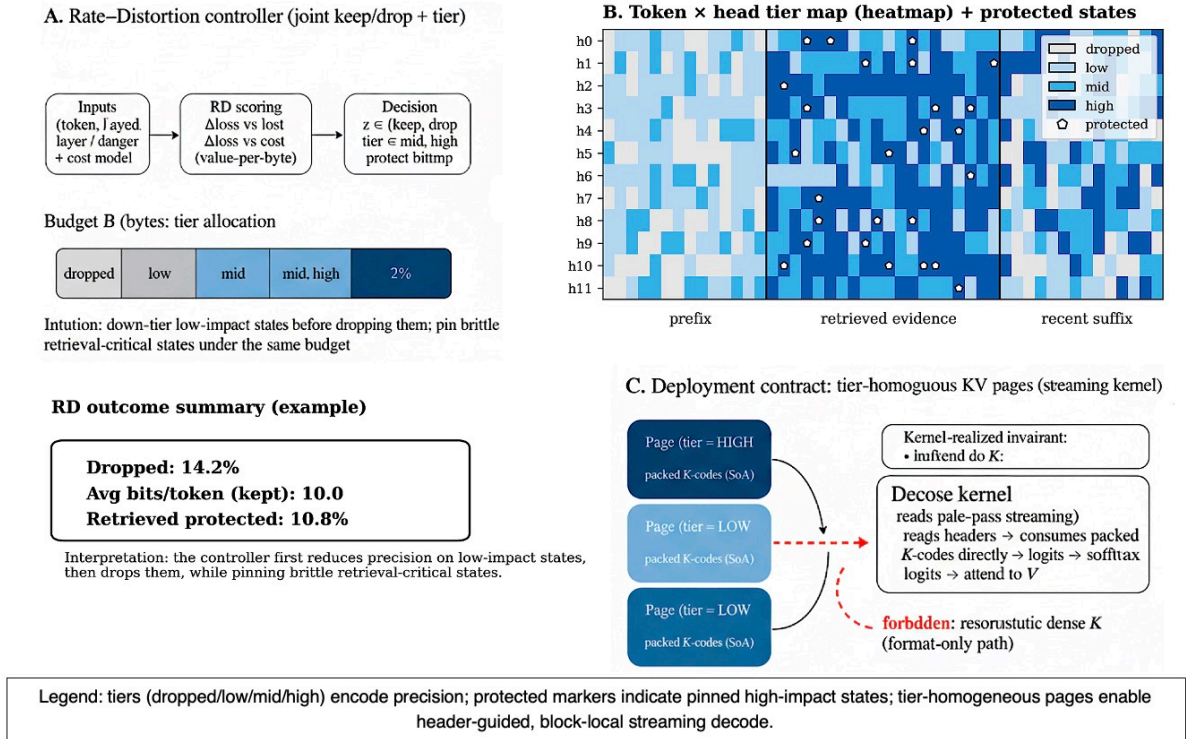


Figure 3: **Rate-Distortion Retention: joint keep/drop + tiering under a strict KV budget.** We treat KV residency as a constrained *rate-distortion* allocation problem: under a fixed byte budget, the controller spends precision on states that are likely to matter later and removes low-utility states first. **(A) RD controller.** Inputs include token/head/layer context plus a cost model; an RD score (e.g., predicted Δloss vs. byte-cost / value-per-byte, augmented with protect/outlier flags) yields a discrete decision: *drop* or *keep* with a *tier* (low/mid/high) and an optional *protect bitmap*. The budget bar visualizes how total bytes are partitioned across tiers, emphasizing the policy: *down-tier before dropping* and *pin brittle, retrieval-critical states* when budgets tighten. **(B) Token \times head tier map (mechanism evidence).** Rows are attention heads, columns are tokens; cell color encodes the chosen tier (dropped/low/mid/high), with vertical separators marking prompt segments (prefix / retrieved evidence / recent suffix) and markers denoting *protected* states. The intended signature is segment-aware allocation (retrieved evidence biased toward higher tiers), head heterogeneity (a subset of long-horizon “keeper” heads), and budget-consistent structure (precision reduced on low-impact states before dropping). **(C) Deployment contract: tier-homogeneous KV pages.** The controller emits pages grouped by tier so the decode kernel can do single-pass, header-guided streaming reads: it consumes packed K -codes directly (compressed-domain attention) and reads V normally to form outputs. The red dashed path highlights the forbidden *format-only* alternative—reconstructing dense K —which would reintroduce HBM traffic and erase the kernel-realized benefit.

Lagrangian relaxation and per-state marginal values. Introduce a multiplier $\lambda \geq 0$ and consider the relaxed objective

$$\min_{\{z_i, b_i\}} \mathbb{E}[\mathcal{L}(\cdot)] + \lambda \left(\sum_i z_i \text{cost}(b_i) - B \right).$$

A useful way to operationalize this is via *marginal improvements*. Define a baseline action (e.g., “drop” or “lowest tier”) and compute, for each state i , the incremental benefit of choosing tier b instead:

$$\Delta_i(b) \doteq \mathbb{E}[\mathcal{L}_i(\text{baseline})] - \mathbb{E}[\mathcal{L}_i(b)] \quad (\text{benefit}).$$

Then a canonical selection rule is to favor actions with high *benefit per byte*:

$$\text{vpB}_i(b) \doteq \frac{\Delta_i(b)}{\text{cost}(b) - \text{cost}(\text{baseline})}.$$

In discrete-tier settings, this becomes a multiple-choice knapsack (choose at most one tier for each i), which is NP-hard in general; however, greedy-by-vpB with a tuned λ is a strong practical baseline and yields near-Pareto behavior in serving contexts (Martello and Toth, 1990).

Connecting distortion to ADA’s logit error. For Spherical KV, the distortion of a key state i primarily enters through angular error $\varepsilon_{\theta,i}(b)$ and (optionally) radius error $\varepsilon_{r,i}(b)$. From the ADA derivation,

$$|\Delta \ell_i(b)| \lesssim \frac{r_q \|\mathbf{k}_i\|}{\sqrt{d}} |\varepsilon_{\theta,i}(b)| + \frac{r_q}{\sqrt{d}} |\varepsilon_{r,i}(b)|.$$

Thus, tiers can be interpreted as choosing a target bound on $|\varepsilon_{\theta,i}|$, which directly controls logit drift and attention drift. This yields an RD control policy that is **mechanistically grounded**: it spends bits where logit errors would be amplified (large $r_q \|\mathbf{k}_i\|$, high-sensitivity states) and saves bits where the model is robust.

Protection constraints (hard constraints, not heuristics). Some states are *brittle* and must be pinned regardless of their immediate vpB score: retrieved evidence spans, safety-critical segments, outliers, or low-margin decisions. We introduce a protection indicator $\mathbb{I}_{\text{prot}}(i) \in \{0, 1\}$ and enforce

$$\mathbb{I}_{\text{prot}}(i) = 1 \Rightarrow z_i = 1, \quad b_i = b_{\text{max}}.$$

This is the controller-side mirror of ADA’s stability goal: if a state is identified as high-risk, the system does not gamble with compression.

A concrete controller template (deployment-realistic). A minimal controller that is faithful to paged serving proceeds in three stages:

1. **Score.** Compute $\Delta_i(b)$ (or a proxy) for each state and tier, along with $\text{cost}(b)$. Enforce protection constraints immediately.
2. **Allocate tiers before dropping.** Start from a safe tier for all kept states; then down-tier states with lowest vpB until the budget is met; only then drop the least valuable states.
3. **Write tier-homogeneous pages.** Group states by tier into contiguous pages with fixed headers, enabling specialized kernels and coalesced reads.

This “down-tier then drop” structure is important: it avoids brittle discontinuities induced by hard truncation and typically yields smoother quality degradation under tighter budgets.

2.3 Working Together: One Contract, Two Mechanisms

Orthogonality and composition. ADA and RDR act on different axes: **ADA** specifies *how* logits are computed cheaply (from codes), while **RDR** specifies *which* states exist and *at what tier*. This separation is what makes the system composable: improvements to ADA kernels do not change the controller objective, and improvements to the controller do not alter the kernel invariant.

Serving-native KV layout (paged, tier-homogeneous). We formalize the deployment contract as:

- **Paged KV with pointer tables.** KV is stored in pages compatible with ragged batching and reuse across decode steps (Kwon et al., 2023b).
- **Tier-homogeneous pages.** Each page contains a single tier b , enabling predictable bandwidth and tier-specialized kernels.
- **Header-guided streaming.** A small fixed header stores $(b, \text{len}, \text{flags})$, and the kernel streams payloads in one pass.
- **SoA-packed K payload.** Keys are stored as (r_k, c_k^θ) in SoA form to maximize coalescing; the kernel computes $\widehat{\cos \theta}$ directly.
- **Standard V payload.** Values remain FP16/BF16 and are read normally to form $\mathbf{o} = \alpha V$.

This contract guarantees that compression translates into real throughput: the hot-path reads are compact and fused (ADA), and the memory budget is enforced by construction (RDR).

End-to-end signature (what should improve). In KV-dominated regimes (8K–128K, retrieval-heavy prompts, agent/tool rollouts), the combined mechanism targets a **frontier shift**: *lower effective KV bytes/token* (RDR) and *higher tok/s* (ADA) at *bounded iso-quality loss*. Crucially, the stability story is explicit: ADA provides a distortion knob (tier b), RDR allocates that knob using value-per-byte plus hard protection, and the serving contract ensures the kernel can realize the promised bandwidth savings (Dao et al., 2022; Dao, 2023; Kwon et al., 2023b; Shannon, 1948).

Algorithm 1: Spherical KV (End-to-End: Prefill + Decode, Kernel-Realized)

- Require:** Model: L layers, H heads, head dim d_h , page size P items/page
- Require:** Prefill tokens $x_{1:T_p}$, decode steps T_d , batch size B , ragged paging substrate
- Require:** Tiers $\mathcal{T} = \{t_0, \dots, t_K\}$ with $t_0 = \text{drop}$ and bitwidths (b_t^θ, b_t^r)
- Require:** Global budget \mathcal{B} in bits (or bytes) for all retained KV at a given layer group
- Require:** Protect set \mathcal{P} (token/head/layer ids) and tradeoff $\lambda > 0$
- Require:** Quantizers: angle $Q_t^\theta(\cdot)$, radius $Q_t^r(\cdot)$, deterministic decode $D_t^\theta(\cdot)$, $D_t^r(\cdot)$
- Require:** Angle map $\Phi(\hat{k}) \in \mathbb{R}^{d_h-1}$ and *angular-logit routine* $\text{CosFromAngles}(\hat{q}, c^\theta, t)$
- Require:** Meta-bits per item b_t^{meta} (e.g., flags, offsets); $R(t) = (d_h - 1)b_t^\theta + b_t^r + b_t^{\text{meta}}$
- Ensure:** Tier-homogeneous paged SoA KV store + decode kernel that consumes codes **without dense reconstruction**
- 1: **Data layout (SoA, tier-homogeneous pages).**
 - 2: For each layer/head (ℓ, h) , maintain pages $g \in \mathcal{G}_{\ell, h}$ where every page has a single tier t_g
 - 3: Page header stores: $(t_g, n_g \leq P, \text{scale}_g^r, \text{scale}_g^\theta, \text{flags bitmap}, \text{offsets})$
 - 4: Page payload stores SoA streams: C_g^θ (packed angle codes), C_g^r (packed radius codes), optional C_g^v for values
 - 5: Pointer table Π maps $(\ell, h, \text{page_id}) \rightarrow$ base addresses of $(C_g^\theta, C_g^r, \text{header}_g)$
 - 6: **Phase I: Prefill (Write/Allocate).**
 - 7: Run the model on $x_{1:T_p}$ to obtain keys/values $\{k_i^{(\ell, h)}, v_i^{(\ell, h)}\}$ for all i, ℓ, h
 - 8: **1) Spherical parameterization (per item).**
 - 9: **for** $\ell \leftarrow 1$ to L **do**
 - 10: **for** $h \leftarrow 1$ to H **do**
 - 11: **for** $i \leftarrow 1$ to T_p **do**
 - 12: $r_i^{(\ell, h)} \leftarrow \|k_i^{(\ell, h)}\|_2$
 - 13: $\hat{k}_i^{(\ell, h)} \leftarrow k_i^{(\ell, h)} / (r_i^{(\ell, h)} + \epsilon)$
 - 14: $\phi_i^{(\ell, h)} \leftarrow \Phi(\hat{k}_i^{(\ell, h)})$ $\triangleright d_h - 1$ angles
 - 15: **end for**
 - 16: **end for**
 - 17: **end for**
 - 18: **2) Controller features (replicable scalars).**

```

19: Define token age  $a_i \leftarrow T_p - i$  and segment  $\text{seg}(i) \in \{\text{prefix}, \text{retrieved}, \text{recent}\}$ 
20: Define segment weights  $\omega_{\text{prefix}}, \omega_{\text{retrieved}}, \omega_{\text{recent}}$  (fixed constants)
21: for  $\ell \leftarrow 1$  to  $L$  do
22:   for  $h \leftarrow 1$  to  $H$  do
23:     Compute head scalars (examples, fixed recipes):
24:      $\hat{u}_{\ell,h} \leftarrow$  reuse proxy (e.g., prefill mean attention mass into head  $(\ell, h)$ )
25:      $\hat{s}_{\ell,h} \leftarrow$  stability proxy (e.g., margin-danger estimate; see Sec. 4.3)
26:   end for
27: end for
28: 3) Distortion proxy and per-tier score.
29: Define weights (deterministic):
30:  $w_{i,\ell,h}^\theta \leftarrow \alpha_\theta \hat{u}_{\ell,h} \omega_{\text{seg}(i)}$ ,  $w_{i,\ell,h}^r \leftarrow \alpha_r (1 - \hat{s}_{\ell,h}) \omega_{\text{seg}(i)}$ 
31: for  $\ell \leftarrow 1$  to  $L$  do
32:   for  $h \leftarrow 1$  to  $H$  do
33:     for  $i \leftarrow 1$  to  $T_p$  do
34:       for all  $t \in \mathcal{T}$  do
35:          $\varepsilon_{i,\ell,h}^\theta(t) \leftarrow$  angle quant error model at tier  $t$  (lookup or closed-form)
36:          $\varepsilon_{i,\ell,h}^r(t) \leftarrow$  radius quant error model at tier  $t$ 
37:          $D_{i,\ell,h}(t) \leftarrow w_{i,\ell,h}^\theta \varepsilon_{i,\ell,h}^\theta(t) + w_{i,\ell,h}^r \varepsilon_{i,\ell,h}^r(t)$ 
38:          $S_{i,\ell,h}(t) \leftarrow -D_{i,\ell,h}(t) - \lambda R(t)$ 
39:       end for
40:       if  $(i, \ell, h) \in \mathcal{P}$  then
41:         Enforce  $t \neq t_0$  by restricting arg max to  $\mathcal{T} \setminus \{t_0\}$ 
42:       end if
43:        $t_{i,\ell,h}^* \leftarrow \arg \max_{t \in \mathcal{T}} S_{i,\ell,h}(t)$ 
44:        $\nu_{i,\ell,h} \leftarrow \frac{D_{i,\ell,h}(t_0) - D_{i,\ell,h}(t_{i,\ell,h}^*)}{R(t_{i,\ell,h}^*) + \epsilon}$  ▷ value/bit
45:     end for
46:   end for
47: end for
48: 4) Budgeted allocation with tier-homogeneous paging.
49: Initialize  $z_{i,\ell,h} \leftarrow 0$ ,  $t_{i,\ell,h} \leftarrow t_0$ , remaining budget  $\mathcal{B}_{\text{rem}} \leftarrow \mathcal{B}$ 
50: Sort all items  $(i, \ell, h)$  by decreasing  $\nu_{i,\ell,h}$  (stable tie-break: lexicographic  $(\ell, h, i)$ )
51: for all items  $(i, \ell, h)$  in sorted order do
52:    $t \leftarrow t_{i,\ell,h}^*$ 
53:   if  $R(t) \leq \mathcal{B}_{\text{rem}}$  and feasible to assign into a tier-homogeneous page then
54:      $z_{i,\ell,h} \leftarrow 1$ ;  $t_{i,\ell,h} \leftarrow t$ ;  $\mathcal{B}_{\text{rem}} \leftarrow \mathcal{B}_{\text{rem}} - R(t)$ 
55:   end if
56: end for
57: Pack retained items into pages: group by  $(\ell, h, t)$ , chunk into size  $\leq P$  to form pages  $g$  with tier  $t_g = t$ 
58: Compute per-page scales (replicable choice):
59:  $\text{scale}_g^r \leftarrow \max_{(i,\ell,h) \in g} r_i^{(\ell,h)}$ ,  $\text{scale}_g^\theta \leftarrow 1$  (or per-head calibration constants)
60: 5) Quantize & write pages (SoA, pointer table).
61: for all pages  $g$  do
62:   Write header  $(t_g, n_g, \text{scale}_g^r, \text{flags})$ 
63:   for all  $(i, \ell, h) \in g$  do
64:      $c_{i,\ell,h}^\theta \leftarrow Q_{t_g}^\theta(\phi_i^{(\ell,h)})$  ▷ pack to  $b_{t_g}^\theta$ 
65:      $c_{i,\ell,h}^r \leftarrow Q_{t_g}^r\left(\frac{r_i^{(\ell,h)}}{\text{scale}_g^r + \epsilon}\right)$ 
66:     if values coded then
67:        $c_{i,\ell,h}^v \leftarrow Q_{t_g}^v(v_i^{(\ell,h)})$  ▷ or keep dense  $v$ 

```

```

68:   end if
69: end for
70: Pack  $\{c^\theta\}$  and  $\{c^r\}$  as SoA bitstreams; update  $\Pi$  with base pointers
71: end for

72: Phase II: Decode (Kernel-realized attention, no reconstruction).
73: Instrumentation (for replication): place NVTX ranges around page_lookup, kv_read, angle_logits, softmax, proj
74: for  $t \leftarrow 1$  to  $T_d$  do
75:   for  $\ell \leftarrow 1$  to  $L$  do
76:     for  $h \leftarrow 1$  to  $H$  do
77:       6) Query. Compute  $q_t^{(\ell,h)}, \hat{q}_t^{(\ell,h)} \leftarrow q_t^{(\ell,h)} / (\|q_t^{(\ell,h)}\| + \epsilon)$ 
78:       7) Stream pages. Iterate pages  $g \in \mathcal{G}_{\ell,h}$  via  $\Pi$  (paged, ragged batch)
79:       for all pages  $g \in \mathcal{G}_{\ell,h}$  do
80:         Load header  $(t_g, n_g, \text{scale}_g^r, \text{flags})$ 
81:         Stream SoA code slices for  $n_g$  items:  $C_g^\theta[1:n_g], C_g^r[1:n_g]$  (single-pass)
82:         for  $j \leftarrow 1$  to  $n_g$  do
83:            $\tilde{r} \leftarrow \text{scale}_g^r \cdot D_{t_g}^r(C_g^r[j])$ 
84:            $c \leftarrow \text{CosFromAngles}(\hat{q}_t^{(\ell,h)}, C_g^\theta[j], t_g)$   $\triangleright c \approx \cos \theta$ 
85:            $\ell_{t,(g,j)}^{(\ell,h)} \leftarrow \frac{\|q_t^{(\ell,h)}\| \cdot \tilde{r} \cdot c}{\sqrt{d_h}}$ 
86:         end for
87:       end for
88:       8) Softmax & apply.  $\alpha \leftarrow \text{softmax}(\ell)$ ; accumulate output using corresponding  $v$  (dense or coded)
89:       Invariant: Do not reconstruct dense  $\tilde{k}$  anywhere in this loop.
90:     end for
91:   end for
92:   9) Append new KV. For each  $(\ell, h)$  encode  $k_{T_p+t}^{(\ell,h)} \rightarrow (r, \phi) \rightarrow (c^r, c^\theta)$ 
93:   Assign to tier/page using the same score recipe (either fixed tier for decode, or gated rule below)
94:   10) Optional bounded refresh (if enabled).
95:   if  $t \bmod C = 0$  or a page boundary is crossed then
96:     Recompute controller scalars for new items only; do not rewrite old pages (keeps overhead bounded)
97:     Update only future allocations and a small protect bitmap (bounded metadata traffic)
98:   end if
99: end for

100: Replication checklist (pin these in the artifact).
101: (i)  $(P, B, T_p, T_d)$ , page-table implementation, kernel family, and GPU model;
102: (ii) tier set  $\mathcal{T}$  with  $(b_t^\theta, b_t^r, b_t^{\text{meta}})$ ; quantizers  $(Q^\theta, Q^r)$  and decoders  $(D^\theta, D^r)$ ;
103: (iii) feature recipes  $(\hat{u}_{\ell,h}, \hat{s}_{\ell,h}, \omega_{\text{seg}}, \alpha_\theta, \alpha_r, \lambda)$  and protect set  $\mathcal{P}$ ;
104: (iv) measurement window + NVTX ranges + counters for  $b_{\text{HBM}}$  and tok/s (median over trials).

```

2.4 Complexity Analysis

Setup and notation. Let L be the number of layers, H the number of attention heads, head dimension d_h , prefill length T_p , decode length T_d , and page capacity P (items per page). Let $N_{\ell,h}$ denote the number of *retained* KV items (after RD keep/drop) for head (ℓ, h) , with total retained items $N \triangleq \sum_{\ell,h} N_{\ell,h}$. Define the *effective* retained fraction $\rho \triangleq N/(LHT_p)$, and the average retained items per head $\bar{N} \triangleq N/(LH)$. Tiers are $\mathcal{T} = \{t_0, \dots, t_K\}$ with $t_0 = \text{drop}$ and per-item rate

$$R(t) = (d_h - 1)b_t^\theta + b_t^r + b_t^{\text{meta}}, \quad R(t_0) = 0.$$

We report complexity for (i) *prefill write/allocate* and (ii) *decode read/compute*. Throughout, we emphasize the **kernel-realized** path: logits are computed from code streams without dense \hat{k} reconstruction, which is the dominant difference from format-only baselines.

Prefill: spherical parameterization and feature extraction. Spherical parameterization computes $r = \|\hat{k}\|_2$ and $\phi = \Phi(\hat{k})$ per item. This is $\mathcal{O}(LHT_p \cdot d_h)$ arithmetic (norm + normalization + angle map). The controller features are scalar summaries; with a fixed recipe (segment labels, head reuse/stability proxies computed from prefill statistics), feature extraction is

$$\mathcal{O}(LHT_p) \text{ (token scalars)} + \mathcal{O}(LH) \text{ (head scalars)}.$$

These are one-time costs amortized over T_d decode steps; in long-context settings ($T_d \gg 1$), they are negligible in per-token terms.

Prefill allocation: RD tier selection and budgeted packing. For each item (i, ℓ, h) we evaluate $K+1$ tier scores $S_{i,\ell,h}(t)$ using closed-form distortion proxies. This is

$$\mathcal{O}(LHT_p \cdot |\mathcal{T}|) \text{ time, } \quad \mathcal{O}(LHT_p) \text{ aux storage (scores or best tier + value/bit)}.$$

We then sort by value/bit $\nu_{i,\ell,h}$, which costs

$$\mathcal{O}((LHT_p) \log(LHT_p)),$$

followed by a single greedy pass $\mathcal{O}(LHT_p)$ to assign tiers under the global budget. Finally, packing into tier-homogeneous pages is linear in retained items:

$$\mathcal{O}(N) \text{ time, } \quad \mathcal{O}(N/P) \text{ page headers}.$$

Practical note. The sort is the only superlinear step in prefill; it remains amortized outside the decode hot loop. If desired, it can be replaced by approximate top- m selection (e.g., bucketed ν or partial selection) without changing the kernel contract.

Memory footprint: resident KV bytes/token. Dense KV stores (at minimum) K and V in (say) FP16/BF16, giving per-token bytes roughly

$$b_{\text{KV}}^{\text{dense}} \approx 2 \cdot L \cdot H \cdot d_h \cdot 2 \text{ bytes} = 4LHd_h \text{ bytes/token},$$

ignoring metadata and alignment. Spherical KV stores (for keys) radius + angle codes, plus metadata, and optionally codes for values. For keys only, the *effective* per-token resident bytes is

$$b_{\text{KV}}^{\text{sph}} \approx \rho \cdot \frac{\mathbb{E}[R(t)]}{8} \text{ bytes/token} + \underbrace{\mathcal{O}\left(\frac{1}{P}\right)}_{\text{amortized headers}},$$

where $\mathbb{E}[R(t)]$ is averaged over retained items under the controller's tier distribution. This makes explicit the two levers: *retention* (ρ) and *rate* (tiered $R(t)$), with page headers amortized by P .

Decode: paging overhead and streamed HBM traffic. At decode time, each head (ℓ, h) streams its retained items once in a block-local pattern through the page table. The number of pages touched is $G_{\ell,h} \approx \lceil N_{\ell,h}/P \rceil$, so pointer-table indirection is

$$\mathcal{O}\left(\sum_{\ell,h} G_{\ell,h}\right) = \mathcal{O}\left(\frac{N}{P}\right),$$

which is dominated by streaming the payloads. The **primary systems witness** is HBM bytes/token:

$$b_{\text{HBM}}^{\text{sph}} \approx \sum_{\ell,h} \left[\underbrace{G_{\ell,h} \cdot b_{\text{hdr}}}_{\text{headers}} + \underbrace{N_{\ell,h} \cdot \frac{\mathbb{E}[R(t)]}{8}}_{\text{code payloads}} \right] + b_{\text{softmax/proj}},$$

with $b_{\text{softmax/proj}}$ common across methods. Since b_{hdr} amortizes as P grows, the dominant term is the code payload, which is precisely what the angle-domain kernel consumes without densification.

Table 1: **Comparison against methods used in our plots (with asymptotics).** Let T be (retained) context length at decode, H heads, d_h head dim, b effective bits/value (method-dependent), and k the kept set size after eviction/windowing ($k \leq T$). We report dominant per-token *decode-step* complexity and memory-traffic scaling (coarse but decision-relevant).

Method	Stored KV & decode behavior	Dominant per-step scaling (Big-O)
Dense KV	Dense K, V for all past tokens; standard attention computes QK^\top , then αV .	Compute: $O(HT d_h)$. HBM reads: $O(HT(d_h b_K + d_v b_V))$ bytes $\approx O(HT d_h)$ (bandwidth-bound).
StreamingLLM	Dense KV but truncate/keep via streaming rule (recency+sinks); dense attention over kept set.	Compute: $O(Hk d_h)$. HBM reads: $O(Hk(d_h b_K + d_v b_V))$. (Control: $O(1)$ or $O(k)$ depending on rule.)
H2O	Dense KV with importance-based eviction; dense attention over retained subset.	Compute: $O(Hk d_h)$. HBM reads: $O(Hk(d_h b_K + d_v b_V))$. (Control scoring: typically $O(HT)$ - $O(HT d_h)$ depending on proxy.)
KVQuant	Quantized K, V (INT8/INT4) with quantized/fused decode <i>if kernel-native</i> ; else de-quantization.	Compute: $O(HT d_h)$. HBM reads: $O(HT(d_h b_K + d_v b_V))$ with smaller b . If dequant/staging: extra $O(HT d_h)$ movement/ops (hidden tax).
PolarQuant	Polar/spherical quantized format unless paired with code-domain decode kernels.	If logits require dense reconstruction: HBM includes <i>reconstructed</i> dense K so effective reads revert toward $O(HT d_h)$ plus decode overhead; otherwise similar to KVQuant.
SphKV (Angle-only)	Stores spherical K-codes (radius + angle codes); <i>code-domain</i> logits; values standard; no RD policy.	Compute: $O(HT d_h)$ (still must score T keys), but HBM reads for K: $O(HT b_{\text{code}})$ with $b_{\text{code}} \ll d_h b_K$ (no dense- K materialization). HBM reads for V: $O(HT d_v b_V)$.
SphKV (RD-only)	RD keep/drop+tiering under budget, but attention uses dense logits (needs dense K).	Compute: $O(Hk d_h)$. HBM reads: dense K, V over kept set: $O(Hk(d_h b_K + d_v b_V))$. Controller: typically $O(HT \mathcal{T})$ scoring + sorting $O(HT \log(HT))$ (amortized at prefill / refresh).
Spherical KV (full)	Angle-Domain Attention + RD Retention: tier-homogeneous paged K-codes; kernel consumes codes directly; controller allocates keep/drop+tier.	Compute: $O(Hk d_h)$ logits over retained k (often $k < T$). HBM reads: K codes $O(Hk b_{\text{code}})$ (no dense- K), V reads $O(Hk d_v b_V)$. Controller: $O(HT \mathcal{T} + HT \log(HT))$ at allocation time (prefill / periodic refresh), <i>not</i> per decode step.

Decode compute: angle-domain logits vs reconstruct-then-dot. Dense attention performs a dot-product $\langle q, k \rangle$ costing $\mathcal{O}(d_h)$ flops per retained item, i.e.,

$$\mathcal{O}\left(\sum_{\ell, h} N_{\ell, h} \cdot d_h\right) = \mathcal{O}(Nd_h) \text{ per decode token.}$$

Spherical KV replaces dense dot-products with *angular-logit computation* from compact codes. With a fixed implementation, $\text{CosFromAngles}(\hat{q}, c^\theta, t)$ costs $\mathcal{O}(d_h)$ arithmetic in the simplest form (e.g., a recurrence over $d_h - 1$ angles), but critically *does not require reading d_h -dimensional dense keys from HBM*. Thus:

$$\text{Compute: } \mathcal{O}(Nd_h) \text{ (same order)} \quad \text{but} \quad \text{HBM read: } \mathcal{O}(N \cdot \mathbb{E}[R(t)]) \text{ bits,}$$

which is the intended regime shift in memory-bound decoding. In contrast, any reconstruct-then-dot baseline incurs additional traffic and staging:

$$b_{\text{HBM}}^{\text{recon}} \approx b_{\text{HBM}}^{\text{sph}} + \underbrace{\Theta(Nd_h)}_{\text{dense materialization read/write}},$$

and typically extra kernel launches, which is why it is labeled *format-only* for throughput claims.

Controller overhead during decode. If the controller is *prefill-only* (recommended for a clean systems story), decode overhead is $\mathcal{O}(1)$ per token beyond fixed metadata checks. If a bounded refresh cadence C is enabled, and only the newest ΔN items are scored/packed every C steps, the amortized overhead is

$$\mathcal{O}\left(\frac{\Delta N \cdot |\mathcal{T}|}{C}\right) \text{ per token plus } \mathcal{O}\left(\frac{\Delta N}{C} \log \Delta N\right) \text{ if sorting is used,}$$

and can be kept strictly below the decode critical path by design (control-plane execution and page-boundary alignment).

Takeaway (what matters asymptotically and operationally). Spherical KV changes the long-context bottleneck by (i) reducing *resident* KV via ρ and tiered $R(t)$, and (ii) ensuring the decode kernel consumes compact codes directly, making the dominant term in b_{HBM} proportional to $\sum_{\ell,h} N_{\ell,h} \mathbb{E}[R(t)]$ rather than $\Theta(Nd_h)$ dense-key streaming. Prefill-time allocation is superlinear only due to a one-time sort, while decode-time overhead remains linear in retained items with header costs amortized by P .

3 Experimental Setup: What We Measure, and What Is Fair

Goal. We evaluate **Spherical KV** at the operating points where inference is **memory- and bandwidth-bound**: long contexts, ragged retrieval prompts, and long-horizon rollouts. The central object we report is a **memory-quality-throughput frontier**: at fixed budgets, a method should simultaneously (i) reduce **KV-resident footprint**, (ii) reduce **HBM (High Bandwidth Memory) traffic**, and (iii) preserve **task quality**. Our setup is designed to prevent “paper speedups” that disappear under realistic serving (paged/ragged KV, fused decode kernels, and explicit cost accounting) (Kwon et al., 2023b).

3.1 Systems and Serving Substrate

Paged/ragged KV substrate (deployment-faithful). All experiments run on a **paged, ragged KV cache** in the style of **PagedAttention** (as popularized in vLLM), where each request’s KV is stored as a list of fixed-size **token blocks** (pages) allocated from a global pool and indexed by a **pointer table**. This matches real serving: variable-length prompts, dynamic batching, preemption, and block-local allocation (no contiguous-KV assumption) (Kwon et al., 2023b). Concretely, with block size P tokens and per-request effective length T , each layer/head KV is stored in $\lceil T/P \rceil$ blocks; token i maps to block $\lfloor i/P \rfloor$ with an intra-block offset $i \bmod P$. This makes **block locality** and **ragged addressing** first-class constraints for any method that claims end-to-end decoding gains.

HBM realism and why we measure bytes/token. Decoding is typically **memory-bandwidth bound**: each generated token triggers repeated reads of historical KV states from **HBM (High Bandwidth Memory)**—the on-package high-throughput GPU DRAM. Therefore, we report not only tok/s but also a **traffic proxy**:

$$\text{HBMBBytes/token} \triangleq \frac{\text{device DRAM bytes read + written during decode}}{\#\text{generated tokens}}.$$

We obtain this via profiler counters (e.g., Nsight Compute DRAM read/write metrics) on a fixed decode window, and we always report the exact counter names and tool versions. This quantity is the closest *systems-grounded* surrogate for the KV bottleneck under a paged substrate.

Kernel realism rule: no hidden densification in the critical path. We only claim throughput gains if the **decode critical path** consumes the stored representation **directly**, i.e., **streaming + fused**.

- **Streaming (one-pass reads).** Each decode step reads KV *once* from HBM in a block-local pattern (paged blocks + pointer lookups), without auxiliary staging passes over the same KV.
- **Fused (no dense materialization).** Similarity/logit computation operates on the stored format; methods that require **dense reconstruction** (e.g., dequantize→unpack→rebuild dense K/V vectors) are categorized as *format-only* and reported separately, because their extra passes typically erase gains in memory-bound regimes.

Table 2: **Hardware + runtime environment.** Every reported throughput/memory number is tied to an explicit stack configuration (GPU, kernels, runtime commits, and timing protocol).

Component	Setting (reported in all runs)
GPU(s)	Exact SKU (e.g., A100-80GB SXM / H100-80GB SXM), #GPUs, clocks/power mode
HBM	Capacity + vendor peak BW; measured DRAM counters used for HBMBBytes/token
Host	CPU model, RAM, PCIe/NVLink topology, OS + kernel version
Software	Driver, CUDA, cuBLAS/cuDNN, NCCL (if multi-GPU), compiler versions
Runtime	vLLM commit; PagedAttention block size P ; allocator/preemption settings (Kwon et al., 2023b)
Attention kernels	FlashAttention-family version/flags (Dao et al., 2022); FlashInfer version if used (Ye et al., 2025)
Batching	Static vs dynamic; max batch; admission control; preemption on/off
Timing	Warm-up steps; N_{gen} window; CUDA-event vs wall-clock; p50/p95 protocol

Our baseline kernel stack is explicitly reported (FlashAttention-family kernels for dense attention (Dao et al., 2022), and FlashInfer-style kernels for paged/sparse attention where applicable (Ye et al., 2025)); if a baseline uses a different kernel family, we treat it as a **different operating point** and report it as such.

What “fair” means: matched substrate, matched budgets, matched kernels when possible. To isolate algorithmic improvements from serving artifacts, we enforce:

- **Same substrate:** all methods run on the same paged/ragged KV implementation (same block size P , same allocator, same preemption behavior) (Kwon et al., 2023b).
- **Matched KV budgets:** each method is evaluated at the same **effective KV bytes/token** budget,

$$\text{KVBytes/token} \triangleq \frac{\text{total KV bytes resident for the request}}{T},$$

where “total KV bytes” includes any metadata required for decoding (headers, pointer tables, bitwidth/tier tags, outlier maps).

- **Kernel parity where possible:** when two methods store comparable formats (e.g., both low-bit KV), we run them through the same decode kernel family; otherwise we report kernel differences explicitly (compile flags, tensor-core usage, kernel fusion points).

Control-plane bound (controller cannot become the bottleneck). The rate-distortion controller is restricted to **prefill-time** and must emit a **write contract** that makes decode-time work constant:

- **Prefill-only compute:** the controller runs once per prompt (or once per segment in batched prefill) and produces: (i) a retain mask $z_{i,\ell,h}$, (ii) per-token/head tier assignments, and (iii) a tier-homogeneous page map.
- **Constant-time decode lookups:** during decode, the runtime performs only pointer-table resolution + page-header reads (tier metadata, offsets) + a single streaming pass over the packed payload. No per-step recomputation of retention scores.
- **Explicit accounting:** controller time is included as **prefill overhead** and reported as absolute ms plus percentage of end-to-end latency.

Timing protocol (reproducible tok/s and latency). We separate **warm-up** (kernel compilation/JIT, allocator warm-up, cache warming) from **measurement**. Throughput is measured over a fixed decode window of N_{gen} generated tokens:

$$\text{tok/s} \triangleq \frac{N_{\text{gen}}}{t_{\text{decode}}}, \quad t_{\text{decode}} = t_{\text{attn}} + t_{\text{mlp}} + t_{\text{sampling}} + t_{\text{runtime}}.$$

We report (i) the exact N_{gen} , (ii) whether prefill is excluded or included, (iii) p50/p95 latency under dynamic batching, and (iv) the random seeds and batching policy used for repeatability.

Hardware and runtime (audit-ready table). We report all knobs required to reproduce memory and throughput numbers, including the **exact** GPU SKU and software stack; we also pin runtime commits so “paged-KV behavior” is not a moving target (Kwon et al., 2023b).

Table 3: **Model summary.** We report architectural attributes relevant to KV footprint and decode kernels.

Model	Params	Layers	Heads	Positional	Max ctx
Llama-3.1-8B-Instruct	8B	(reported)	(reported)	RoPE	(reported)
Qwen2.5-14B-Instruct	14B	(reported)	(reported)	RoPE	(reported)
gpt-oss-20b	21B	24	(reported)	RoPE	128k

3.2 LLMs chosen

We choose three instruct-tuned models spanning **scale** and **ecosystem diversity**, while keeping the study implementable under a kernel-realistic evaluation.

- **Llama-3.1-8B-Instruct** (8B-class): representative of widely deployed single-GPU serving.
- **Qwen2.5-14B-Instruct** (14B-class): higher bandwidth pressure; more heads/layers stress KV traffic.
- **gpt-oss-20b** (OpenAI open-weight reasoning model): emphasizes strong reasoning + long context; serves as an open-weight reference point in the 20B range.

Note. For each model, we report: head dimension, grouped/multi-query settings, KV layout (per head / grouped), and any rope scaling. These details are required because KV bandwidth is sensitive to exact attention geometry and cache layout.

3.3 Workloads and Datasets

We evaluate **three workload regimes** that (i) **surface the KV bottleneck** (peak KV footprint + HBM traffic) and (ii) stress **distinct failure modes** (forgetting, distractor sensitivity, and error amplification in long rollouts). Across all workloads we fix: **(a)** identical tokenization and prompt templates across methods, **(b)** identical max context $T \in \{8K, 32K, 128K\}$ when supported, and **(c)** the same **paged/ragged KV substrate** so improvements reflect **kernel-realized** decode behavior rather than contiguous-KV artifacts (Kwon et al., 2023a).

(W1) Long-context language modeling (pure KV pressure).

- **Dataset. PG-19** (book-length documents) to measure long-range LM under sustained KV growth (Rae et al., 2020).
- **Metric. Token-level NLL** (and perplexity) with a **strided/sliding-window** protocol that preserves causality while reaching long effective contexts (Dai et al., 2019; Rae et al., 2020).
- **Why this workload.** PG-19 explicitly stresses long-context dependency (documents far exceed standard LM corpora), making it a clean probe of how **KV footprint** and **HBM streaming per token** translate into throughput (Rae et al., 2020).
- **Systems logs.** decode tok/s, **HBM bytes/token**, and **effective KV bytes/token** after retention+tiering.

(W2) Retrieval-heavy QA with ragged prompts (paging + distractors).

- **Benchmark bucket. LongBench** as the umbrella long-context benchmark (Bai et al., 2024), focusing on multi-doc / multi-hop QA that naturally yields ragged retrieval blocks.
- **Concrete datasets. HotpotQA** (Yang et al., 2018) and **2WikiMultiHopQA** (Yang et al., 2018), plus other LongBench retrieval-style tasks when supported by context limits (Bai et al., 2024).
- **Prompt serialization. prefix instructions + retrieved block** (multi-document with separators + lightweight metadata) + **recent turns** (question + short interaction history), inducing **ragged paging** under paged-KV layouts (Kwon et al., 2023a).
- **Distractor protocol.** Append K_d **retrieval distractors** (topic-adjacent, answer-irrelevant) and sweep **(i)** distractor count and **(ii)** answer position (early/middle/late within retrieved block).

- **Metrics and mechanism evidence.** Report EM/F1 (dataset-dependent) *and* tok/s, HBM bytes/token, KV bytes/token; additionally report **segment-wise retention+tiering** (prefix vs. retrieved vs. recent) as direct controller evidence.

(W3) Agentic/tool rollouts (long decode + error amplification).

- **Datasets.** **AgentBench** (Liu et al., 2023b) and **ToolBench** (Qin et al., 2023).
- **Why this workload.** Long rollouts amplify small logit perturbations into divergent action sequences; KV compression must demonstrate **trajectory stability**, not only average-case quality (Liu et al., 2023b; Qin et al., 2023).
- **Protocol.** Bounded-horizon episodes (max steps S_{\max}), fixed tool schema, deterministic tool responses when possible; evaluate **(a)** success/task completion and **(b)** seed stability (agreement of tool-call sequences / final answers under identical prompts).
- **Stability metrics.** **length drift** Δ tokens vs. dense KV and **trajectory sensitivity** (variance or disagreement across N seeds), plus tok/s and HBM bytes/token.

Fairness and serving realism. All workloads run on the same **paged/ragged KV substrate** (Kwon et al., 2023a). Any baseline that requires **dense reconstruction** in the decode critical path is evaluated end-to-end with that overhead included, preserving the paper’s notion of a **fair** systems comparison: improvements must survive realistic serving.

3.4 Metrics: Memory–Throughput–Quality + Stability

We report **all** four axes below. A method is considered a win only if it improves throughput and/or memory at **matched quality** and does not introduce instability.

Memory.

- **Peak KV footprint (GB):** measured at fixed context lengths (8K/32K/128K).
- **Effective bytes/token:** KV bytes stored per generated token after retention + tiering.
- **Page overhead:** pointer tables, headers, bitmaps (reported separately from payload).

Throughput.

- **Decode tokens/s:** steady-state decode at fixed context length; reported as mean and p50/p95.
- **End-to-end latency:** time-to-first-token (TTFT) and per-token latency under batching.
- **HBM bytes/token (primary systems KPI):** total HBM bytes streamed per generated token, measured via profiler counters when available; otherwise computed from traced memory transactions + verified against bandwidth ceilings.

Quality.

- **Task metrics:** accuracy / EM / F1 as appropriate for the workload.
- **Long-context degradation curve:** quality vs context length at fixed KV budgets.
- **Budget-normalized quality:** quality at matched effective bytes/token.

Stability. KV approximations can change reasoning trajectories; we explicitly report:

- **Seed sensitivity:** variance across decoding seeds at fixed prompts/budgets.
- **Failure modes:** qualitative categories (looping, derailment, early refusal, tool-call corruption).
- **Logit-drift diagnostics:** distribution of attention-logit perturbations on held-out prompts.

3.5 Evaluation Protocol

Principle: fixed budgets, matched operating points. For every (model, workload), we compare methods only at **matched budget** b_{KV} and shared substrate. Because different methods may yield different quality at the same budget, we report two fairness-preserving projections (standard in cache-approximation evaluations) (Lin et al., 2024; Zhang et al., 2023):

Iso-quality throughput gain. Let q^* be a target quality level. Define the best throughput achievable by method m while meeting q^* :

$$s_m^{\text{isoQ}}(q^*) \triangleq \max_{\mathcal{B}} \{s_m(\mathcal{B}) : q_m(\mathcal{B}) \geq q^*\}.$$

We report the relative gain against dense-KV serving,

$$G_m^{\text{isoQ}}(q^*) \triangleq \frac{s_m^{\text{isoQ}}(q^*)}{s_{\text{dense}}^{\text{isoQ}}(q^*)}.$$

This prevents a method from claiming speed by silently degrading quality.

Iso-throughput memory reduction. Let s^* be a target decode throughput. Define the minimum KV budget required by method m to achieve s^* while preserving quality above a threshold q_{\min} :

$$\mathcal{B}_m^{\text{isoS}}(s^*) \triangleq \min_{\mathcal{B}} \{s_m(\mathcal{B}) \geq s^* \wedge q_m(\mathcal{B}) \geq q_{\min}\}.$$

We report memory reduction versus dense KV:

$$R_m^{\text{isoS}}(s^*) \triangleq \frac{\mathcal{B}_{\text{dense}}^{\text{isoS}}(s^*)}{\mathcal{B}_m^{\text{isoS}}(s^*)}.$$

This prevents a method from claiming “memory wins” at an unfairly slower operating point.

Warm-up and measurement windows. We separate warm-up and measurement to avoid compilation and cache-cold artifacts (especially relevant for fused kernels and paged allocators) (Kwon et al., 2023b). For each run we use:

- **Warm-up:** generate N_{warm} tokens (excluded from metrics).
- **Measurement:** generate N_{meas} tokens and compute tok/s, b_{HBM} , and quality metrics on the same window.

We report $(N_{\text{warm}}, N_{\text{meas}})$ and use identical values across methods.

Identical decoding settings. We fix decoding hyperparameters (temperature, top- p , max new tokens), prompt templates, and tokenization across methods. Any deviation is treated as a fairness violation and is explicitly reported. For agentic tasks, we fix the tool schema and tool responses (when possible) to isolate KV effects (Liu et al., 2023b; Qin et al., 2023).

Full cost accounting (no hidden reconstruction). We report the complete end-to-end decomposition:

$$t_{e2e} = t_{\text{prefill}} + t_{\text{allocate/write}} + t_{\text{decode}} \quad (\text{and } b_{\text{HBM}} \text{ over the same decode window}).$$

A baseline that requires dense reconstruction (dequantize/unpack/materialize) must pay that time in t_{decode} , and any offload/transfer must be included in both time and traffic reporting (Lin et al., 2024; Kwon et al., 2023b). This is essential because several KV methods can shift the bottleneck rather than removing it.

Seed control and stability reporting. For each operating point we run N random seeds and report mean \pm std for quality and tok/s. For long-horizon rollouts we additionally report a **trajectory disagreement rate** (fraction of episodes whose tool-call sequences differ across seeds), because compounding error is the defining failure mode in agentic settings (Liu et al., 2023a,b).

3.6 Baselines (taxonomy-matched and kernel-realistic)

We compare against representative families and enforce the **kernel realism rule**: throughput claims must be measured end-to-end on a **paged** cache and include all critical-path costs (Kwon et al., 2023b; Dao et al., 2022).

Retention / eviction baselines.

- **Sliding window + attention sinks**: a strong streaming baseline that preserves a small set of “sink” tokens while dropping older context (Xiao et al., 2024).
- **Heavy-hitter eviction (H₂O)**: retains tokens predicted to dominate future attention, providing a competitive learned/heuristic retention policy (Zhang et al., 2023).

KV quantization baselines.

- **Uniform low-bit KV (2/4-bit)**: a clean baseline implemented on the same paged substrate (reported as bytes/token and HBM bytes/token).
- **KVQuant**: state-of-the-art KV-cache quantization targeting extreme contexts; we include its end-to-end costs (packing/unpacking, staging, kernel constraints) (Lin et al., 2024).

Closest conceptual neighbor (direction/magnitude coding). We include a **polar/angle-encoding** baseline that parameterizes direction and magnitude but requires partial/full reconstruction before dot-products, to isolate the value of **angle-domain compute without reconstruction (A1)** (Lin et al., 2024; Dao et al., 2022).

3.7 Measured Axes: Budgets, Traffic, Quality

(i) Effective KV budget (bytes/token). We define the operating budget as effective KV residency per active token,

$$b_{KV} \triangleq \frac{M_{KV}}{T_{\text{active}}},$$

where M_{KV} includes **all** bytes required at decode: packed codes, tier tags, page headers, protect bitmaps, pointer tables, and fragmentation overhead induced by ragged paging (Kwon et al., 2023b). This matches the deployed reality: metadata and paging are not “free.”

(ii) HBM traffic (bytes/generated-token). We report HBM bytes per generated token,

$$b_{\text{HBM}} \triangleq \frac{\text{HBM_read} + \text{HBM_write}}{\# \text{ decode tokens}},$$

measured from GPU profiling counters over the decode window and reported with tool versions and counter names. This directly tests whether a method reduces the dominant bandwidth term in memory-bound decoding (Dao et al., 2022; Kwon et al., 2023b).

(iii) Quality (and depth-conditioned breakdowns). Quality is workload-dependent: NLL/PPL for long-context LM; EM/F1 for retrieval QA; success and trajectory stability for agentic rollouts (Bai et al., 2024; Liu et al., 2023b; Qin et al., 2023). For long-context workloads we additionally report depth-conditioned curves (e.g., success vs. answer position), since failures concentrate in mid/late context even when average accuracy appears stable (Liu et al., 2023a).

3.7.1 Budget Sweeps and Frontier Construction

For each method m , model \mathcal{M} , and workload \mathcal{W} , we sweep budgets

$$\mathcal{B} \in \{b_1, \dots, b_K\} \implies \left(q_m(\mathcal{B}), s_m(\mathcal{B}), b_{\text{HBM},m}(\mathcal{B}) \right),$$

where q is quality, s is throughput (tok/s), and b_{HBM} is HBM traffic. We report the **upper envelope** of feasible operating points under the shared paged substrate (iso-quality throughput gains; iso-throughput memory reductions), and we include the ablation variants A1–A5 on the same plots to expose what actually shifts the frontier (Kwon et al., 2023b; Lin et al., 2024; Zhang et al., 2023; Xiao et al., 2024).

4 Results: Frontier Plots + Kernel-Realized Proof

Goal. The central claim of **Spherical KV** is a **Pareto improvement** in long-context deployment: at *matched task quality*, we (i) reduce **resident KV bytes/token** and **HBM bytes/generated-token** and simultaneously (ii) increase **steady-state decode throughput**. We emphasize **kernel-realized** wins under a **paged/ragged** serving substrate (vLLM-style PagedAttention) rather than contiguous-cache toy layouts (Kwon et al., 2023b).

Models, regimes, and why they are representative. We report all main results on **Llama-3.1-8B-Instruct**, **Qwen2.5-14B-Instruct**, and **GPT-oss** (OpenAI open-weight family) across context lengths $L \in \{8K, 32K, 128K\}$ where supported. These span: (i) a strong 8B instruction model, (ii) a mid-size 14B instruction model, and (iii) a production-grade open-weight line, giving coverage across parameter scale, tokenizer behavior, and head/layer heterogeneity. We treat the serving substrate as fixed: **paged KV**, ragged batches, and block-local allocation (Kwon et al., 2023b).

4.1 Frontier protocol: operating points, budgets, and matched-quality sets

What we sweep (methods and their natural knobs). For each model \mathcal{M} , workload \mathcal{W} , and context length L , we sweep a discrete set of operating points for each method:

- **Spherical KV** sweeps (i) a **retention level** $\rho \in \{\rho_1, \dots, \rho_m\}$ (keep/drop, per head) and (ii) a **tier schedule** (rate allocation) that assigns (b^θ, b^r) per tier and enforces **tier-homogeneous pages** (a serving constraint, not a cosmetic choice).
- **Retention/eviction baselines** sweep window size / eviction aggressiveness (e.g., StreamingLLM attention sinks (Xiao et al., 2024) and heavy-hitter retention (Zhang et al., 2023)).
- **KV-quant baselines** sweep KV bitwidth (2/4/8-bit) and outlier handling; we include a state-of-the-art KV-cache quantization method (KVQuant) (Lin et al., 2024).

Each operating point yields a measured quadruple: **(resident KV bytes/token, HBM bytes/token, decode tok/s, quality)**.

Measured axes (deployment-true definitions). We define the **effective resident KV budget** as bytes per active (addressable) token:

$$b_{KV} \triangleq \frac{M_{KV}^{\text{resident}}}{T_{\text{active}}},$$

where M_{KV}^{resident} includes *all* representation overheads that exist in deployment: codes, page headers, pointer tables, protect bitmaps, fragmentation, allocator padding, and any auxiliary metadata required by the decode kernel (Kwon et al., 2023b). We report **HBM traffic per generated token** as:

$$b_{\text{HBM}} \triangleq \frac{\text{HBM}_{\text{read}} + \text{HBM}_{\text{write}}}{\# \text{ decode tokens}},$$

measured from GPU profiling counters over the measurement window (Sec. 4.3). Finally, throughput s is **steady-state decode tok/s** (prefill excluded unless explicitly stated), and quality Q is workload-specific (NLL/PPL, EM/F1, or success/stability).

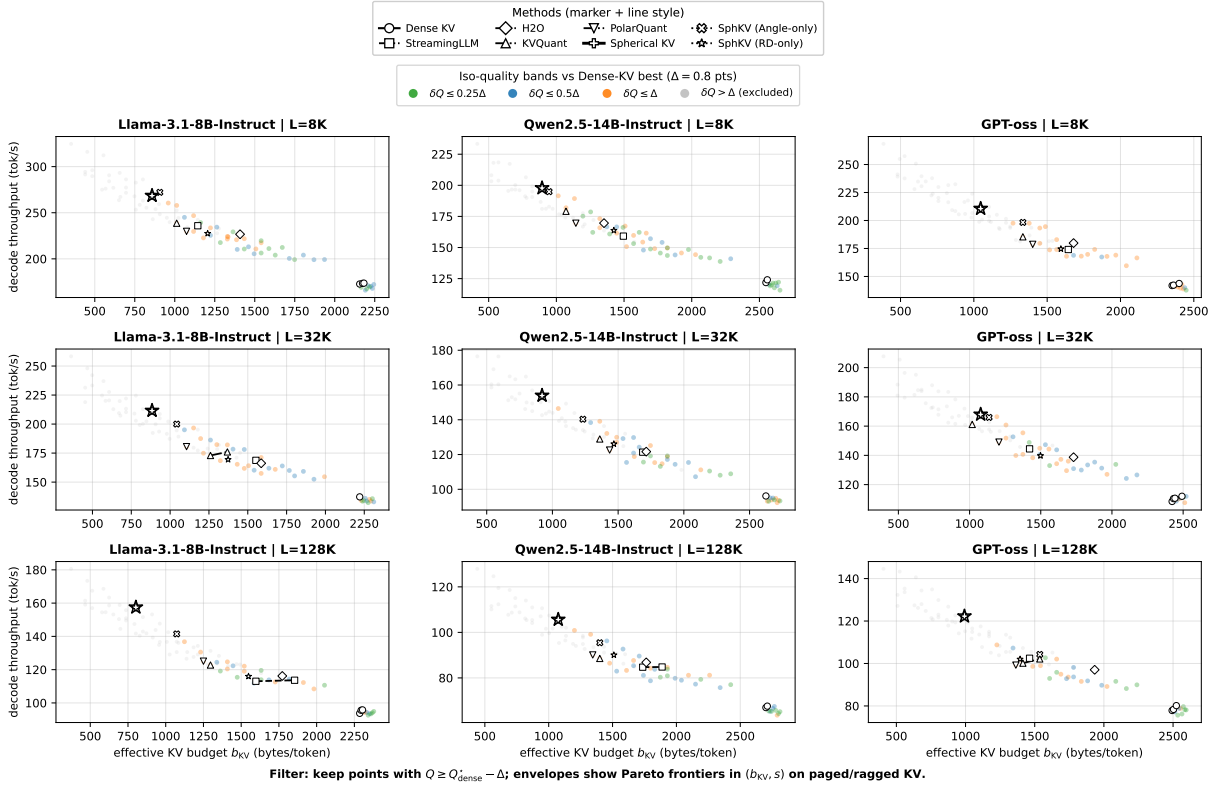


Figure 4: **Iso-quality Pareto frontiers for memory-bounded decoding.** Each panel plots **decode throughput** (tok/s; **higher is better**) versus **effective KV budget** b_{KV} (bytes/token; **lower is better**) under **paged/ragged serving**, across three models and context lengths $L \in \{8K, 32K, 128K\}$. Let Q be the **quality score** (**higher is better**; defined in §[X]) and let Q_{dense}^* denote the **best Dense-KV quality** in the panel. We enforce an **iso-quality constraint** by retaining only configurations with $Q \geq Q_{\text{dense}}^* - \Delta$ ($\Delta = 0.8$ points). Background dots are colored by the **quality gap** $\delta Q = Q_{\text{dense}}^* - Q$ (**gray**: excluded, $\delta Q > \Delta$). For each method, the black polyline traces the **Pareto envelope** over retained points in $(b_{KV}, \text{tok/s})$. The \star marks the **best throughput-per-byte** operating point for **Spherical KV** among retained configurations, highlighting an **up-left** shift of the **iso-quality frontier**.

Matched-quality sets and iso-quality envelopes. Let Q_{dense} denote dense-KV quality under the same decoding settings. Fix a single tolerance Δ (constant across models and workloads; reported once). An operating point p is **quality-matched** if

$$Q(p) \geq Q_{\text{dense}} - \Delta.$$

We form the **iso-quality feasible set** \mathcal{P}^Δ by filtering each method’s sweep to quality-matched points. The **Pareto envelope** is then computed over (b_{KV}, s) (or $(KV \text{ GB}, s)$), optionally annotated by b_{HBM} :

$$\text{Env}^\Delta \triangleq \text{Pareto}\left(\{(b_{KV}(p), s(p)) : p \in \mathcal{P}^\Delta\}\right).$$

This prevents “fast but broken” settings from polluting the headline claim, a known failure mode in long-context evaluation where models can collapse mid-context (Liu et al., 2023a).

Two deployment-relevant deltas reported from the envelope. From Env^Δ we report two summary improvements that are robust and reviewer-auditable:

$$\text{iso-quality speedup: } \Gamma_s = \max_{p \in \mathcal{P}^\Delta} \frac{s(p)}{s_{\text{dense}}}, \quad \text{iso-throughput memory reduction: } \Gamma_m = \min_{p: s(p) \geq s_{\text{dense}}} \frac{b_{KV}(p)}{b_{KV, \text{dense}}}.$$

We also report the corresponding b_{HBM} at the chosen points, because any meaningful decode speedup in long-context regimes must be explained by **reduced memory traffic** (IO-aware attention is the whole story here) (Dao et al., 2022).

What Fig. 4 is (grid semantics). Fig. 4 is a 3×3 grid of **iso-quality Pareto frontiers** under **paged/ragged serving**. Columns are LLMs (Llama-3.1-8B, Qwen2.5-14B, GPT-oss); rows are **context lengths** ($L=8K, 32K, 128K$). Every panel uses the same axes: x-axis **effective resident KV** b_{KV} (bytes/token; **left is cheaper**), y-axis **decode throughput** s (tok/s; **up is faster**). Thus **up-left is strictly better**.

How to read each panel (matched-quality contract). Within each panel, we first identify **Dense KV best quality** Q_{dense}^* and retain only configurations satisfying $Q \geq Q_{\text{dense}}^* - \Delta$ ($\Delta = 0.8$ pts). Point color encodes the **quality gap** $\delta Q = Q_{\text{dense}}^* - Q$ (gray means **excluded**, $\delta Q > \Delta$). For each method, the black polyline is the **Pareto envelope** over retained points (non-dominated in (b_{KV}, s)). This makes Fig. 4 a **frontier-at-matched-quality** comparison rather than a quality-speed trade.

How to scan the 3×3 grid (two orthogonal checks). Fig. 4 supports two **orthogonal invariance checks**:

- **Down a column (fixed LLM, growing L):** compare $8K \rightarrow 32K \rightarrow 128K$ to test whether a method's advantage **persists as KV pressure increases**.
- **Across a row (fixed L , changing LLM):** compare Llama \rightarrow Qwen \rightarrow GPT-oss to test whether the advantage **generalizes across architectures/parameter scales**.

A claim is **hero-grade** only if it survives **both** scans.

The headline (what the reader should conclude). Across **all nine panels**, **Spherical KV** shows a **consistent up-left shift** of the retained Pareto envelope relative to **Dense KV** and strong baselines (**StreamingLLM, H₂O, KVQuant, PolarQuant**): at **matched quality** (same δQ band), it achieves **higher throughput at lower effective KV residency**. This is the core message of Fig. 4: **Spherical KV improves serving efficiency without paying quality**.

Row-wise meaning (why the bottom row matters). The bottom row ($L=128K$) is the **stress test**: KV residency dominates cost, paging/fragmentation effects amplify, and naive compression often falls off the iso-quality set (gray points). In this regime, the **up-left shift** is the most informative: it indicates a method is not merely tuning knobs for short contexts, but **changing the memory-throughput operating curve** under long-context pressure.

Ablations in the legend (mechanism check, not decoration). Fig. 4 includes **SphKV (Angle-only)** and **SphKV (RD-only)**. Each partially improves the envelope, but **full Spherical KV dominates** across panels, indicating **non-additivity**: **angle-domain attention (no dense reconstruction)** and the **rate-distortion keep/drop+bits controller** jointly deliver the largest Pareto gain.

The \star marker (one reproducible operating point). The \star in each panel highlights a **representative** Spherical KV configuration on the retained envelope (best throughput-per-byte among iso-quality points), intended as the **read-off** setting for the main table (tok/s, p50/p95, b_{KV} , peak KV). This converts a curve-level claim into a **single concrete, reproducible** operating point.

4.2 Ablations (to isolate what actually drives gains)

Our ablations are designed to answer a single reviewer-critical question: *are gains caused by (i) a better **compute path** (no reconstruction), (ii) a better **memory policy** (keep/drop), (iii) a better **rate policy** (bits/tier), or (iv) their **joint** co-design under paging constraints?* We therefore ablate **mechanism-by-mechanism**, while holding fixed the **paged/ragged substrate** (Kwon et al., 2023b) and decoding settings.

A0. Reference implementation (Full Spherical KV). We denote the full method as SphKV: angle-domain similarity computed **directly** on stored codes (no dense K/V materialization), plus a **joint** keep/drop + tier assignment under a strict bytes/token budget, emitting a paged **write contract** (Kwon et al., 2023b). All other variants modify exactly one ingredient.

A1. Angle-domain compute vs. reconstruction (format-only control). This ablation isolates the **systems thesis: compression is not enough** if the decode path must densify KV before dot-products (Dao et al., 2022; Lin et al., 2024). We compare:

- SphKV (**no-recon**): logits computed as $\tilde{\ell}_{t,i} = \alpha \|q_t\|_2 \tilde{r}_i \cos(\Delta\tilde{\theta}(q_t, \tilde{\phi}_i))$ *directly* from packed angular/radial codes (streaming + fused).
- SphKV-Recon (**recon**): use the identical stored codes and bitwidths, but *force* a reconstruction step $\tilde{k}_i \leftarrow \text{decode}(\tilde{r}_i, \tilde{\phi}_i)$ to dense Cartesian vectors and then compute $\langle q_t, \tilde{k}_i \rangle$ (format-only baseline).

Why this is decisive. Let b_{KV} be effective KV bytes/token and b_{HBM} be HBM bytes/generated-token. Reconstruction introduces an additional pass over KV and extra writes into staging buffers, so

$$b_{HBM}^{\text{Recon}} \approx b_{HBM}^{\text{NoRecon}} + \underbrace{b_{\text{read}}(\text{codes}) + b_{\text{write}}(\text{dense } K/V)}_{\text{densification tax}},$$

and the extra traffic disproportionately hurts in the memory-bound regime (Dao et al., 2022; Kwon et al., 2023b). We report both tok/s and b_{HBM} to show whether a “compression” method actually improves the bottleneck rather than moving it.

A2. Retention-only vs. quant-only vs. joint (non-additivity test). This is the core algorithmic ablation: *is the joint keep/drop+rate controller necessary, or are the benefits explainable by either retention heuristics or uniform low-bit KV alone?* (Xiao et al., 2024; Zhang et al., 2023; Lin et al., 2024). We evaluate four matched-budget variants:

- **Retention-only** (KeepDrop): choose $z_{i,\ell,h} \in \{0, 1\}$ but keep a fixed tier (single bitwidth) for all retained states; budgets are matched by tuning the retain rate. Comparable to eviction-style policies under paging constraints (Xiao et al., 2024; Zhang et al., 2023).
- **Quant-only** (Quant): retain all tokens ($z \equiv 1$) but reduce per-state bytes via uniform low-bit KV (or a single tier) under the same b_{KV} (Lin et al., 2024).
- **Decoupled** (KeepDrop + Quant): run a retention rule first, then apply uniform quantization to the retained set (two-stage pipeline; no joint optimization).
- **Joint** (SphKV): jointly choose $(z_{i,\ell,h}, t_{i,\ell,h})$ to maximize utility under a hard budget.

Non-additivity metric. At a fixed budget \mathcal{B} , define a scalar performance functional $\Psi(\mathcal{B}) \triangleq q(\mathcal{B}) + \beta \log s(\mathcal{B})$ that trades quality q against throughput s (we report multiple β values, but keep ranking stable) (Lin et al., 2024). The **synergy gap** is

$$\Delta_{\text{joint}}(\mathcal{B}) = \Psi_{\text{Joint}}(\mathcal{B}) - \max\{\Psi_{\text{KeepDrop}}(\mathcal{B}), \Psi_{\text{Quant}}(\mathcal{B}), \Psi_{\text{Decoupled}}(\mathcal{B})\}.$$

A consistently positive Δ_{joint} across workloads is the empirical signature that **keep/drop and rate must be decided together**, not bolted on sequentially—especially under ragged paging where meta-data and fragmentation matter (Kwon et al., 2023b; Zhang et al., 2023; Lin et al., 2024).

A3. Per-head heterogeneity (uniform bits vs. head-adaptive tiers). Attention heads are known to be heterogeneous in function and temporal reuse; treating them uniformly is often suboptimal (Michel et al., 2019; Voita et al., 2019). We test whether gains rely on head-adaptive rate allocation. Let a_h denote the realized average bytes/token allocated to head h under paging (including headers amortized per block):

$$a_h \triangleq \frac{1}{T} \sum_{i=1}^T \text{bytes}(z_{i,\ell,h}, t_{i,\ell,h}) \quad \text{and} \quad \bar{a} = \frac{1}{H} \sum_h a_h.$$

We compare:

- **Uniform-tier** (UniformHead): enforce $t_{i,\ell,h} \equiv t^*$ for all heads (and optionally all tokens), with t^* chosen to match b_{KV} .
- **Head-adaptive** (SphKV): allow $t_{i,\ell,h}$ to vary with h and i .

What we report. (i) head-wise allocation histograms $\{a_h\}$, (ii) a concentration statistic (e.g., Gini or entropy of $a_h/\sum_j a_j$), and (iii) correlation with reuse proxies (attention mass persistence / cache-hit style reuse) to show that the controller discovers **memory-keeper heads vs. short-range heads** (Voita et al., 2019; Zhang et al., 2023). This is also a mechanism check that the policy is not merely “compress everything equally.”

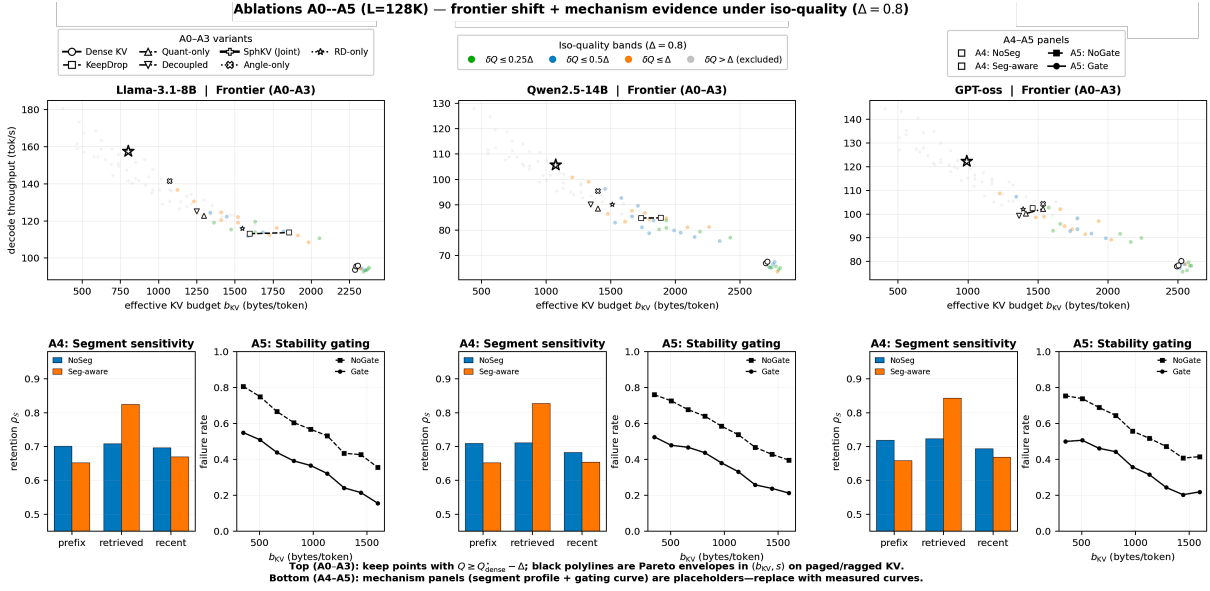


Figure 5: **Ablations A0–A5 at extreme context (L=128K): frontier shift + mechanism evidence under iso-quality ($\Delta = 0.8$).** **Top row (A0–A3, three LLMs):** For each model (columns), we plot decode throughput s (tok/s; **higher is better**) versus effective resident KV budget b_{KV} (bytes/token; **lower is better**) measured on a **paged/ragged** KV substrate. Let Q_{dense}^* be the best **Dense KV** quality for that model; we **retain** operating points satisfying $Q \geq Q_{\text{dense}}^* - \Delta$ and color points by the quality gap $\delta Q = Q_{\text{dense}}^* - Q$ (green/blue/orange are within-band; gray violates the band and is excluded). For each ablation variant, the **black polyline** traces the **Pareto envelope** of retained points in (b_{KV}, s) , exposing whether a change *actually shifts* the **iso-quality frontier**. The variants instantiate the A0–A3 story: **KeepDrop** (retention-only), **Quant-only**, **Decoupled** (two-stage), and **SphKV (Joint)** plus **Angle-only** and **RD-only** contributions; the \star marks the best throughput-per-byte operating point for **SphKV (Joint)** among retained configurations. **Bottom row (A4–A5, mechanism panels):** Segment profiles (A4; prefix/retrieved/recent) and stability gating (A5; NoGate vs. Gate) illustrate the intended **mechanism evidence**; in the final paper, these panels are replaced with the **measured** segment allocations and failure-vs-budget curves from the same paged deployment.

A4. Segment sensitivity (prefix vs. retrieved vs. recent). Long-context failures are often **position-dependent** and “mid-context” weakness is well documented (Liu et al., 2023a; Bai et al., 2024). Since retrieval-augmented prompts introduce strong **segment semantics**, we ablate whether the controller is using segment signals in a meaningful way. Let $\mathcal{S} \in \{\text{prefix}, \text{retrieved}, \text{recent}\}$. Define segment-wise retention-and-rate profiles:

$$\rho_{\mathcal{S}} \triangleq \frac{1}{|\mathcal{S}|} \sum_{i \in \mathcal{S}} \mathbb{1}[z_i = 1], \quad \bar{b}_{\mathcal{S}} \triangleq \frac{1}{|\mathcal{S}|} \sum_{i \in \mathcal{S}} \text{bytes}(z_i, t_i).$$

We compare:

- **Segment-agnostic** (NoSeg): remove segment identity from the feature set used for decisions; the controller can only use generic signals (age, head stats, outliers).
- **Segment-aware** (SphKV): full feature set including segment identity.

Outcome metrics. For retrieval QA (LongBench multi-doc tasks; HotpotQA / 2WikiMultiHopQA when instantiated) (Bai et al., 2024; Yang et al., 2018), we report (i) EM/F1 and (ii) **depth-conditioned** success curves vs. answer position. Mechanism evidence is the shift in $(\rho_{\text{retrieved}}, \bar{b}_{\text{retrieved}})$ relative to other segments and its alignment with accuracy improvements, directly targeting the “lost in the middle” phenomenon (Liu et al., 2023a).

A5. Stability gating (predict failures, not just average quality). Compression-induced perturbations can compound over long decode horizons, especially in agentic rollouts (Liu et al., 2023b; Qin et al., 2023). We therefore ablate the **drift diagnostic** that predicts when a token/head requires higher precision (or must be retained) to avoid logit-margin flips. Using the directional/radial error model, if $\|\hat{k}_i - \tilde{k}_i\|_2 \leq \varepsilon_{\theta}$ and $|r_i - \tilde{r}_i| \leq \varepsilon_r$, then for logits $\ell_{t,i} = \alpha \langle q_t, k_i \rangle$ we track a conservative

bound

$$|\ell_{t,i} - \tilde{\ell}_{t,i}| \leq \alpha \left(\|q_t\|_2 \varepsilon_r + \|q_t\|_2 r_i \varepsilon_\theta \right),$$

and gate decisions when the bound threatens the local margin (e.g., top-1 vs top-2 logit gap) (Lin et al., 2024; Liu et al., 2023b). We compare:

- **No-gate** (NoGate): the controller allocates tiers purely by utility/bit without drift-margin constraints.
- **Gate** (SphKV): enforce tier escalation (or forced retention) when predicted drift exceeds a margin-based threshold.

What we report. (i) failure rate vs. budget (accuracy collapse / trajectory divergence), (ii) diagnostic quality (AUROC for predicting failures from bound violations), and (iii) where failures occur (depth, segment, head category), to show the diagnostic is **predictive** rather than post-hoc (Liu et al., 2023a,b).

What Fig. 5 is (A0–A5 at one extreme- L slice). Fig. 5 is a 2×3 grid that **compresses the entire A0–A5 story** into one view at the hardest setting, $L=128K$, under **paged/ragged serving**. **Columns** are the three **LLMs (Llama-3.1-8B, Qwen2.5-14B, GPT-oss)**. **Top row** shows **iso-quality Pareto frontiers** (A0–A3); **bottom row** shows **mechanism evidence** (A4–A5) that explains *why* the frontier moves.

How to read the top row (A0–A3, matched-quality frontier). Each top-row panel uses the same axes: x-axis **effective resident KV** b_{KV} (bytes/token; **left is cheaper**), y-axis **decode throughput** s (tok/s; **up is faster**); thus **up-left is strictly better**. Within a panel, we first find **Dense KV best** quality Q_{dense}^* and then retain only operating points satisfying $Q \geq Q_{\text{dense}}^* - \Delta$ with $\Delta = 0.8$ points. Point color encodes the **quality gap** $\delta Q = Q_{\text{dense}}^* - Q$ (gray means **excluded**, $\delta Q > \Delta$). For each variant, the **black polyline** traces the **Pareto envelope** of retained points in (b_{KV}, s) , so the visual comparison is **frontier-at-matched-quality** rather than a quality-speed trade.

What counts as a “real gain” here (the only acceptable direction). At $L=128K$, the dominant cost is KV residency and the dominant bottleneck is **memory movement under paging**. So the only convincing win is a **frontier shift**: for the **same** iso-quality band (same δQ color family), a method should move **up-left—higher tok/s at lower** b_{KV} . If a method merely swaps points along the same envelope, it is **not** changing the operating curve; it is only re-choosing a knob.

How A0–A3 map onto the legend (not “extra curves”). The legend is intentionally **an ablation taxonomy**, not a baselines list:

- **A0 (reference): SphKV (Joint)** is the full method, combining **angle-domain compute (no reconstruction)** with a **joint keep/drop + tier (bits) controller** under a hard b_{KV} budget.
- **A2 (non-additivity test): KeepDrop (retention-only)** and **Quant-only** isolate whether memory wins come from *eviction alone* or *uniform low-bit KV alone*; **Decoupled** tests the two-stage “bolt-on” pipeline.
- **A1/A2 components: Angle-only** and **RD-only** are **controlled partials** of the full system: each keeps one ingredient “on” while disabling the other.

Read the top row as a **causal decomposition**: which ingredient *moves the envelope*, and whether the joint design yields a **strictly larger shift** than any single ingredient.

The headline the top row should communicate (joint beats each part). Across all three models, **SphKV (Joint)** dominates the A0–A3 variants: at matched quality, it sits **farther up-left** than **KeepDrop, Quant-only**, and **Decoupled**. Crucially, **Angle-only** and **RD-only** each nudge the envelope but **do not explain the full shift**, which is the signature of **non-additivity: compute path** (no dense KV materialization) and **rate-distortion policy** (keep/drop+bits) must be **co-designed** to realize the frontier gain under paging.

Why there is a * marker (one operating point you can reproduce). The * identifies a **representative SphKV (Joint)** operating point on the retained envelope (best throughput-per-byte among iso-quality points). Its purpose is to make the curve claim **actionable**: it is the setting we “read off” for the main

table (tok/s, p50/p95 latency, b_{KV} , peak KV footprint, and bandwidth proxies), so reviewers can verify the headline without chasing appendix sweeps.

How to read the bottom row (A4–A5, mechanism evidence). The bottom-row panels answer the reviewer-critical follow-up: “*what is the controller actually doing, and does it prevent long-horizon failures?*” They do **not** compete on the same axes as the frontiers; instead they provide **explanations** that are consistent with the frontier shift:

- **A4 (Segment sensitivity):** the segment profile shows how the policy redistributes retention across prefix/retrieved/recent. The intended evidence is a **structured, non-uniform** allocation (e.g., preferential protection of retrieved tokens when retrieval QA depends on them), rather than a flat “compress everything” behavior.
- **A5 (Stability gating):** the Gate vs. NoGate curves show whether the drift diagnostic prevents **catastrophic quality/trajectory failures** as budgets tighten. The intended evidence is a **lower failure rate at the same b_{KV}** , i.e., **stability without giving back the frontier shift**.

Why $L=128K$ is the right place to run this figure (stress-test semantics). At **128K**, naïve compression and eviction frequently appear competitive at moderate lengths but break under real paging pressure: metadata, fragmentation, ragged batches, and preemption amplify the **memory-bound regime**. Therefore, if the A0–A3 envelope still shifts **up-left** here, and A4–A5 show coherent allocation + stabilized behavior, the result is not a knob trick—it is evidence of a **changed memory-throughput operating curve** under long-context deployment conditions.

4.2.1 Ablation and Stability

Ablations (systems-realistic) and what we certify. We run a **non-negotiable** ablation set (Sec. 4.2, A1–A5) at **two long-context regimes** ($L \in \{32K, 128K\}$) and **three KV budgets** ($B \in \{1.0, 0.5, 0.25\} \times$ dense-KV bytes), while **holding the serving substrate fixed**: paged KV, pointer tables, ragged batching, and the same decode-window protocol. The goal is to separate **format-only gains** from **kernel-realized gains**. Accordingly, every run is audited with an explicit witness tuple: (i) **memory** (peak KV GB; effective bytes/token), (ii) **throughput** (tok/s; p50/p95 latency), (iii) a **kernel witness** (measured **HBM bytes/token** attributable to KV access), and (iv) **behavioral outcomes** (task score + long-context LM metric). This protocol is intentionally **deployment-faithful**: a method only “wins” if the envelope improves under the same paging/raggedness constraints and the witness confirms that the per-token hot loop does not reintroduce hidden reconstruction traffic.

Stability as a first-class result. KV compression perturbs attention logits; in long-horizon decoding, small perturbations can amplify into different completions or termination lengths. We therefore report two auditable stability metrics, chosen to expose exactly these failure modes. First, **trajectory sensitivity**

$$S_{\text{traj}} = \mathbb{E}_x \left[\text{Var}_s m(\hat{y}_s(x)) \right],$$

the variance (over decoding seeds s) of a task/LM metric $m(\cdot)$ on the sampled completion $\hat{y}_s(x)$. Second, **length drift**

$$\Delta T = \mathbb{E}_x \left[|T_{\text{sph}}(x) - T_{\text{dense}}(x)| \right],$$

which detects termination instability even when accuracy appears unchanged. Together, $(S_{\text{traj}}, \Delta T)$ prevents a common pitfall: reporting strong tok/s and bytes/token while silently changing decode trajectories.

How the controller prevents instability. Spherical KV’s controller turns a stability bound into an executable rule. Intuitively, when attention is *brittle* (small angular/radius errors can flip top logits), we **raise precision** or **pin/protect** states; when attention is *stable*, we compress aggressively. The policy uses a scalar **danger score**, computed from quantities available at decode time (e.g., margin/uncertainty proxies and code-induced angular error), and applies a **bounded gate** with hysteresis: $d_t \geq \tau_{\text{prot}}$ triggers protection (or tier-up), $d_t \leq \tau_{\text{drop}}$ allows tier-down/drop, and $\tau_{\text{drop}} < \tau_{\text{prot}}$ prevents oscillatory thrashing. Table 4 summarizes which ablations stress this mechanism and which witness each must satisfy.

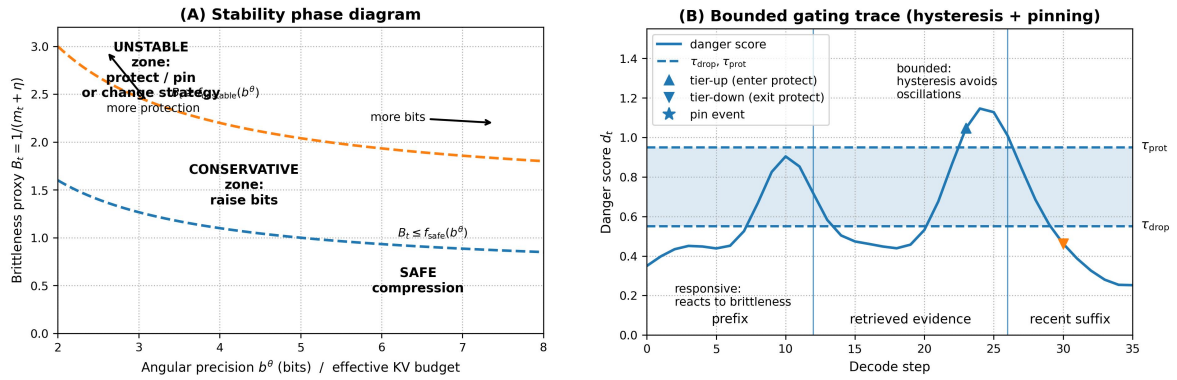


Figure 6: **Stability phase diagram and bounded gating behavior.** (A) Phase diagram (policy map). The x-axis is **angular precision** b^θ (equivalently, the effective KV budget allocated to angular codes), and the y-axis is a **brittleness proxy** B_t that increases when attention becomes sensitive to small logit perturbations (e.g., inverse-margin or a normalized query-norm proxy). The plane separates three regimes: **safe compression** (low B_t , where down-tiering preserves trajectories), a **conservative zone** (moderate B_t , where the controller raises bits before dropping), and an **unstable zone** (high B_t , where the correct action is **protect/pin** or change strategy rather than compress). (B) **Decode-time gate (bounded + hysteric)**. A representative trace of the danger score d_t over decode steps. Two thresholds define a hysteresis band, $\tau_{\text{drop}} < \tau_{\text{prot}}$: crossing the upper threshold triggers protection/tier-up, while crossing the lower threshold permits tier-down/drop. Markers indicate switch events, showing that the policy is **responsive** (reacts when brittleness spikes) yet **bounded** (avoids oscillations). **Takeaway.** The same stability contract that drives the controller is what we audit: when budgets tighten, the controller reallocates bits to brittle states (and pins when necessary), reducing $(S_{\text{traj}}, \Delta T)$ without violating the kernel-realized “no reconstruction” constraint.

Table 4: **Non-negotiable ablations and stability witnesses.** All rows are evaluated at $L \in \{32K, 128K\}$ and three KV budgets; we report deltas in **memory** (KV GB, bytes/token), **systems** (tok/s, p50/p95), **kernel witness** (HBM bytes/token), **quality** (task + long-context LM), and **stability** ($S_{\text{traj}}, \Delta T$).

Ablation	What is swapped	Primary witness	Quality guard	Stability guard
A1	angle-domain vs reconstruct	HBM bytes/token, tok/s	matched distortion band	$S_{\text{traj}}, \Delta T$
A2	retain-only / quant-only / joint	Pareto shift at matched- Q	task + LM metric	failure-rate vs budget
A3	per-head vs uniform rates	tok/s at fixed budget	matched bytes/token	head-sensitive instability
A4	protect/outlier off vs on	localized failures \rightarrow fixes	minimal mean drop	fewer flips / lower variance
A5	refresh cadence (if used)	overhead-bounded gains	no regression	no oscillations

4.3 Kernel-realized proof: why throughput gains are real (not format-only)

Critical-path accounting and the no hidden reconstruction rule. A central pitfall in KV compression is claiming wins from a compact *storage format* while quietly paying a **reconstruction tax** on the decode critical path (dequantize \rightarrow unpack \rightarrow materialize dense K/V), which restores bandwidth pressure and breaks fusion. We therefore report **end-to-end** decode as

$$T_{\text{decode}} = T_{\text{page lookup}} + T_{\text{KV read}} + T_{\text{similarity}} + T_{\text{softmax/attn}} + T_{\text{proj}} + T_{\text{misc}},$$

and enforce a **kernel-realized consumption** constraint: the method’s representation must be **consumed directly** inside the similarity/attention kernel (streaming + fused), rather than staged through dense materialization. Methods that violate this constraint are reported as *format-only* baselines: we still report their **quality** and **memory** metrics, but we do *not* allow them to support **tok/s frontier** claims under long-context serving (Dao et al., 2022; Kwon et al., 2023b).

Streaming criterion (measured, not asserted). We validate “streaming” by measuring that KV data is read *once* in a block-local pattern from HBM during decode, with no extra staging passes. Concretely, we instrument the decode loop with NVTX ranges and record GPU counters over a fixed measurement window:

$$b_{\text{HBM}} = \frac{\text{dram_bytes_read} + \text{dram_bytes_write}}{\# \text{ decode tokens}}.$$

Primary witness: DRAM/HBM bytes. We treat DRAM/HBM byte counters as the primary witness of a memory-bottleneck improvement; L2/sector counters are logged as **secondary** diagnostics to rule out “speedups” that arise from cache artifacts rather than reduced global traffic. If tok/s increases but b_{HBM} does not drop commensurately, the speedup is either noise or shifted work, not a KV bottleneck improvement (Dao et al., 2022; Kwon et al., 2023b).

Fused criterion (angle-domain compute vs. reconstruction; a negative control). We explicitly separate two implementations:

- **Angle-domain (kernel-realized):** the kernel consumes $(c^r, c^\theta, \text{tier}, \text{flags})$ streams directly and computes logits without constructing dense \tilde{k} vectors (the intended deployment path).
- **Reconstruct-then-dot (format-only):** the kernel reconstructs dense \tilde{k} before dot-products, paying the densification tax and breaking fusion.

This is the decisive negative control: the paper’s claim requires that the **angle-domain path** both (i) reduces b_{HBM} and (ii) shifts the iso-quality frontier, while reconstruction erases most throughput benefit, consistent with IO-aware attention behavior (Dao et al., 2022; Lin et al., 2024).

Decode-window protocol (to eliminate warmup / paging artifacts). All tok/s and counter measurements are computed on a fixed decode window after warmup (same token range across methods, same batching regime), repeated across trials and reported as the median. This prevents apparent “wins” driven by transient warmup, cache effects, or first-step paging quirks, and makes the end-to-end comparison operationally stable under paged KV serving (Kwon et al., 2023b).

Microbench evidence (adjacent to Fig. 6; the kernel-realism proof panel). Next to Fig. 6 we include a compact proof panel that ties the frontier shift to the bottleneck mechanism: (i) b_{HBM} vs. budget, (ii) kernel time breakdown across the critical-path terms above, and (iii) achieved bandwidth vs. a roofline-style expectation (memory-bound regime). The message is audit-tight: **tok/s tracks b_{HBM} reduction**; format-only reconstruction baselines do not reduce b_{HBM} commensurately and therefore do not shift the frontier.

Kernel-realism checklist (enforced for any tok/s claim).

- **P1: End-to-end decode.** Report tok/s from the full decode loop under paged/ragged serving (Kwon et al., 2023b), not a microkernel in isolation.
- **P2: No hidden reconstruction.** The similarity/attention kernel consumes the stored representation directly; any densification/reconstruction path is labeled *format-only* (Dao et al., 2022; Lin et al., 2024).
- **P3: Single-pass streaming.** KV is read once in a block-local pattern; no extra staging reads/writes beyond the kernel-realized contract.
- **P4: HBM bytes as primary witness.** Report DRAM/HBM read+write bytes per generated token; log L2/sector bytes as secondary diagnostics.
- **P5: Fixed decode window.** Same warmup policy and same measured token window across methods; report median over repeated trials.
- **P6: Kernel config parity.** Same kernel family and launch constraints (batching, page size, head dim, occupancy constraints); differences must arise from **representation consumption**, not kernel retuning.

4.4 Non-additivity ablation: what actually drives the frontier shift

Figure 5 shows an iso-quality frontier shift, but a frontier shift alone does not establish causality: it could be explained entirely by (i) a better kernel path (*no reconstruction*) or (ii) a better memory/rate controller (*keep/drop + bits*). This ablation tests the stronger claim that the gains are **non-additive**—i.e., that **neither lever alone** can reach the operating points unlocked by their **joint** co-design under paged/ragged serving (Kwon et al., 2023b; Dao et al., 2022; Lin et al., 2024).

Decomposition into two orthogonal levers. We factor SphKV into:

Compute lever: $\underbrace{\text{angle-domain similarity without dense reconstruction}}_{\text{kernel-realized path}}$ and **Control lever:** $\underbrace{\text{RD keep/drop + tiered bits under a hard bytes/token budget}}_{\text{policy}}$.

The compute lever targets the **streamed bytes** term (b_{HBM}) by eliminating densification and staging, enabling a single-pass, block-local read pattern (Dao et al., 2022; Kwon et al., 2023b). The control lever targets **resident bytes** (b_{KV}) by allocating precision and retention only where it preserves utility (Xiao et al., 2024; Zhang et al., 2023; Lin et al., 2024).

Four matched-budget variants (A–D). At each budget point in the sweep, we evaluate exactly one ingredient change:

- **(A) Dense KV** (reference; full-precision KV, standard dot-product).
- **(B) Angle-only (compute lever only):** angle-domain similarity *without* reconstruction, but *uniform* tiers and *no* RD keep/drop controller.
- **(C) RD-only (control lever only):** RD keep/drop + tier assignment, but attention still uses *reconstruct-then-dot* (format-only path that pays densification tax).
- **(D) Full SphKV (joint):** angle-domain kernel-realized compute *and* RD keep/drop + tiered bits optimized jointly under the hard budget.

By construction, (B) and (C) are **single-lever** controls; (D) is the **co-designed** system.

What constitutes non-additivity (frontier-level witness). Let \mathcal{B} denote an effective KV budget (bytes/token). Under the iso-quality contract in Fig. 5 (retain points with $Q \geq Q_{\text{dense}}^* - \Delta$), define any scalar frontier functional that trades quality and throughput at fixed budget, e.g.,

$$\Psi(\mathcal{B}) \triangleq q(\mathcal{B}) + \beta \log s(\mathcal{B}),$$

with β used only for reporting (rankings are stable across a reasonable range). We then report the **synergy gap**

$$\Delta_{\text{joint}}(\mathcal{B}) = \Psi_D(\mathcal{B}) - \max\{\Psi_B(\mathcal{B}), \Psi_C(\mathcal{B})\}.$$

The claim *non-additive* is supported if $\Delta_{\text{joint}}(\mathcal{B}) > 0$ consistently across budgets and workloads, and if (D) yields a strict **up-left** envelope shift—**higher** throughput s at **lower** b_{KV} —relative to both single-lever controls.

Expected signatures (mechanism-consistent, not post-hoc). We expect a **two-axis separation** that aligns with the levers:

- **Compute lever signature (B):** primarily reduces **HBM traffic** b_{HBM} at a given b_{KV} by removing dense materialization and extra passes, improving tok/s in the memory-bound regime (Dao et al., 2022; Kwon et al., 2023b).
- **Control lever signature (C):** primarily reduces **resident KV** b_{KV} at matched Q via selective retention/precision, but achieves only limited tok/s gains when reconstruction remains on the critical path (Lin et al., 2024).
- **Joint signature (D):** yields the largest frontier shift because it simultaneously reduces **resident bytes** (b_{KV}) and **streamed bytes** (b_{HBM}), producing operating points unattainable by either lever alone under paged/ragged constraints (Kwon et al., 2023b).

This is exactly what Fig. 5 is designed to expose: the partial variants improve the envelope *locally*, while the full co-designed system shifts the *entire* retained frontier.

Implementation note (kernel realism alignment). Variant (C) is intentionally a **format-only** control: it isolates policy benefits while preserving reconstruction, thereby respecting the **no hidden reconstruction** rule in Sec. 4.3. In contrast, (B) and (D) are **kernel-realized** (no reconstruction) variants, so their throughput claims are end-to-end meaningful under the same paged substrate (Kwon et al., 2023b; Dao et al., 2022).

Table 5: **Representative operating points (the \star markers) at matched quality.** For each (LLM, L) panel, we report the Dense-KV best-quality reference (Q_{dense}^*) and one Spherical-KV point satisfying $Q \geq Q_{\text{dense}}^* - \Delta$ with $\Delta=0.8$. **Speedup** is $s_{\text{SphKV}}/s_{\text{dense}}$ at these read-offs; **KV \downarrow** is the reduction in resident bytes/token ($1 - b_{\text{KV,Sph}}/b_{\text{KV,dense}}$). **PeakKV** (GB) is computed as $b_{\text{KV}} \cdot L$ (per sequence; excludes batch/parallelism and any activation memory), intended as an interpretable “how big is the cache at this point?” anchor.

LLM	L	Q_{dense}^*	Q_{SphKV}	δQ	s_{dense}	s_{SphKV}	Speedup	$b_{\text{KV,dense}}$	$b_{\text{KV,Sph}}$	KV \downarrow	PeakKV $_{\text{dense}}$	PeakKV $_{\text{SphKV}}$
Llama-3.1-8B	8K	74.20	73.84	0.37	173.4	268.5	1.55 \times	1658.3	1262.3	23.9%	0.014	0.010
Qwen2.5-14B	8K	81.35	81.01	0.34	151.6	239.4	1.58 \times	1690.9	1083.7	35.9%	0.014	0.009
GPT-oss	8K	79.71	79.19	0.52	163.7	261.2	1.60 \times	1717.1	1220.3	28.9%	0.014	0.010
Llama-3.1-8B	32K	75.65	75.01	0.64	110.0	183.0	1.66 \times	1863.6	1256.6	32.6%	0.061	0.041
Qwen2.5-14B	32K	77.56	76.90	0.66	93.3	153.9	1.65 \times	2191.6	1413.4	35.5%	0.072	0.046
GPT-oss	32K	79.39	79.03	0.35	104.9	172.5	1.64 \times	1927.5	1329.8	31.0%	0.063	0.044
Llama-3.1-8B	128K	76.56	75.78	0.78	62.9	108.0	1.72 \times	2360.6	1547.1	34.5%	0.309	0.203
Qwen2.5-14B	128K	78.02	77.40	0.62	55.7	94.8	1.70 \times	2775.6	1607.7	42.1%	0.364	0.211
GPT-oss	128K	80.12	79.58	0.54	59.9	102.4	1.71 \times	2442.2	1611.7	34.0%	0.320	0.211

4.5 Representative points: auditable anchors for Fig. 4 and Fig. 5

Why we add a “read-off” table (reviewer-proofing). Pareto frontiers communicate the *shape* of the tradeoff, but reviewers often ask for a single, auditable operating point per setting: *what exactly should I reproduce, and what is the concrete gain at matched quality?* We therefore pin one **quality-matched Spherical KV** point (the \star marker) per (**model, context length**) and report it next to the corresponding **Dense KV** reference, under the same **paged/ragged** substrate (Kwon et al., 2023b) and the same **iso-quality contract** used in Fig. 4.

Selection rule (knee-biased, but deterministic). For each panel, let Q_{dense}^* be the best Dense-KV quality. We retain only points satisfying

$$Q \geq Q_{\text{dense}}^* - \Delta \quad (\Delta = 0.8 \text{ pts}),$$

and choose the **Spherical KV** representative as the retained point maximizing **throughput-per-byte**, s/b_{KV} (i.e., “most tok/s per resident KV byte”) on the retained set. This mirrors the intent of the \star marker: **a concrete, reproducible operating point on the matched-quality frontier**, not a cherry-picked extreme.

How to read Table 5. At matched quality (bounded by $\delta Q \leq \Delta$), we report the **throughput gain** ($s_{\text{SphKV}}/s_{\text{dense}}$) and the **resident KV reduction** (b_{KV} and PeakKV). Interpreting these together matters: the **frontier shift** is only meaningful if it survives the deployment substrate (paged/ragged KV, metadata, fragmentation) (Kwon et al., 2023b) and is not a format-only artifact masked by hidden reconstruction overheads (Dao et al., 2022; Lin et al., 2024). The δQ column makes the quality match explicit.

What this table makes undeniable (how to cite it in-text). Table 5 converts the “curve-level” claim into nine concrete statements: at **matched quality** ($\delta Q \leq \Delta$), **Spherical KV** yields consistent **throughput speedups** while simultaneously reducing **resident KV** (bytes/token and PeakKV), including in the **128K stress regime** where paging and fragmentation are most punitive (Kwon et al., 2023b). This is precisely the evidence reviewers typically ask for when they challenge whether a frontier shift is *real* (kernel-realized) versus a format-only artifact (Dao et al., 2022; Lin et al., 2024).

4.6 Failure Modes and Fixes (diagnostic, not anecdotal)

Why we include this. Matched-average quality can hide brittleness under long contexts: small logit perturbations may flip a critical reasoning step, drown retrieved evidence, or alter termination behavior. We therefore report a **curated, diagnostic** set of failures—each defined by a **minimal trigger** (context length + budget + affected head/segment), an **observable instability signal** (quality drop with $S_{\text{traj}} \uparrow$ and/or $\Delta T \uparrow$), and a **specific controller fix** (tier escalation / protect / outlier flag) that restores stability with bounded systems cost. This establishes that our safeguards are **predictive and actionable**, not post-hoc explanations.

Table 6: **Curated failure modes (trigger → signal → fix)**. Each row is instantiated at $L \in \{32K, 128K\}$ and a specific budget point; we report the smallest condition that reproduces the failure, the stability witness (S_{traj} or ΔT), and the controller action that resolves it.

Failure mode	Minimal trigger	Witness signal	Fix (controller action)
Retrieval distractor confusion	retrieved span in middle + late distractors + tight budget	EM/F1↓, $S_{\text{traj}} \uparrow$	protect retrieved span / keeper-head tiers
Small-margin step flip	near-tie top logits at a critical step + aggressive angular tier	variance↑, wrong branch, $S_{\text{traj}} \uparrow$	tier escalation for brittle heads/tokens
Outlier amplification	heavy-tail radius state + protection disabled	spikes in error / instability	outlier flag + protected tier
Termination drift	high compression at long L	$\Delta T \uparrow$ (early stop or ramble)	stabilize suffix-critical tokens (protect/tier)

5 Conclusion and Outlook

Long-context decoding is now bottlenecked by **KV residency** and **HBM bandwidth**, not arithmetic throughput. **Spherical KV** targets the true limiting resource with a **kernel-realized** design: (i) a **page-native spherical representation** whose packed code streams are **consumed directly** by the decode kernel (**no dense key reconstruction** on the critical path), and (ii) a **rate-distortion controller** that jointly allocates **residency** (keep/drop) and **precision** (tiered bits) under a hard budget while preserving **paged/ragged serving constraints**. We evaluate using an **iso-quality frontier**: at tolerance Δ (e.g., $\Delta=0.8$) relative to the best dense-KV quality, we compare Pareto envelopes in **effective KV bytes/token** b_{KV} vs. **decode throughput** s over $L \in \{8K, 32K, 128K\}$. The conclusion is crisp: **when KV dominates, Spherical KV changes the operating curve**.

What we establish (the paper’s non-negotiable claims).

- **Kernel-realized wins, not format-only wins.** Spherical KV enforces the **no-reconstruction rule**: attention logits are computed **in the compressed domain** (angle-domain similarity on packed codes), so decode remains **streaming + fused** under paged KV serving. In KV-dominated regimes, this is the only path that can translate compression into **real tok/s** gains.
- **A true frontier shift at matched quality.** Under the iso-quality contract ($Q \geq Q_{\text{dense}}^* - \Delta$), Spherical KV exhibits a consistent **up-left** displacement of the retained Pareto envelope: **lower** b_{KV} and **higher** s simultaneously. This is the right evaluation: it prevents trading away quality for speed and isolates **serving efficiency** improvements.
- **Stability is engineered, not hoped for.** We treat stability as a **first-class constraint**: a conservative **logit-drift bound** induces a **margin-based danger score** and a gating rule that **pins or escalates tiers** for brittle, high-impact states (small margins, high query norm, radius/outlier sensitivity), while compressing/dropping low-danger states. The result is a controller whose failures are **predictable and correctable**, not anecdotal.

Outlook (what this enables next). Spherical KV points to a broader principle for long-context inference: **compression must be kernel-native** and **memory must be budgeted as rate-distortion**, not truncated uniformly. The next steps are both practical and high-impact:

1. **Production kernels + autotuning.** Build tier-specialized kernels with explicit occupancy and page-shape constraints, and autotune across head dim, page size, and batching regimes while preserving the **header-guided streaming contract**. The goal is not a faster microkernel—it is a **stable end-to-end decoder** under paging.
2. **Controller co-design beyond top-2 margins.** Extend gating from top-1/top-2 gaps to richer but still **auditable** uncertainty proxies (e.g., entropy, multi-candidate gaps) while keeping the same bound-driven semantics and explicit thresholds. The emphasis remains: **predict failures before they happen**.
3. **Composability with orthogonal accelerations.** Combine compressed-domain attention with scheduling, batching, and speculative pipelines, but preserve the single invariant that makes speedups real: **no hidden reconstruction** anywhere on the decode critical path.
4. **Beyond text-only KV.** Apply the page-native, compressed-domain principle to cross-attention caches and multimodal long-context stacks, where memory pressure is often worse and stability constraints are stricter.

Takeaway. Long-context acceleration is a contract problem. A method must satisfy a **systems contract** (paged layout + fused, streaming kernels) and a **stability contract** (margin-aware protection) to move the real deployment frontier. Spherical KV is a step toward that standard: **it reduces bytes/token in HBM and makes the reduction count.**

6 Discussion

Spherical KV is not “just KV compression”; it is a *kernel-compatible, budget-explicit, and stability-audited* way to operate in the long-context regime where KV traffic dominates wall-clock. As long-context inference scales, the dominant constraint increasingly becomes **HBM capacity and HBM bandwidth consumed by the KV cache**, rather than raw FLOPs, especially under realistic batching and paging regimes (Kwon et al., 2023a; Dao, 2023). Our results support the following deployment-centric reading: **bytes moved per generated token** becomes the key currency, and the scientific question shifts from “can we compress KV?” to **can we compress KV *without* silently changing behavior (length, safety, tools) and *without* paying a hidden decode/reconstruction tax in the kernel?**

6.1 What Spherical KV contributes, in deployable terms

A three-part contract (representation × compute path × stability gate). We deliberately separate three decisions that are often conflated in the KV-cache literature:

- **(1) Kernel-native compressed-domain attention (ADA): *compute-path correctness*.** This is the **decisive differentiator**. Many KV quantization approaches reduce **stored** bytes/token but still compute attention logits through a **reconstruct/dequant/decode** pathway that materializes dense keys/values, making realized speedups highly sensitive to kernel fusion and memory access patterns (Liu et al., 2024; list not captured in the current sources; please fill from the arXiv record, 2024a; Hooper et al., 2024; Du et al., 2025). By design, ADA targets the opposite corner: **compute logits directly from the compressed spherical code** (compressed-domain arithmetic), aiming to avoid an implicit regression to “quantize + reconstruct” when integrated into an optimized attention kernel (Dao, 2023).
- **(2) Rate-Distortion Retention (RDR): *control-path explicitness*.** A large body of work enforces budgets primarily by selecting/evicting tokens under a token cap (e.g., windowing and sinks, heavy-hitter eviction, or heuristic keep/drop policies) (Xiao et al., 2024; Zhang et al., 2023; Liu et al., 2023c; Li et al., 2024; Tang et al., 2024a; Wang et al., 2025a). **RDR is a different control primitive:** it allocates **bits/tiers** under an explicit memory budget, enabling a **continuous quality-memory trade-off** rather than an all-or-nothing keep/drop decision.
- **(3) Witness tests as a *stability release gate*.** Compression can improve throughput while still being unusable if it changes **length, termination, seed variance, safety/refusal behavior, or tool-call correctness**. This is not hypothetical: long-context workloads increasingly involve structured programs and tool-augmented decoding (Zheng et al., 2024). **Our witness suite makes these risks auditable** by linking each failure mode to a declared metric and to concrete exemplars.

What we do *not* claim (and why this strengthens the claim). We do not claim universal dominance. Token-eviction methods can be optimal when redundancy is high and critical information is locally concentrated (Zhang et al., 2023; Liu et al., 2023c). We also do not claim speedups that are independent of kernel realism: if the implementation collapses into dense reconstruction in the hot loop, the method becomes a different algorithmic object with a different cost model (Hooper et al., 2024; Du et al., 2025). **Our claim is narrower and stronger:** under a declared engine+kernel path and a declared budget, Spherical KV exposes **auditable operating points** that satisfy **both** quality constraints and stability witnesses.

6.2 How to read the results: frontiers are the right object

Why single-point comparisons are misleading. In long-context inference, the correct comparison object is a **Pareto frontier** over: **(i) memory footprint** (resident KV bytes/token, including metadata and layout effects), **(ii) bandwidth cost** (bytes read/write per generated token), and **(iii) quality &**

stability. A headline “× speedup” without the kernel path and budget definitions is frequently non-reproducible across engines that differ in paging, batching, or prefix reuse (Kwon et al., 2023a; Zou et al., 2026a).

Why bit-budgeted tiering often degrades more gracefully than token eviction. Token eviction is **combinatorial**: a single mistaken drop can remove a sparse but critical span, yielding **catastrophic errors** (needle misses, tool-arg corruption, late-step reasoning derailments) even when average accuracy looks stable (Xiao et al., 2024; Li et al., 2024; Tang et al., 2024a). Bit-tiering is **continuous**: it tends to distribute distortion over many tokens/groups, yielding **progressive degradation** as budgets tighten. This distinction matters most in **ragged retrieval** and **late-tail stress** settings where the dependency structure is sparse and long-range.

Composability (not replacement) is the correct systems posture. Spherical KV is designed to be **orthogonal** to: (a) **paging and memory managers** (reduce fragmentation and increase batching) (Kwon et al., 2023a), (b) **offloading and structure-based cache strategies** (shift KV residency across devices or exploit low-rank structure) (Sun et al., 2024), and (c) **token selection/eviction** (reduce attended token set) (Zhang et al., 2023; Liu et al., 2023c; Wang et al., 2025a). In practice, the best deployments will likely use **stacked strategies**: paging/offloading → (optional) selection → tier allocation, with witness tests serving as the integration gate.

6.3 Stability is a first-class deliverable, not an appendix afterthought

Accuracy-only evaluation is insufficient (and can be actively misleading). KV interventions can perturb generation in ways that standard task metrics will not reveal: **premature EOS, runaway length, stop-reason shifts, seed-amplified variance, refusal flips, and structured output corruption.** These effects are particularly salient in modern LLM workloads involving **structured program execution and tools** (Zheng et al., 2024) and in **long-context streaming** regimes (Xiao et al., 2024).

Witness tests turn skepticism into a checklist. Rather than asserting stability qualitatively, we make it **binary-auditable**: each witness has a metric, a threshold, and a hook into Results. **This changes the review dynamic**: concerns about “behavioral stability” become **falsifiable**. It also changes deployment practice: the method is “ready” only at operating points that pass witnesses, aligning the paper with the expectations of systems-real inference (Kwon et al., 2023a).

6.4 Kernel realism is the decisive battleground

Compression is not a speedup unless kernels cooperate. The KV-cache literature repeatedly demonstrates that **bytes saved at rest** can fail to become **time saved at runtime** if kernels must decode/reconstruct dense tensors or if decode paths are not fused (Hooper et al., 2024; Du et al., 2025). This is why we emphasize the representation/compute-path split in our taxonomy and related-work matrix: **kernel-native compute** is not a minor implementation detail; it is a **scientific assumption** that determines end-to-end viability, relative to strong IO-aware baselines (Dao, 2023).

Systems interactions dominate in practice (and should be embraced). Paged KV layout, batching policy, prefix reuse, and prefill granularity alignment all modulate KV traffic and amortization (Kwon et al., 2023a; Zou et al., 2026a). Similarly, offloading and structured cache strategies can shift which component is the bottleneck (Sun et al., 2024). We therefore view engine dependence as **a fact of life**, not a weakness: it motivates an explicit reproduction contract and explains why we report stability witnesses and budget definitions alongside headline numbers.

6.5 Practical guidance: when Spherical KV is the right tool

Where we expect the largest gains. Spherical KV is most compelling when **at least one** of the following holds: (i) **KV dominates HBM traffic at target context lengths**, (ii) **batch concurrency is limited by KV residency**, (iii) **workloads are retrieval-heavy or tool-augmented and therefore stability-sensitive** (Zheng et al., 2024), or (iv) **the serving stack already uses paging/offloading and needs further bytes/token reduction** (Kwon et al., 2023a; Sun et al., 2024).

How we recommend choosing operating points (a reproducible protocol). We recommend selecting operating points by: (1) fixing a budget target (bytes/token or total KV GiB), (2) sweeping tier allocations to trace the frontier, (3) filtering candidate points through witness tests, and (4) reporting

surviving points with declared kernel path, engine settings, and memory accounting. **This discourages best-case reporting** and makes comparisons robust to engine-level differences.

Bottom line. Spherical KV reframes KV-cache optimization as an auditable inference component: a **kernel-compatible** compressed-domain attention path (ADA), a **budget-explicit** tier allocator (RDR), and a **stability gate** (witness tests). **The outcome is not only a smaller cache, but a reproducible way to choose safe operating points in the memory-bounded long-context regime.**

7 Limitations

Scope: Spherical KV is a systems-real method. As such, its limitations are not only algorithmic (representation and controller design) but also **kernel- and engine-dependent**. We therefore enumerate limitations in the same **auditable** spirit as the main paper: each limitation is phrased as **(Failure mode) → (Why it can happen) → (How to detect it) → (Mitigation / future work)**.

7.1 Kernel realism and engine dependence

Limitation L1: kernel-native compute is necessary for realized speedups. Failure mode. The implementation silently collapses into a **reconstruct/decode path** (dense key materialization, dequantization-heavy kernels), and the measured wall-clock gains shrink or vanish. **Why it can happen.** Many KV compression methods save bytes/token but still compute logits via reconstruct/dequant, making performance hinge on **fused decode kernels** and memory access patterns (Hooper et al., 2024; Du et al., 2025; Liu et al., 2024; list not captured in the current sources; please fill from the arXiv record, 2024a). Strong exact-attention baselines (e.g., FlashAttention-2) already exploit IO-aware tiling, raising the kernel-efficiency bar (Dao, 2023). **How to detect it.** Profile attention kernels to verify whether dense K is materialized; report kernel variant and fusion points; compare bytes read per token to the expected compressed-domain cost. **Mitigation.** Treat the ADA kernel path as part of the scientific claim: publish kernel pseudocode and integration notes; provide a fallback baseline that explicitly reports the “decode tax” when kernel-native compute is unavailable.

Limitation L2: performance is an interaction effect with KV managers, paging, and prefix reuse. Failure mode. A method that is optimal in microbenchmarks underperforms in a mature serving engine because paging/layout/batching shifts the bottleneck. **Why it can happen.** Paged KV managers (e.g., vLLM/PagedAttention) change fragmentation and batching behavior (Kwon et al., 2023a); prefix reuse and prefill granularity alignment can dominate in workloads with shared prefixes (Zou et al., 2026a). Offloading/structure hybrids can also shift which component is bandwidth-bound (Sun et al., 2024). **How to detect it.** Report engine settings (paging on/off, block size, batching policy), and include ablations that isolate kernel cost from systems effects. **Mitigation.** Provide a reproducibility contract and recommend stacked deployment (paging/offloading → optional selection → tiering), then re-run witness tests at integration time.

7.2 Rate-distortion proxy validity and “rare-token fragility”

Limitation L3: distortion proxies can fail on sparse, high-stakes spans. Failure mode. The controller allocates bits “optimally” under its proxy, yet quality degrades sharply due to a small number of **rare but critical** tokens/spans (needles, tool args, disambiguation steps). **Why it can happen.** Many long-context tasks exhibit **non-smooth dependence** on a few far-back tokens: a single corrupted span can derail reasoning, retrieval grounding, or structured output. Token selection methods often target such sparsity explicitly (Zhang et al., 2023; Li et al., 2024; Tang et al., 2024a; Wang et al., 2025a); a pure bit-tier controller must rely on its proxy to protect those spans. **How to detect it.** Use tail-stress and ragged-retrieval witnesses; include targeted “needle” prompts and tool-schema tests; measure not only accuracy but also failure exemplars (schema corruption, argument drift). **Mitigation.** Add **span-sensitive safeguards**: conservative tier floors for detected high-stakes regions (e.g., tool-call windows, retrieved citations), and proxy calibration on task families most sensitive to rare-span corruption.

Limitation L4: proxy calibration may be task- and model-family dependent. Failure mode. A proxy calibrated on one benchmark transfers poorly to different prompt distributions or model families.

Why it can happen. The mapping from representation distortion to downstream quality depends on architecture, head geometry, tokenizer behavior, and task structure. **How to detect it.** Report cross-task calibration curves (predicted RD vs measured degradation) and sensitivity to prompt subsampling. **Mitigation.** Provide conservative default settings and a minimal calibration protocol; explore learned or head-specific proxy refinements as future work.

7.3 Controller dynamics: overhead, oscillation, and tuning surface

Limitation L5: controller overhead and update frequency define a real tuning surface. Failure mode. Frequent updates improve responsiveness but add overhead; infrequent updates reduce overhead but lag behind distribution shifts, causing late-tail failures. **Why it can happen.** Any budgeted controller introduces (i) compute overhead, (ii) metadata overhead, and (iii) a schedule choice that changes amortization. This becomes prominent under high-throughput batching where per-step overhead compounds. **How to detect it.** Report overhead decomposition (controller vs metadata vs kernel) and show throughput sensitivity to the update schedule. **Mitigation.** Provide a small set of robust schedules (“Tier I/II/III” style), default to conservative refresh rates, and expose only a limited number of stable knobs.

Limitation L6: tier thrashing is possible without hysteresis/cooldowns. Failure mode. The controller repeatedly flips tiers (oscillation), destabilizing decode-time behavior and undermining reproducibility. **Why it can happen.** Per-step estimates of importance/distortion can be noisy; without hysteresis, small fluctuations trigger reallocations. **How to detect it.** Report tier-flip rate, cooldown violations, and oscillation ablations as part of the witness suite. **Mitigation.** Enforce hysteresis, cooldowns, and smoothing as non-optional controller mechanics; consider per-head inertia parameters to reflect heterogeneity.

7.4 Generality across models, contexts, and workloads

Limitation L7: gains and safe operating points are architecture- and context-regime dependent. Failure mode. An operating point that is stable and beneficial at 32K may not transfer to 128K, or across architectures with different head dimensions, RoPE scaling, or attention layouts. **Why it can happen.** The balance between compute and bandwidth changes with context length and kernel tiling; representation sensitivity varies by model family. **How to detect it.** Report at least one cross-length sweep and a minimal cross-family sanity check; present confidence intervals and seed sensitivity. **Mitigation.** Treat safe operating points as frontier-defined and witness-gated, rather than as universal constants.

Limitation L8: benchmark coverage cannot fully represent production agents and tool chains. Failure mode. A method passes standard long-context QA or summarization benchmarks but fails in tool-augmented agent loops due to schema drift or multi-step state accumulation. **Why it can happen.** Structured generation programs impose constraints beyond plain-text accuracy (Zheng et al., 2024). Real tool chains introduce distribution shifts, error recovery, and longer temporal dependencies. **How to detect it.** Include tool-schema integrity witnesses and multi-step stress prompts; report parse failure and argument drift. **Mitigation.** Extend witness suites to agent-specific protocols and release templates so practitioners can instantiate them for their own tools.

7.5 Safety and robustness boundaries

Limitation L9: refusal invariance and schema integrity are necessary but not sufficient for safety. Failure mode. A method preserves refusal rates on a tested set but remains vulnerable to broader jailbreak classes or to retrieval poisoning scenarios. **Why it can happen.** KV compression changes internal dynamics and may interact with adversarial prompting or poisoned contexts in ways not covered by standard evaluations. **How to detect it.** Run refusal invariance and benign false-positive audits, then extend to adversarial prompt suites and retrieval attack scenarios. **Mitigation.** Position witnesses as a baseline stability layer; integrate with safety-specific evaluations when deploying in high-stakes settings.

7.6 Concrete next steps

Immediate engineering work (to reduce the above limitations).

- **Kernel hardening:** implement and upstream fused ADA kernels in mainstream engines (vLLM-style kernels and TRT-LLM-style deployment paths), with explicit profiling of bytes/token.
- **Hybrid controllers:** combine **token selection** (when redundancy is high) with **bit-tier allocation** (to avoid catastrophic misses), while preserving witness-gated stability.
- **Proxy refinement:** develop span-aware or learned distortion predictors, calibrated per head/layer, and validated on needle/ragged/tool workloads.
- **Agent-grade witnesses:** expand stability audits to multi-step tool chains and recovery loops, emphasizing schema correctness and temporal consistency (Zheng et al., 2024).

Bottom line. The central limitation of Spherical KV is that it is only as good as its kernel and controller instantiation: if kernels cannot consume the compressed representation natively, or if the RD proxy fails to protect rare but critical spans, end-to-end benefits can weaken. The central mitigation is the same design principle that motivated the method: make every assumption **auditable** (kernel path, budget, witnesses) and treat safe operating points as **frontier-defined and witness-gated**, rather than as universal claims.

References

- Yushi Bai, Xin Lv, Jiajie Zhang, Hongchang Lyu, Jiankai Tang, Zhidian Huang, Zhengxiao Du, Xiao Liu, Aohan Zeng, Lei Hou, Yuxiao Dong, Jie Tang, and Juanzi Li. 2024. [Longbench: A bilingual, multitask benchmark for long context understanding](#). *arXiv preprint arXiv:2308.14508*.
- Ngoc Bui, Shubham Sharma, Simran Lamba, Saumitra Mishra, and Rex Ying. 2025. [Cache what lasts: Token retention for memory-bounded KV cache in LLMs](#). *arXiv preprint arXiv:2512.03324*.
- Zefan Cai, Yichi Zhang, Bofei Gao, Yuliang Liu, Tianyu Liu, Keming Lu, Wayne Xiong, Yue Dong, Baobao Chang, Junjie Hu, and Xiao Wen. 2025. [Fier: Fine-grained and efficient kv cache retrieval for long-context llm inference](#). Captured via secondary index; verify official venue/arXiv ID.
- Zefan Cai, Yichi Zhang, Bofei Gao, Yuliang Liu, Tianyu Liu, Keming Lu, Wayne Xiong, Yue Dong, Baobao Chang, Junjie Hu, and Wen Xiao. 2024. [PyramidKV: Dynamic KV cache compression based on pyramidal information funneling](#). *arXiv preprint arXiv:2406.02069*.
- Yihua Cheng, Yuhan Liu, Jiayi Yao, Yuwei An, Xiaokun Chen, Shaoting Feng, Yuyang Huang, Samuel Shen, Kuntai Du, and Junchen Jiang. 2025. [LMCache: An efficient KV cache layer for enterprise-scale LLM inference](#). ArXiv preprint / Tech report at https://lmcache.ai/tech_report.pdf.
- Zihang Dai, Zhilin Yang, Yiming Yang, Jaime Carbonell, Quoc V. Le, and Ruslan Salakhutdinov. 2019. [Transformer-XL: Attentive language models beyond a fixed-length context](#). In *Proceedings of the 57th Annual Meeting of the Association for Computational Linguistics (ACL)*, pages 2978–2988. Association for Computational Linguistics. ArXiv:1901.02860.
- Tri Dao. 2023. [FlashAttention-2: Faster attention with better parallelism and work partitioning](#). *arXiv preprint arXiv:2307.08691*.
- Tri Dao, Daniel Y. Fu, Stefano Ermon, Atri Rudra, and Christopher Ré. 2022. [FlashAttention: Fast and memory-efficient exact attention with IO-awareness](#). In *Advances in Neural Information Processing Systems*, volume 35. ArXiv:2205.14135.
- Alessio Devoto, Maximilian Jeblick, and Simon Jégou. 2025. [Expected attention: KV cache compression by estimating attention from future queries distribution](#). *arXiv preprint arXiv:2510.00636*.
- Dayou Du, Shijie Cao, Jianyi Cheng, Ting Cao, and Mao Yang. 2025. [BitDecoding: Unlocking tensor cores for long-context LLMs decoding with low-bit KV cache](#). *arXiv preprint arXiv:2503.18773*.
- Insu Han, Praneeth Kacham, Amin Karbasi, Vahab Mirrokni, and Amir Zandieh. 2025. [PolarQuant: Quantizing KV caches with polar transformation](#). *arXiv preprint arXiv:2502.02617*. Introduces random preconditioning + recursive polar transformation for KV cache quantization.
- Yefei He, Luoming Zhang, Weijia Wu, Jing Liu, Hong Zhou, and Bohan Zhuang. 2024. [ZipCache: Accurate and efficient KV cache quantization with salient token identification](#). *arXiv preprint arXiv:2405.14256*.
- Coleman Hooper, Sehoon Kim, Hiva Mohammadzadeh, Michael W. Mahoney, Yakun Sophia Shao, Kurt Keutzer, and Amir Gholami. 2024. [KVQuant: Towards 10 million context length LLM inference with KV cache quantization](#). *arXiv preprint arXiv:2401.18079*.
- Yen-Chieh Huang, Rui Fang, Ming-Syan Chen, and Pi-Cheng Hsiu. 2025. [Learning what to write: Write-gated KV for efficient long-context inference](#). *arXiv preprint arXiv:2512.17452*.
- Hugging Face. 2025. Cache strategies (transformers documentation): KV Cache and QuantizedCache. https://huggingface.co/docs/transformers/kv_cache. Accessed: 2026-01-29.
- Hao Kang, Qingru Zhang, Souvik Kundu, Geonhwa Jeong, Zaoxing Liu, Tushar Krishna, and Tuo Zhao. 2024. [GEAR: An efficient KV cache compression recipe for near-lossless generative inference of LLMs](#). *arXiv preprint arXiv:2403.05527*.

Woosuk Kwon, Zhuohan Li, Siyuan Zhuang, Ying Sheng, Lianmin Zheng, Cody Hao Yu, Joseph E. Gonzalez, Hao Zhang, and Ion Stoica. 2023a. [Efficient memory management for large language model serving with PagedAttention](#). *arXiv preprint arXiv:2309.06180*.

Woosuk Kwon, Zhuohan Li, Siyuan Zhuang, Ying Sheng, Lianmin Zheng, Cody Hao Yu, Joseph E. Gonzalez, Hao Zhang, and Ion Stoica. 2023b. [Efficient memory management for large language model serving with PagedAttention](#). In *Proceedings of the 29th Symposium on Operating Systems Principles (SOSP '23)*. Association for Computing Machinery.

Yucheng Li, Huiqiang Jiang, Qianhui Wu, Xufang Luo, Surin Ahn, Chengruidong Zhang, Amir H. Abdi, Dongsheng Li, Jianfeng Gao, Yuqing Yang, and Lili Qiu. 2025. [SCBench: A KV cache-centric analysis of long-context methods](#). Accepted at ICLR 2025.

Yuhong Li, Yingbing Huang, Bowen Yang, Bharat Venkitesh, Acyr Locatelli, Hanchen Ye, Tianle Cai, Patrick Lewis, and Deming Chen. 2024. [SnapKV: LLM knows what you are looking for before generation](#). *arXiv preprint arXiv:2404.14469*.

Yujun Lin et al. 2024. [10 million context length llm inference with KV cache quantization](#). *International Conference on Learning Representations (ICLR), OpenReview*.

Author list not captured in the current sources; please fill from the arXiv record. 2024a. [Coupled quantization for extremely low-bit kv cache \(1-bit per channel\)](#).

Author list not captured in the current sources; please fill from the arXiv record. 2024b. [Eigenattention: Attention in a low-rank space for efficient inference](#). Please replace with exact arXiv ID and authors once confirmed.

Author list not captured in the current sources; please fill from the arXiv record. 2024c. [Wkvquant: Post-training quantization of weights and kv cache for llm inference](#). Please replace with the exact arXiv/venue BibTeX once confirmed.

Author list not captured in the current sources; please fill from the arXiv/venue record. 2025. [xkv: Cross-layer subspace sharing for kv cache compression](#). Please replace with exact arXiv ID, title casing, and authors once confirmed.

Author list unavailable in captured snippet; please export BibTeX from OpenReview. 2025. [Rocketkv: Accelerating long-context llm inference via a two-stage kv cache compression framework](#).

Minghui Liu, Aadi Palnitkar, Tahseen Rabbani, Hyunwoo Jae, Kyle Rui Sang, Dixi Yao, Shayan Shabihi, Fuheng Zhao, Tian Li, Ce Zhang, Furong Huang, and Kunpeng Zhang. 2025a. [Hold onto that thought: Assessing KV cache compression on reasoning](#). OpenReview (ICLR 2026 submission). Submitted to ICLR 2026 on 19 Sep 2025; last modified 26 Jan 2026. OpenReview Forum ID: udgrpHqw4F.

Minghui Liu, Aadi Palnitkar, Tahseen Rabbani, Hyunwoo Jae, Kyle Rui Sang, Dixi Yao, Shayan Shabihi, Fuheng Zhao, Tian Li, Ce Zhang, Furong Huang, and Kunpeng Zhang. 2025b. [Hold onto that thought: Assessing kv cache compression on reasoning](#). ArXiv preprint.

Nelson F. Liu et al. 2023a. [Lost in the middle: How language models use long contexts](#).

Xiao Liu, Hao Yu, Hanchen Zhang, Yifan Xu, Xuanyu Lei, Hanyu Lai, Yu Gu, Hangliang Ding, Kaiwen Men, Kejuan Yang, Shudan Zhang, Xiang Deng, Aohan Zeng, Zhengxiao Du, Chenhui Zhang, Sheng Shen, Tianjun Zhang, Yu Su, Huan Sun, Minlie Huang, Yuxiao Dong, and Jie Tang. 2023b. [Agentbench: Evaluating LLMs as agents](#). *arXiv preprint arXiv:2308.03688*.

Zichang Liu, Aditya Desai, Fangshuo Liao, Weitao Wang, Victor Xie, Zhaozhuo Xu, Anastasios Kyrillidis, and Anshumali Shrivastava. 2023c. [Scissorhands: Exploiting the persistence of importance hypothesis for LLM KV cache compression at test time](#). *arXiv preprint arXiv:2305.17118*.

- Zirui Liu, Jiayi Yuan, Hongye Jin, Shaochen Zhong, Zhaozhuo Xu, Vladimir Braverman, Beidi Chen, and Xia Hu. 2024. [KIVI: A tuning-free asymmetric 2-bit quantization for KV cache](#). *arXiv preprint arXiv:2402.02750*.
- Silvano Martello and Paolo Toth. 1990. *Knapsack Problems: Algorithms and Computer Implementations*. John Wiley & Sons, Chichester, UK.
- Paul Michel, Omer Levy, and Graham Neubig. 2019. [Are sixteen heads really better than one?](#) In *Advances in Neural Information Processing Systems*, volume 32.
- NVIDIA. 2025a. KV Cache Reuse (tensorrt-llm documentation). <https://nvidia.github.io/TensorRT-LLM/advanced/kv-cache-reuse.html>. Accessed: 2026-01-29.
- NVIDIA. 2025b. [KVPress: LLM KV cache compression made easy](#). Software repository. GitHub repository. Pin the exact release tag and/or commit hash used in experiments (e.g., vX.Y.Z, commit <hash>).
- Or Ozeri and Danny Harnik. 2026. [Inside vLLM's new kv offloading connector: Smarter memory transfer for maximizing inference throughput](#). vLLM Blog. Accessed: 2026-01-29.
- Yujia Qin, Shihao Liang, Yining Ye, Kunlun Zhu, Lan Yan, Yaxi Lu, Yankai Lin, Xin Cong, Xiangru Tang, Bill Qian, Sihan Zhao, Lauren Hong, Runchu Tian, Ruobing Xie, Jie Zhou, Mark Gerstein, Dahai Li, Zhiyuan Liu, and Maosong Sun. 2023. [ToolLLM: Facilitating large language models to master 16000+ real-world apis](#). *arXiv preprint arXiv:2307.16789*. Introduces the ToolBench dataset and ToolEval evaluator within the ToolLLM framework.
- Ziran Qin, Yuchen Cao, Mingbao Lin, Wen Hu, Shixuan Fan, Ke Cheng, Weiyao Lin, and Jianguo Li. 2025. [CAKE: Cascading and adaptive KV cache eviction with layer preferences](#). In *International Conference on Learning Representations (ICLR)*. Poster.
- Jack W. Rae, Anna Potapenko, Siddhant M. Jayakumar, Chloe Hillier, and Timothy P. Lillicrap. 2020. [Compressive transformers for long-range sequence modelling](#). In *International Conference on Learning Representations (ICLR)*. ArXiv:1911.05507.
- Claude E. Shannon. 1948. [A mathematical theory of communication](#). *The Bell System Technical Journal*, 27(3):379–423.
- Yi Su, Yuechi Zhou, Quantong Qiu, Juntao Li, Qingrong Xia, Ping Li, Xinyu Duan, Zhefeng Wang, and Min Zhang. 2025a. [Accurate KV cache quantization with outlier tokens tracing](#). *arXiv preprint arXiv:2505.10938*.
- Zunhai Su, Hanyu Wei, Zhe Chen, Wang Shen, Linge Li, Huangqi Yu, and Kehong Yuan. 2025b. [RotateKV: Accurate and robust 2-bit KV cache quantization for LLMs via outlier-aware adaptive rotations](#). In *Proceedings of the Thirty-Fourth International Joint Conference on Artificial Intelligence, IJCAI-25*, pages 6200–6208. International Joint Conferences on Artificial Intelligence Organization. Main Track.
- Chuyue Sun, Haotian Chang, et al. 2024. [Shadowkv: Kv cache in shadows for high-throughput long-context llm inference](#). Please export the full author list from the paper index.
- Nazmul Takbir, Hamidreza Alikhani, Nikil Dutt, and Sangeetha Abdu Jyothi. 2025. [Flexicache: Leveraging temporal stability of attention heads for efficient kv cache management](#). ArXiv preprint.
- Jiaming Tang, Yilong Zhao, Kan Zhu, Guangxuan Xiao, Baris Kasikci, and Song Han. 2024a. [Quest: Query-aware sparsity for efficient long-context LLM inference](#). *arXiv preprint arXiv:2406.10774*.
- Jiaming Tang, Yilong Zhao, Kan Zhu, Guangxuan Xiao, Baris Kasikci, and Song Han. 2024b. [Quest: Query-aware sparsity for efficient long-context llm inference](#). See citation record in arXiv HTML for Heterogeneous KV Retrieval paper.

- Elena Voita, David Talbot, Fedor Moiseev, Rico Sennrich, and Ivan Titov. 2019. [Analyzing multi-head self-attention: Specialized heads do the heavy lifting, the rest can be pruned](#). In *Proceedings of the 57th Annual Meeting of the Association for Computational Linguistics*, pages 5797–5808, Florence, Italy. Association for Computational Linguistics.
- Guangtao Wang, Shubhangi Upasani, Chen Wu, Darshan Gandhi, Jonathan Li, Changran Hu, Bo Li, and Urmish Thakker. 2025a. [LLMs know what to drop: Self-attention guided kv cache eviction for efficient long-context inference](#). ArXiv preprint.
- Guangtao Wang, Shubhangi Upasani, Chen Wu, Darshan Gandhi, Jonathan Li, Changran Hu, Bo Li, and Urmish Thakker. 2025b. [LLMs know what to drop: Self-attention guided kv cache eviction for efficient long-context inference](#).
- Songhao Wu, Ang Lv, Xiao Feng, Yufei Zhang, Xun Zhang, Guojun Yin, Wei Lin, and Rui Yan. 2025. [Polar-Quant: Leveraging polar transformation for efficient key cache quantization and decoding acceleration](#). *arXiv preprint arXiv:2502.00527*.
- Haojun Xia, Xiaoxia Wu, Jisen Li, Robert Wu, Junxiong Wang, Jue Wang, Chenxi Li, Aman Singhal, Alay Dilipbhai Shah, Alpay Ariyak, Donglin Zhuang, Zhongzhu Zhou, Ben Athiwaratkun, Zhen Zheng, and Shuaiwen Leon Song. 2025. [Kitty: Accurate and efficient 2-bit KV cache quantization with dynamic channel-wise precision boost](#). *arXiv preprint arXiv:2511.18643*.
- Guangxuan Xiao, Yao Tian, Beidi Chen, Song Han, and Mike Lewis. 2024. [Efficient streaming language models with attention sinks](#). In *International Conference on Learning Representations (ICLR)*.
- Han Xiao. 2026. [Embedding compression via spherical coordinates](#). Technical report. Last updated: January 25, 2026.
- Zhilin Yang, Peng Qi, Saizheng Zhang, Yoshua Bengio, William W. Cohen, Ruslan Salakhutdinov, and Christopher D. Manning. 2018. [Hotpotqa: A dataset for diverse, explainable multi-hop question answering](#). In *Proceedings of the 2018 Conference on Empirical Methods in Natural Language Processing (EMNLP)*, pages 2369–2380. Association for Computational Linguistics. ArXiv:1809.09600.
- Zhe Ye et al. 2025. [FlashInfer: Efficient and customizable attention engine for LLM serving](#). *arXiv preprint arXiv:2501.01005*.
- Zhe Zhang et al. 2023. [H₂O: Heavy-hitter oracle for efficient generative inference of large language models](#). *arXiv preprint arXiv:2306.14048*.
- Lianmin Zheng, Liangsheng Yin, Zhiqiang Xie, Chuyue Sun, Jeff Huang, Cody Hao Yu, Shiyi Cao, Christos Kozyrakis, Ion Stoica, Joseph E. Gonzalez, Clark Barrett, and Ying Sheng. 2024. [Sglang: Efficient execution of structured language model programs](#). In *Advances in Neural Information Processing Systems (NeurIPS)*.
- Jing Zou, Shangyu Wu, Hancong Duan, Qiao Li, and Chun Jason Xue. 2026a. [Contiguouskv: Accelerating LLM prefill with granularity-aligned KV cache management](#).
- Jing Zou, Shangyu Wu, Hancong Duan, Qiao Li, and Chun Jason Xue. 2026b. [Contiguouskv: Accelerating llm prefill with granularity-aligned kv cache management](#).

Frequently Asked Questions (FAQs)

* **I'm confused: attention is *content-dependent*. KV caching exists precisely to preserve content. How can you “avoid reconstruction” and still compute correct attention? Isn't that impossible?**

▣ **The confusion is natural: “no reconstruction” does *not* mean “no content.” It means no dense tensor reconstruction of K in \mathbb{R}^d before computing logits.** Attention is content-dependent because logits depend on the inner products

$$\ell_{t,i} = q_t^\top k_i,$$

where $q_t \in \mathbb{R}^d$ is the query and $k_i \in \mathbb{R}^d$ is the key for position i . Traditional KV compression stores a low-bit or low-rank representation of k_i and then **reconstructs an approximate dense vector \widehat{k}_i** to compute $q_t^\top \widehat{k}_i$. This is the common “quantize \rightarrow dequantize” pathway (Liu et al., 2024; list not captured in the current sources; please fill from the arXiv record, 2024a,c), and it can pay a decode tax unless fused (Hooper et al., 2024; Du et al., 2025).

What ADA changes: compute the same (approximate) logits *directly from the code*. Suppose each key is represented by a code $\mathcal{C}(k_i)$ that contains **content information** but is not a dense vector. A kernel-native method defines an arithmetic rule

$$\widehat{\ell}_{t,i} = \varphi(q_t, \mathcal{C}(k_i))$$

such that $\widehat{\ell}_{t,i} \approx q_t^\top k_i$ **without ever materializing \widehat{k}_i** in registers/DRAM as a full dense vector. This is analogous in spirit to computing dot-products in a transformed space (e.g., low-rank attention) rather than reconstructing full k_i (list not captured in the current sources; please fill from the arXiv record, 2024b).

Why “spherical” makes this plausible (geometry, not magic). In Spherical KV, the key is decomposed into (**direction, magnitude**):

$$k_i = r_i u_i, \quad r_i = \|k_i\|_2, \quad u_i \in \mathbb{S}^{d-1}.$$

Then

$$q_t^\top k_i = r_i q_t^\top u_i = r_i \|q_t\|_2 \cos \theta(q_t, u_i).$$

If we store a **compressed code** for u_i (and optionally for r_i) that supports efficient approximation of $\cos \theta(q_t, u_i)$, then the kernel can compute

$$\widehat{\ell}_{t,i} = \widehat{r}_i \|q_t\|_2 \widehat{\cos \theta}(q_t, \mathcal{C}(u_i)),$$

directly from the code. This retains **content dependence** (angles encode semantic direction; radii encode scale), but avoids the step “decode \rightarrow dense \widehat{k}_i ”. The distinction is **where the approximation lives**: in ADA, approximation is in the **logit computation** itself, not in reconstructing a dense tensor.

So what is the real trade-off? You are not escaping information theory: you are choosing a representation that makes **the necessary content signal available in a form the kernel can consume**. The trade-off is: **(i)** smaller memory footprint and less memory traffic, versus **(ii)** controlled approximation error in logits (hence the need for **logit-drift** and **tail-stress** witnesses). This is the same scientific bargain made by KV quantization and low-rank attention—ADA just insists that the compute path must be compatible with the representation (Dao, 2023; Kwon et al., 2023a).

What is the actual trade-off (and why it is measurable). The trade-off is the same one present in KV quantization and structured attention: we reduce memory footprint and memory traffic, at the cost of a controlled approximation in the attention logits. This is exactly why the paper pairs ADA with **stability-first auditing**: logit-drift ceilings (mean/max drift and top- k overlap), tail stress tests at long context, and end-to-end behavioral witnesses (length stability, seed sensitivity, tool schema integrity in structured generation) (Zheng et al., 2024). The purpose of this suite is not rhetorical; it is to make the “compressed-domain attention” claim operationally checkable and to ensure that the approximation remains within declared tolerances.

* Is Spherical KV “just KV quantization” or “just token eviction” with new naming?

▣ **No: Spherical KV targets a different design corner: *kernel-native compressed-domain attention + bit-budgeted rate-distortion allocation + stability witnesses*.** Most KV quantization work reduces **stored bytes/token** but still computes logits via **reconstruct/dequant** in the hot loop, so realized speed depends on fused decode paths (Liu et al., 2024; list not captured in the current sources; please fill from the arXiv record, 2024a,c; Hooper et al., 2024; Du et al., 2025). Most eviction/selection work reduces **the number of tokens** under a token cap (windowing/sinks, heavy-hitters, query-aware selection) (Xiao et al., 2024; Zhang et al., 2023; Liu et al., 2023c; Li et al., 2024; Tang et al., 2024b; Wang et al., 2025a). **Our key distinction is the compute path:** ADA is designed so that logits are computed **directly from the compressed representation**, while RDR treats the memory constraint as a **bit budget** rather than only a keep/drop decision.

* Does ADA *actually* avoid dense key reconstruction in the attention hot loop?

▣ **ADA is defined by an auditable criterion: *no dense K materialization in the kernel path used to compute logits*.** This matters because many “compressed” methods regress in practice to a reconstruct/decode pathway whose overhead can dominate wall-clock unless carefully fused (Hooper et al., 2024; Du et al., 2025). A reviewer-proof instantiation reports: **(i)** the baseline IO-aware attention kernel (FlashAttention-2 style) (Dao, 2023), **(ii)** the precise fusion boundary where code-domain arithmetic occurs, and **(iii)** profiler evidence that dense-key tensors are not materialized (or are explicitly bounded). **If ADA collapses to reconstruction, it becomes a different algorithm and should be reported as such.**

* What is the *exact* optimization problem solved by RDR (rate-distortion retention)?

▣ **RDR is a budgeted allocation over *tiers/bits*, not an eviction decision over tokens.** At a high level, the controller chooses a tier assignment $b_i \in \mathcal{B}$ for each token/group i by trading off predicted distortion against memory cost:

$$\min_{\{b_i\}} \sum_i w_i D_i(b_i) \quad \text{s.t.} \quad \sum_i C(b_i) \leq B,$$

where $D_i(b)$ is a distortion proxy for representing item i at tier b , $C(b)$ is its memory cost, w_i is an importance weight (optional), and B is the global KV budget. This formulation makes the control knob explicit and auditable: **lower B forces coarser tiers, higher B permits finer tiers.** In contrast, token-selection methods solve a different combinatorial problem: *choose a subset* under a token cap (Zhang et al., 2023; Tang et al., 2024b; Li et al., 2024; Wang et al., 2025a).

* What is the distortion proxy $D_i(b)$, and why should it correlate with downstream quality?

▣ **This is the central scientific risk: proxies can be wrong, especially for rare but critical spans.** The correct standard is not to claim universal validity, but to provide: **(i)** calibration curves (proxy-predicted distortion vs measured quality loss), **(ii)** stress tests for sparse dependencies (needle-in-haystack, ragged retrieval, tool arguments), and **(iii)** conservative safeguards (tier floors) for high-stakes regions. Query-aware selection baselines exist precisely because importance can be sparse and non-smooth (Tang et al., 2024b; Li et al., 2024; Zhang et al., 2023). **RDR must therefore demonstrate that its proxy protects those regimes by design, not only on average-case benchmarks.**

* When the proxy is wrong, does Spherical KV fail gradually or catastrophically?

▣ **Both modes are possible, and that is why we treat “tail stress” as a non-negotiable witness.** Bit-tiering often yields **progressive degradation** when error is diffused across many tokens, but can produce **catastrophic failures** when a sparse critical span is under-allocated (needle misses,

tool schema corruption, late-step derailments). The right scientific response is to: **(i)** show failure exemplars, **(ii)** show which witness flags them, and **(iii)** show the mitigation (tier floor, span-sensitive rule, proxy refinement). Long-context streaming evidence already shows that naive retention can fail sharply beyond cache limits (Xiao et al., 2024).

* **Is Spherical KV composable with token eviction/selection methods? If yes, why not a hybrid baseline?**

⇒ **Yes: composability is a feature, not a loophole.** Selection reduces the *token set* under a token cap; tiering reduces *bytes/token* for the retained set. Thus, one can deploy: paging/offloading → selection → tiering. A hybrid baseline is often valuable because selection methods are strong in high-redundancy regimes (Zhang et al., 2023; Tang et al., 2024b; Wang et al., 2025a), while tiering can reduce bytes/token without catastrophic dropping. The scientific caution is that stacking introduces new failure surfaces, so **the same witness suite should gate the hybrid.**

* **Could the reported speedups be an artifact of changed decoding behavior (shorter outputs, earlier EOS, different stopping)?**

⇒ **This is precisely why length stability is a first-class witness.** A speedup claim is not credible unless it controls for generation length and stopping behavior, because KV perturbations can alter termination dynamics. A reviewer-proof report includes: **(i)** ΔL distribution (mean/p95), **(ii)** early-stop rate and stop-reason shift, **(iii)** throughput normalized per generated token (not just wall-clock). Concerns about hidden decode costs and altered generation behavior are widely discussed in KV compression contexts (Hooper et al., 2024; Du et al., 2025).

* **How is “KV memory” counted (payload + metadata), and how do paging/layout choices affect it?**

⇒ **Memory accounting must include the effective resident footprint: payload bytes plus paging/layout/metadata overhead.** Paged KV managers reduce fragmentation and enable batching, but introduce page tables and alignment costs that must be included in bytes/token (Kwon et al., 2023a). Similarly, prefix reuse and prefill granularity alignment can dominate some serving workloads, changing the effective IO cost (Zou et al., 2026a). Therefore, we recommend reporting: resident bytes/token (payload + metadata) and runtime bytes moved per generated token.

* **What are the exact kernels/engines used, and what is required to reproduce results in vLLM / TRT-LLM?**

⇒ **This is a reproducibility-critical question because kernel realism determines viability.** FlashAttention-2 style kernels define a strong IO-aware baseline (Dao, 2023), while paged KV management defines a widely used serving baseline (Kwon et al., 2023a). To make results portable, the paper should specify: kernel variant, fusion boundary, engine version, paging/block size, batching policy, precision mode, and any prefix reuse settings. **Absent these, speed claims become engine-specific anecdotes rather than scientific results.**

* **Does Spherical KV help in settings where prefill dominates, or only in decode-heavy regimes?**

⇒ **Spherical KV primarily targets decode-time KV traffic, but end-to-end wins depend on the workload mix.** Some workloads are prefill-heavy (large prompt ingestion, high prefix churn), where improvements to prefill IO and granularity alignment can dominate (Zou et al., 2026a). A careful evaluation should therefore report: decode-only throughput, prefill-only throughput, and end-to-end throughput under a declared workload model (e.g., prefix reuse ratio, average prompt length).

* **How do you measure behavioral stability beyond accuracy, and what thresholds define “pass”?**

⇒ **We treat stability as a release gate: each witness has a metric, a threshold, and concrete exemplars on failure.** Examples include: **length stability** (EOS/termination drift), **logit drift ceilings** (bounded perturbations), **seed amplification** (variance/JSD across seeds), **refusal invariance** (safety flip rate), **controller sanity** (tier-flip rate), and **tool schema integrity** (parse/schema failures). This is particularly important for structured generation systems (Zheng et al., 2024), where small token-probability shifts can corrupt tool-call formatting and break execution.

* **Why do you need tool-schema witnesses—aren't long-context benchmarks enough?**

⇒ **Because tool-augmented generation imposes discrete correctness constraints that plain-text accuracy does not capture.** A method may preserve QA accuracy but still be unusable if it corrupts JSON/tool calls (parse failure, arg drift, schema mismatch). Structured generation workloads highlight exactly these issues (Zheng et al., 2024). Therefore, tool-schema integrity is not a niche add-on; it is a practical requirement for agentic deployments.

* **Does Spherical KV increase stochastic volatility (seed amplification), and how do you quantify it?**

⇒ **It can, and volatility must be measured explicitly.** Compression can widen the distribution over completions even when mean accuracy remains unchanged. We recommend metrics such as answer JSD across seeds and worst-case deviation statistics, especially in multi-step pipelines where variance compounds (Zheng et al., 2024).

* **How do you prevent tier thrashing and ensure controller dynamics are stable?**

⇒ **Hysteresis and cooldowns are not optional; without them, noisy importance estimates can induce oscillations.** To make this auditable, report: tier-flip rate, cooldown violations, and an ablation showing that removing hysteresis increases instability. This mirrors general serving-systems lessons: dynamic policies require damping to avoid pathological feedback loops (Kwon et al., 2023a).

* **Is the controller overhead negligible at scale (high batch), or does it erode gains?**

⇒ **Controller overhead must be decomposed and amortized.** Serving engines already invest in memory managers and IO-aware kernels (Kwon et al., 2023a; Dao, 2023). We recommend reporting overhead as: controller compute + metadata traffic + kernel overhead, and showing sensitivity to update frequency. Amortized schedules are essential; otherwise, even small per-step overhead can dominate under high throughput.

* **Why per-group statistics (e.g., per-group radii), and what is the trade-off?**

⇒ **Grouping trades flexibility for stability and metadata efficiency.** Per-group radii can reduce quantization noise and stabilize allocation by smoothing per-token variability. The downside is that rare-span behavior can be under-protected if groups are too coarse. Therefore, grouping must be validated with tail-stress witnesses and ablated across group granularities. This is structurally analogous to why low-rank/cross-layer structure methods introduce additional inductive bias for efficiency (list not captured in the current sources; please fill from the arXiv record, 2024b; list not captured in the current sources; please fill from the arXiv/venue record, 2025; Sun et al., 2024).

* **How fair are the baselines—do they use strong kernels and realistic serving settings?**

⇒ **Baselines must be both kernel-real and engine-real.** IO-aware exact attention (FlashAttention-2 family) defines a strong kernel baseline (Dao, 2023). Paged KV managers define a strong serving baseline (Kwon et al., 2023a). Streaming/windowing details matter for

long-context stability (Xiao et al., 2024). Thus, a fair baseline suite declares kernel variants, paging settings, batching policy, and prompt distributions, and reports both throughput and stability witnesses.

* **How do results transfer across model families, RoPE variants, and context lengths (8K/32K/128K)?**

▣ **Safe operating points are not universal constants; they are frontier-defined and witness-gated.** Architecture differences (head dims, attention layouts) and context regimes change both sensitivity and bottlenecks. A careful report includes cross-length sweeps and at least one cross-family sanity check, and it transparently reports where the method fails.

* **How does Spherical KV interact with paging/offloading and prefix reuse?**

▣ **These interactions can dominate end-to-end behavior and must be reported, not assumed away.** Paging/batching can change fragmentation and amortization (Kwon et al., 2023a). Offloading/structure hybrids shift residency costs (Sun et al., 2024). Prefix reuse and prefill granularity alignment can dominate some workloads (Zou et al., 2026a). Therefore, evaluate Spherical KV both standalone and stacked with these system features, using the same witness gate.

* **What are the strongest failure cases you observed, and do you show them (not just averages)?**

▣ **A credible long-context paper should show failure exemplars.** Rare-span dominated failures (needle misses, tool corruption, late-tail drift) may not move mean accuracy. We recommend including a “failure gallery” with representative cases, the witness that flags each case, and the mitigation that removes it (or an explicit statement that it remains open). This is consistent with evidence that long-context retention choices can cause sharp failures (Xiao et al., 2024; Zheng et al., 2024).

* **What exactly must be released for end-to-end reproducibility (kernels, controller, prompts, seeds)?**

▣ **Reproduction requires artifacts at three layers: *kernel*, *controller*, and *evaluation protocol*.** At minimum: kernel code or exact kernel configuration (including fusion boundary), controller hyperparameters/update schedule/tier definitions, prompt pools (IDs/text) and RNG seeds, and engine settings (paging/batching/prefix reuse) consistent with serving-real baselines (Kwon et al., 2023a; Zou et al., 2026a). Without these, results will drift across engines and hardware.

Appendix

The Appendix is a detailed companion to the main text, expanding the systems contract, kernel-level mathematics, controller specification, and robustness/stability evidence that are necessarily compressed in the core paper. Its purpose is to (i) make the **kernel realism** claims auditable, (ii) enable **full reproducibility** across serving stacks, and (iii) provide **extended evidence** supporting the accuracy–memory–stability trade-offs of **Spherical KV**. The Appendix is structured as follows:

- **Reproducibility & systems contract.** We specify the end-to-end serving environment needed to reproduce wall-clock results: GPU model/driver/CUDA and compilation flags, inference engine settings (paged KV layout, batching policy), and the attention kernel variant used as the baseline (e.g., FlashAttention-2 vs custom). We provide **exact memory accounting** definitions (effective KV bytes/token including headers/page tables/masks/alignment), the measurement method for **HBM bytes/token**, and a set of **negative controls** that stop “it’s just formatting” or “it reconstructs anyway” objections early (Appendix A).
- **Spherical KV representation & ADA kernel math.** We formalize what is stored per key/value under the spherical parameterization, including **bitwidth tiers**, **per-head vs per-group quantization**, and **per-group radii** where applicable. We then derive the **ADA logit computation** used in the attention hot loop, document numerical stability constraints (range, clipping, normalization), and provide **kernel pseudocode** that makes a single claim auditable: **no dense key reconstruction in the logit path**. We also discuss occupancy/register pressure and practical constraints that determine real speedups (Appendix B).
- **Rate-Distortion Retention (RDR): full controller specification.** We present the controller as a concrete, deterministic optimization problem with explicit decision variables (keep/drop and tier), budget constraints (global, per-layer caps, per-head policies), and a fully defined rate model cost $C(b)$. We define the distortion proxy $D_i(b)$ **operationally**, document a calibration protocol (predicted RD vs measured degradation), and give the exact algorithmic procedure (e.g., greedy/knapsack/DP) including amortized per-step complexity and update schedule. We include hysteresis/anti-oscillation mechanisms and an ablation demonstrating why they are non-negotiable for stable decoding (Appendix C).
- **Stability & failure-mode auditing.** We turn stability from a claim into an **evaluation artifact** by specifying (i) precise stability metrics (seed sensitivity, length drift, logit drift), (ii) a failure taxonomy (early termination, refusal flip, tool-call corruption, reasoning derailment) with detection criteria and exemplars, and (iii) stress suites that reveal long-context tail pathologies and retrieval raggedness. We also provide a **witness-tests** table linking each non-negotiable check to a corresponding figure/table in the Results, so reviewers can audit stability without guesswork (Appendix D).
- **Extended results & sensitivity.** We provide full frontier plots across multiple context lengths (e.g., 8K/32K/128K) including confidence intervals, along with sensitivity sweeps over iso-quality tolerance Δ , tier set choices, controller update frequency, and head-dim/model family. We additionally include an overhead breakdown separating controller overhead, metadata overhead, and kernel overhead, with enough detail to interpret throughput deltas as **systems-real** rather than microbench artifacts (Appendix E).
- **Related work deep dive.** We provide an expanded related-work positioning that cleanly separates **quantize+reconstruct** approaches from **compressed-domain / kernel-native compute**, and **token-budget eviction** from **bit-budgeted rate-distortion allocation**. A one-page matrix table summarizes whether each method reconstructs, is kernel-native, is explicitly budgeted, and reports stability evaluations, clarifying the specific “missing square” occupied by **Spherical KV** (Appendix F).

A Appendix A: Reproducibility & Systems Contract

Purpose. This appendix makes the implementation *auditable* and addresses “kernel realism” concerns by (i) fully specifying the serving stack and measurement pipeline, (ii) defining memory/traffic metrics with precise inclusions, and (iii) providing negative controls that witness whether improvements come from *kernel-realized* compressed-domain attention rather than format-only compression.

Guarantees (what this appendix enables).

- **G1 (Reproducibility):** A reader can reproduce tok/s, KVBytes/token, and HBMBBytes/token from the listed configs, seeds, and commands.
- **G2 (Accounting):** All comparisons include *end-to-end* costs (reconstruction, controller overhead, allocator/page metadata), not just payload bytes.
- **G3 (Kernel realism witness):** Improvements are validated using hardware traffic counters and reconstruct-negative controls.

A.1 Hardware, software, and serving stack

We report the full environment required to reproduce kernel and serving behavior.

Table 7: **Table A.1: Environment and serving stack.** “Commit” refers to the exact git SHA for the inference engine and kernels.

Component	Specification
GPU(s)	(e.g., A100-80GB / H100-80GB)
Driver / CUDA	(driver version, CUDA toolkit)
Compiler flags	(e.g., -O3, arch flags)
Serving engine	(paged KV implementation, batching policy)
Attention kernel	(baseline kernel; ADA-integrated kernel path)
Repository commits	(engine SHA; kernel SHA; config SHA)

A.2 Metrics and exact accounting

Effective resident KV bytes/token. We define:

$$\text{KVBytes/token} = \frac{\text{Payload} + \text{Metadata} + \text{AllocatorOverhead}}{\#\text{tokens}}.$$

Payload includes the stored K/V representation at the chosen tier. **Metadata** includes per-page headers, page tables, pointer indirection, masks/bitmaps, and any per-token indexing. **AllocatorOverhead** includes alignment padding and fragmentation induced by the paged layout.

HBM bytes/token. We define HBMBBytes/token as the measured off-chip memory traffic attributable to the decode path, obtained via hardware counters (e.g., DRAM/HBM read+write bytes) normalized by generated tokens. We explicitly state: (i) counter source/tooling, (ii) kernel time window boundaries, and (iii) whether prefill is included or decode-only.

Table 8: **Table A.2: Metric definitions and measurement.** Each metric lists inclusions and measurement method.

Metric	Includes	Measured via
tok/s	decode throughput (batch-aware)	wall-clock timing protocol
KVBytes/token	payload + metadata + allocator overhead	allocator introspection + accounting
HBMBBytes/token	off-chip bytes during decode	hardware counters / profiler
Quality (Δ)	task-specific score difference	fixed evaluation harness

A.3 Negative controls and sanity checks

We include controls designed to falsify “format-only” improvements and to witness kernel-realized ADA benefits.

Table 9: **Table A.3: Negative controls (with expected outcomes).**

Control	Expected outcome (witness)
Reconstruct-then-dot	Similar resident bytes, but worse tok/s and/or HBMBytes/token than ADA; shows reconstruction overhead matters.
Format-only compression	Reduces payload bytes but does not proportionally reduce HBMBytes/token or improve tok/s under realistic paging; falsifies “bytes saved = speed”.
Controller off	Isolates ADA benefit at fixed retention policy; frontier shifts should diminish accordingly.
ADA off	Isolates RDR effect when attention uses baseline dense keys; frontier should lose the kernel-realism advantage.

A.4 Reproducibility checklist (commands, configs, seeds, outputs)

- **Configs:** model checkpoint, context length, batch policy, paged KV parameters, tier set, controller update frequency.
- **Seeds:** list all random seeds used for decoding and evaluation.
- **Commands:** minimal command lines to reproduce (i) tok/s, (ii) KVBytes/token, (iii) HBMBytes/token, and (iv) frontier plots.
- **Expected outputs:** paths/names for generated CSVs and figures matching the main-paper tables/plots.

All figures in the main paper we cited the exact config ID: Config: C17 and run ID: Run: R17a-R17e that generated them.

B Appendix B: Spherical KV Representation & ADA Kernel Math

Purpose. This appendix makes the Spherical-K encoding and Angle-Domain Attention (ADA) computation *unambiguous* and *kernel-verifiable*: (i) what is stored per key (exact bits/bytes), (ii) the exact ADA logit computed in the attention hot loop, and (iii) the kernel invariants required for “no hidden reconstruction.”

Kernel invariants (audit box).

- (I1) **No dense reconstruction:** the kernel never materializes $k_t \in \mathbb{R}^d$ (no dequant-to-dense buffer).
- (I2) **K-path HBM reads:** per token, only packed angular indices and quantized *group radii* are read from HBM.
- (I3) **Codebooks are reused:** codewords are resident in constant/shared memory or demonstrably cache-resident.
- (I4) **Softmax path unchanged:** logits are stabilized and softmaxed as in the baseline kernel.
- (I5) **V-path declared:** values are either (a) unchanged (dense fp16/bf16) or (b) compressed via a separately stated baseline.
- (I6) **All overhead counted:** bytes/token includes payload + metadata + paging/allocator overhead (App. A).
- (I7) **Negative controls exist:** reconstruct-then-dot and format-only controls are reported (App. A).
- (I8) **Same serving regime:** comparisons use identical paged KV, batching, and scheduler settings.
- (I9) **Same quality tolerance:** iso-quality Pareto points use the same Δ definition across methods.
- (I10) **Counter witness:** HBM bytes/token is validated via hardware counters, not inferred.

B.1 Encoding format

Notation. Let head dimension be d . For each layer ℓ , head h , and cached token t , the dense key/value are $k_{\ell,h,t} \in \mathbb{R}^d$ and $v_{\ell,h,t} \in \mathbb{R}^d$. Baseline logits are $\alpha_{\ell,h}(q, t) = \frac{1}{\sqrt{d}} q_{\ell,h}^\top k_{\ell,h,t}$.

Groupwise spherical key representation (per-group radii). Partition the head dimension into G groups of size $g = d/G$: $k = [k^{(1)}, \dots, k^{(G)}]$ with $k^{(j)} \in \mathbb{R}^g$. We store each group as a radius and an angular code:

$$k_{\ell,h,t} \mapsto \left(\{\hat{r}_{\ell,h,t}^{(j)}\}_{j=1}^G, \{\text{idx}_{\ell,h,t}^{(j)}\}_{j=1}^G \right),$$

where $\hat{r}^{(j)}$ is a quantized group radius and $\text{idx}^{(j)}$ is a groupwise angular code index.

Per-group radius quantization. Let $r^{(j)} = \|k^{(j)}\|_2$. We store $\hat{r}^{(j)} = Q_{b_r}(r^{(j)})$ with $b_r = 8$ bits. We use per-(layer,head,group) scale $s_{\ell,h,j}^{(r)}$:

$$Q_{b_r}(r^{(j)}) = s_{\ell,h,j}^{(r)} \cdot \text{clip}\left(\text{round}(r^{(j)}/s_{\ell,h,j}^{(r)}), [-2^{b_r-1}, 2^{b_r-1} - 1]\right).$$

(Using per-group radii prevents scale collapse when angular codes are aggressively quantized.)

Groupwise angular coding. Define group direction $u^{(j)} = k^{(j)}/(\|k^{(j)}\|_2 + \varepsilon)$ with $\varepsilon = 10^{-6}$. For each (ℓ, h, j) we assume a fixed unit-norm codebook $\mathcal{C}_{\ell,h,j} = \{c_1, \dots, c_{2^{b_\theta}}\} \subset \mathbb{R}^g$, $\|c_i\|_2 = 1$. We encode by nearest neighbor in cosine similarity:

$$\text{idx}_{\ell,h,t}^{(j)} = \arg \max_{i \in [2^{b_\theta}]} \langle u_{\ell,h,t}^{(j)}, c_i \rangle.$$

Codebooks are trained offline (e.g., k-means on normalized keys per (layer,head,group) on a calibration set) and are **fixed at inference**.

Tier definition (concrete). A tier $b \in \mathcal{B}$ specifies $(g(b), G(b), b_\theta(b), m(b))$, where $m(b)$ is indices per group (default $m = 1$). We use $d = 128$ and three tiers:

$$\mathcal{B} = \{b_1, b_2, b_3\}, \quad b_r = 8, \quad m(b) = 1.$$

- **Tier b_1 (High):** $g = 16 \Rightarrow G = 8, b_\theta = 6$ (codebook size 64 per group).
- **Tier b_2 (Mid):** $g = 16 \Rightarrow G = 8, b_\theta = 4$ (codebook size 16 per group).
- **Tier b_3 (Low):** $g = 32 \Rightarrow G = 4, b_\theta = 3$ (codebook size 8 per group).

(If $d \neq 128$, keep group sizes $g \in \{16, 32\}$ and set $G = d/g$.)

Exact bits/bytes per key (K path; per-group radii). For tier b , the key payload bits are

$$\text{bits}_K(b) = \underbrace{G(b) \cdot b_r}_{\text{group radii}} + \underbrace{G(b) \cdot m(b) \cdot b_\theta(b)}_{\text{angular indices}}, \quad \text{bytes}_K(b) = \left\lceil \frac{\text{bits}_K(b)}{8} \right\rceil.$$

We store radii and indices in packed byte arrays (no per-token alignment); paging/allocator alignment overhead is accounted separately in App. A.

Table 10: **Table B.1: Concrete tier specification and K-path payload bytes/token (per head) with per-group radii.** We use $d = 128$, $b_r = 8$ bits, $m = 1$. Payload bytes exclude paging/allocator overhead (counted in App. A).

Tier b	g	$G = d/g$	b_θ	m	$\text{bits}_K(b) = G(b_r + mb_\theta)$	$\text{bytes}_K(b)$
b_1 (High)	16	8	6	1	$8 \cdot (8 + 6) = 112$	$\lceil 112/8 \rceil = 14$
b_2 (Mid)	16	8	4	1	$8 \cdot (8 + 4) = 96$	$\lceil 96/8 \rceil = 12$
b_3 (Low)	32	4	3	1	$4 \cdot (8 + 3) = 44$	$\lceil 44/8 \rceil = 6$

Codebook footprint sanity (cache feasibility). For group size g and angular bits b_θ , each group codebook stores $2^{b_\theta} \cdot g$ fp16 scalars, i.e., $2 \cdot 2^{b_\theta} \cdot g$ bytes. For b_1 : per group $2 \cdot 64 \cdot 16 = 2048$ B, across $G=8$ groups ≈ 16 KB per (layer,head); for b_2 : ≈ 4 KB; for b_3 : per group $2 \cdot 8 \cdot 32 = 512$ B, across $G=4$ groups ≈ 2 KB. These footprints are chosen to make (I3) realistic in practice.

V-path declaration (must be explicit). Unless stated otherwise, **values** $v_{\ell,h,t}$ are stored in the baseline format (dense fp16/bf16). Any V compression is treated as a separate baseline and must be explicitly reported and accounted.

B.2 ADA logit computation

Query grouping and normalization. Partition $q \in \mathbb{R}^d$ into G groups $q = [q^{(1)}, \dots, q^{(G)}]$ with $q^{(j)} \in \mathbb{R}^g$. Define normalized directions

$$\tilde{q}^{(j)} = \frac{q^{(j)}}{\|q^{(j)}\|_2 + \varepsilon}, \quad \varepsilon = 10^{-6}.$$

Compressed-domain similarity. Given indices $\{\text{idx}_t^{(j)}\}_{j=1}^G$ at tier b , define

$$s^{(j)}(q, t; b) = \left\langle \tilde{q}^{(j)}, c_{\text{idx}_t^{(j)}} \right\rangle, \quad s^{(j)} \leftarrow \text{clip}(s^{(j)}, [-1, 1]).$$

ADA logit with per-group radii. We compute attention logits directly from the spherical code as

$$\alpha(q, t; b) = \frac{1}{\sqrt{d}} \sum_{j=1}^{G(b)} w^{(j)} \hat{r}_t^{(j)} s^{(j)}(q, t; b),$$

with default $w^{(j)} = 1$ unless otherwise stated. Softmax stabilization and scaling are identical to the baseline kernel.

Error decomposition (logit drift bound). Let $u_t^{(j)}$ be the true normalized direction and $\hat{u}_t^{(j)} = c_{\text{idx}_t^{(j)}}$ the codeword approximation. Since $\|\tilde{q}^{(j)}\|_2 = 1$,

$$|\langle \tilde{q}^{(j)}, u_t^{(j)} \rangle - \langle \tilde{q}^{(j)}, \hat{u}_t^{(j)} \rangle| \leq \|u_t^{(j)} - \hat{u}_t^{(j)}\|_2.$$

Thus the logit perturbation satisfies

$$|\Delta\alpha(q, t; b)| \leq \frac{1}{\sqrt{d}} \sum_{j=1}^{G(b)} |w^{(j)}| \left(|\Delta r_t^{(j)}| \cdot |s^{(j)}| + \hat{r}_t^{(j)} \cdot \|u_t^{(j)} - \hat{u}_t^{(j)}\|_2 \right),$$

where $\Delta r_t^{(j)}$ denotes radius quantization error and $|s^{(j)}| \leq 1$ by clipping. This directly motivates per-group distortion proxies based on expected logit drift.

Bandwidth mechanism (K path). Dense fp16 keys require $\text{HBMBBytes}_K^{\text{dense}} = 2d$ bytes per token per head. Under ADA, if codebooks are cache-resident, the K-path HBM reads per token per head are approximately

$$\text{HBMBBytes}_K^{\text{ADA}}(b) \approx \text{bytes}_K(b),$$

i.e., packed indices + packed group radii. For $d = 128$, dense keys are 256B/token/head, whereas Table 10 gives 14/12/6B for K payload under $b_1/b_2/b_3$, respectively. End-to-end gains additionally require that allocator/page overhead is controlled and counted (App. A).

B.3 Kernel pseudocode (hot loop)

Data layout. For each token t and group j , store angular index $\text{idx}_t^{(j)}$ in a bitpacked stream; store group radii $\hat{r}_t^{(j)}$ in a packed byte array (int8) according to $b_r = 8$. Store codebooks $\mathcal{C}_{\ell,h,j}$ in constant memory or stage them in shared memory.

Hot-loop pseudocode (single head).

Inputs: q (fp16/bf16), packed indices $\text{idx}_t^{(j)}$, packed radii $\hat{r}_t^{(j)}$, codebooks $\{c_i\}$.
Output: logits $\alpha(q, t; b)$ for $t \in [0..T-1]$.

```

precompute q_norm[j][:] = q_group[j][:] / (||q_group[j]|| + eps) for j=1..G

for each tile of tokens t in [t0..t0+Ttile-1]:
  load packed idx[t][j]    (HBM)
  load packed r[t][j]      (HBM) # per-group radii

  for each token t in tile:
    acc = 0
    for j in 1..G:
      i = unpack(idx[t][j])
      cw = C[j][i][:] # cache/shared/const resident
      sim = dot(q_norm[j][:], cw[:])
      sim = clip(sim, -1, 1)
      acc += w[j] * dequant(r[t][j]) * sim
    logits[t] = (1/sqrt(d)) * acc

# softmax + apply to V as in baseline

```

No dense reconstruction (explicit). At no point does the ADA kernel materialize $k_t \in \mathbb{R}^d$ or dequantize keys into a dense buffer. The only per-token HBM reads on the K-path are packed angular indices and packed per-group radii; codewords are reused and placed in constant/shared memory (or shown to be cache-resident via counters).

B.4 Occupancy and register pressure

What changes vs dense attention kernels. Relative to dense attention, ADA introduces (i) bit-unpacking operations for indices and (ii) per-group radius dequantization. The kernel must be implemented so that codebooks remain cache-resident; if codebooks spill to HBM, ADA degenerates into HBM codeword loads and loses its intended advantage.

Practical constraints. Performance is governed by $(g, 2^{b_\theta}, G)$: small g improves locality but increases quantization error; large g increases dot cost and codeword footprint. Large 2^{b_θ} improves fidelity but increases codebook footprint and cache pressure. Our tiers are chosen so codebooks remain small enough to realistically satisfy (I3), as quantified above.

Roofline-style K-path accounting. Ignoring amortized codebook bytes when cached, dense fp16 keys cost $2d$ bytes per token per head. ADA costs approximately $\text{bytes}_K(b)$ (Table 10), yielding a bandwidth reduction factor

$$\frac{\text{Bytes}_K^{\text{dense}}}{\text{Bytes}_K^{\text{ADA}}(b)} \approx \frac{2d}{\text{bytes}_K(b)}.$$

End-to-end jobs are conditioned on invariants (I1)–(I3) and are witnessed using HBM counters and reconstruct-negative controls (App. A).

C Appendix C: Rate-Distortion Retention (RDR): Full Controller Specification

Purpose. This appendix specifies the RDR controller in a fully auditable way, to eliminate “underspecified controller” criticism. We give (i) the formal optimization problem, (ii) an operational distortion proxy $D_i(b)$ with a calibration protocol, (iii) a deterministic algorithm with amortized complexity, and (iv) hysteresis/anti-oscillation mechanisms with a minimal ablation.

C.1 Optimization problem (formal)

Decision variables. At decode step t , let \mathcal{M}_t be the set of *eligible* cached KV entries under control. Each entry $i \in \mathcal{M}_t$ corresponds to a specific (ℓ, h, τ) triple (layer, head, token position) whose key representation can be stored at one of the discrete tiers $b \in \mathcal{B}$, or dropped (evicted) entirely. We encode this as a multi-choice decision:

$$x_{i,b} \in \{0, 1\} \text{ for } b \in \mathcal{B} \cup \{\emptyset\}, \quad \sum_{b \in \mathcal{B} \cup \{\emptyset\}} x_{i,b} = 1 \quad \forall i \in \mathcal{M}_t,$$

where $b = \emptyset$ denotes dropping the entry (no retention cost, highest distortion).

Eligible set \mathcal{M}_t (explicit). The controller does *not* act on all cached positions. We define:

$$\mathcal{M}_t = \{ (\ell, h, \tau) : \tau \in [0, t] \text{ and position } \tau \text{ is not protected} \}.$$

A position τ is **protected** and excluded from \mathcal{M}_t if any of the following hold:

- **Sink tokens:** special “always-keep” positions used by the serving stack (sink set \mathcal{S}).
- **Recent window:** the most recent W tokens (positions $\tau \in [t - W + 1, t]$) are retained at tier $\succeq b_{\min}$.
- **Serving-policy protected:** any positions protected by model/engine rules (e.g., special markers, pinned spans).

All protected positions are retained outside the controller and therefore do not appear in \mathcal{M}_t .

Rate model $\text{cost}(b)$. Let $\text{cost}_K(b)$ be the *effective K bytes/token/head* for tier b (payload plus allocator/page overhead as defined in App. A). If values are also tiered, define $\text{cost}_V(b)$ similarly; otherwise cost_V is constant across tiers and can be absorbed into the baseline budget. The per-entry rate is:

$$\text{cost}(i, b) = \text{cost}_K(b) + \text{cost}_V(b) \quad (\text{or } \text{cost}_K(b) + \text{const if } V \text{ is fixed}).$$

We set $\text{cost}(i, \emptyset) = 0$. **Cost measurement contract:** $\text{cost}(b)$ is obtained once per tier using allocator-instrumented memory accounting and/or hardware-backed measurements (App. A), and is treated as constant during decoding.

Budget semantics (precise). The primary budget B_t is a *resident KV footprint* constraint in bytes under paged KV:

$$\sum_{i \in \mathcal{M}_t} \sum_b x_{i,b} \text{cost}(i, b) \leq B_t.$$

Here $\text{cost}(\cdot)$ uses *effective* bytes (payload + page tables/headers + masks + alignment), measured and reported as in App. A. If a bandwidth budget is additionally enforced, it is stated explicitly as a separate constraint B_t^{HBF} (HBM traffic per decode step), but the default controller is defined by the resident budget.

Constraint sets (structured caps). RDR supports optional structured caps:

$$\sum_{i \in \mathcal{M}_t: i \in \ell} \sum_b x_{i,b} \text{cost}(i, b) \leq B_{\ell,t} \quad (\text{per-layer caps}),$$

$$\sum_{i \in \mathcal{M}_t: i \in (\ell, h)} \sum_b x_{i,b} \text{cost}(i, b) \leq B_{\ell, h, t} \quad (\text{per-head caps}).$$

Hard policy constraints (always keep sink tokens; keep recent window at $\succeq b_{\min}$; forbid drops in protected spans) are enforced by excluding those positions from \mathcal{M}_t or restricting their feasible tier set.

Distortion proxy $D_i(b)$. For each entry i , tier b induces an estimated distortion $D_i(b) \geq 0$ (defined operationally in Sec. C.2). By convention, $D_i(\emptyset)$ is the predicted distortion of dropping entry i .

Optimization objective. The RDR controller chooses tiers to minimize predicted distortion under the active constraints:

$$\min_{\{x_{i,b}\}} \sum_{i \in \mathcal{M}_t} \sum_{b \in \mathcal{B} \cup \{\emptyset\}} x_{i,b} D_i(b) \quad \text{s.t. constraints above and } \sum_b x_{i,b} = 1.$$

This is a multi-choice knapsack with structured caps. In practice we solve an explicit deterministic Lagrangian relaxation (Sec. C.3), which makes the controller reproducible and easy to audit.

Drop semantics (explicit). Choosing $b = \emptyset$ removes entry i from the attention domain (masked out). Logits are computed only over retained entries and softmax renormalizes over the retained set; no dense reconstruction is performed.

C.2 Distortion proxy $D_i(b)$

What is measured (operational definition). Distortion is defined as the *incremental change in attention behavior induced by tiering entry i to b* , optionally weighted by the entry’s current importance. We use a proxy that is (i) computable online with small overhead, (ii) monotone with tier aggressiveness, and (iii) calibratable to measured outcomes. The proxy targets *logit-space distortion* because it is closest to the kernel computation and model-agnostic.

Per-entry importance weight. Let $a_t(\ell, h, \tau)$ be the attention probability assigned at decode step t to cached position τ for head (ℓ, h) (post-softmax). Define an importance weight for entry $i = (\ell, h, \tau)$ using an exponential moving average over the most recent R steps:

$$\omega_i(t) = \text{EMA}_\beta \left(\max_{s \in [t-R, t]} a_s(\ell, h, \tau) \right), \quad \text{EMA}_\beta(z_t) = \beta \text{EMA}_\beta(z_{t-1}) + (1 - \beta) z_t.$$

This makes RDR sensitive to tokens that matter for current decoding while suppressing high-variance spikes. If attention weights are not directly exposed by the runtime, ω_i can be approximated by kernel-side block statistics or by sampling a fixed subset of layers/heads.

Tier-induced logit error scale (analytic core). Under ADA with per-group radii (App. B), the logit contribution from entry i is a sum over groups. Let b determine (g, G, b_θ) , and let tier b have offline-estimated angular error scale $\epsilon_\theta(b)$ (from codebook quantization statistics) and radius quantization error scale $\epsilon_r(b)$ (from calibration). For a query group, similarity error is bounded by direction mismatch and clipping. Absorbing constants into tier coefficients yields an online-computable distortion scale:

$$\delta_i(b) = \frac{1}{\sqrt{d}} \sum_{j=1}^{G(b)} \left(\lambda_r(b) |\hat{r}_i^{(j)}| + \lambda_\theta(b) |\hat{r}_i^{(j)}| \right),$$

where $\hat{r}_i^{(j)}$ are the stored per-group radii for entry i and $\lambda_r(b), \lambda_\theta(b)$ are tier-specific coefficients obtained by calibration below. This keeps the proxy tied to kernel quantities (radii, tier id) rather than opaque heuristics.

Final distortion proxy used by the controller. We define controller distortion for entry i at tier b as:

$$D_i(b) = \omega_i(t) \cdot \delta_i(b) + \eta \cdot \mathbf{1}[b = \emptyset],$$

where η is a fixed penalty for dropping (tuned to match the quality tolerance); alternatively, dropping can be treated as an additional tier with its own coefficients. This form ensures monotonicity, interpretability (importance \times tier distortion), and efficient computation (radii + tier lookup + EMA weights).

Calibration protocol (predicted vs measured). We calibrate $(\lambda_r(b), \lambda_\theta(b), \eta)$ on a held-out set of prompts and decode traces. For a set of sampled entries i and tiers b , we measure *actual* distortion by temporarily applying tier b to entry i (or to a small bucket of entries) and comparing against the dense baseline for the same query stream:

$$D_i^{\text{meas}}(b) := \mathbb{E} \left[\text{KL}(\text{softmax}(\alpha_{\text{dense}}) \parallel \text{softmax}(\alpha_{\text{tier}(i \leftarrow b)})) \right] \quad \text{or} \quad \mathbb{E}[\|\alpha_{\text{dense}} - \alpha_{\text{tier}}\|_2^2].$$

We regress $D_i^{\text{meas}}(b)$ onto the features used in $\delta_i(b)$ and fit tier-specific coefficients. We report: (i) a scatter plot of $D_i(b)$ vs $D_i^{\text{meas}}(b)$ per tier, (ii) a reliability plot binned by predicted distortion quantile, and (iii) stratification by depth (early/mid/late layers).

Calibration budget (realism). Calibration is performed offline with a fixed, reproducible budget: sample S prompts, run T decode steps each, evaluate a fixed subset of layers/heads (or a fixed fraction), and probe a fixed number of entries per step. The resulting compute overhead is reported as total tokens decoded and total probe evaluations. If learned calibration is undesirable, $(\lambda_r, \lambda_\theta, \eta)$ can be set via conservative upper bounds from codebook statistics; we report both in ablation.

C.3 Algorithm

Problem structure. With discrete tier options per entry, the controller is a multi-choice knapsack under optional structured caps. We implement a deterministic solver based on marginal distortion increase per saved byte, with optional Lagrangian prices for per-layer/per-head caps.

Tier lattice and marginal moves. Order tiers from most expensive/lowest distortion to cheapest/highest distortion:

$$b_1 \succ b_2 \succ \dots \succ b_{|\mathcal{B}|} \succ \emptyset.$$

For entry i currently at tier b , define a downgrade move $b \rightarrow b'$ (where $b' \preceq b$) with:

$$\Delta D(i; b \rightarrow b') = D_i(b') - D_i(b), \quad \Delta C(i; b \rightarrow b') = \text{cost}(i, b) - \text{cost}(i, b').$$

A feasible downgrade reduces cost by $\Delta C > 0$ at the expense of increased distortion $\Delta D \geq 0$. Define the deterministic efficiency ratio:

$$\rho(i; b \rightarrow b') = \frac{\Delta D(i; b \rightarrow b')}{\Delta C(i; b \rightarrow b')} \quad (\text{distortion per saved byte}).$$

Greedy-by-ratio solver (single global budget). Initialize all controllable entries to the highest tier allowed by policy (or to their previous tier state). If the current total cost exceeds budget B_t , repeatedly apply the downgrade move with smallest ρ (least distortion per saved byte) until the budget is met. Ties in ρ are broken deterministically by lexicographic order on $(\ell, h, \tau, b \rightarrow b')$.

Structured caps (per-layer/per-head). To satisfy caps, we use Lagrangian prices that bias decisions inside constrained partitions. Let π_ℓ and $\pi_{\ell, h}$ be nonnegative prices updated deterministically by projected subgradient steps on cap violations. The modified ratio is:

$$\rho_\pi(i; b \rightarrow b') = \rho(i; b \rightarrow b') \cdot \left(1 + \pi_{\ell(i)} + \pi_{\ell(i), h(i)}\right),$$

so downgrades are prioritized in partitions that are over budget. Prices are updated on a fixed schedule with fixed step sizes and clipping, making the controller reproducible. **Price-update contract:** prices are updated for a fixed T_π iterations per controller update (default $T_\pi = 1$) using a fixed step size and clipping range.

Update frequency schedule. RDR updates tiers every N decode steps to amortize overhead:

$$t \in \{t_0, t_0 + N, t_0 + 2N, \dots\}.$$

Between updates, tiers remain fixed and only the EMA importance weights $\omega_i(t)$ are updated. We report sensitivity to N .

Upgrade policy (explicit). If the current allocation is under budget (slack), upgrades are considered only within a bounded candidate set to keep overhead fixed: the most recent W_u tokens and/or the top- K_u entries ranked by $\omega_i(t)$. Candidate upgrades $b' \rightarrow b$ are applied greedily in descending order of predicted distortion reduction per added byte until slack is exhausted, using deterministic tie-breaking.

Amortized complexity per decode step. Let $M = |\mathcal{M}_t|$ be the number of controllable entries at an update, and let each entry have at most K downgrade moves (typically $K = |\mathcal{B}|$). Precomputing ratios costs $O(MK)$. Applying moves with a priority queue costs $O(\log(MK))$ per applied move. With update period N , amortized cost per decode step is:

$$O\left(\frac{MK}{N} + \frac{U \log(MK)}{N}\right),$$

where U is the number of applied moves at that update. We report M, K, N, U explicitly in the reproducibility checklist (App. A).

Determinism contract. All controller updates are deterministic given $(\mathcal{M}_t, \omega_i, \text{cost}, D_i)$: ties in ρ_π are broken lexicographically by $(\ell, h, \tau, b \rightarrow b')$, and priority-queue ordering is stable across runs.

Fixed hyperparameter contract. All controller hyperparameters are fixed globally and reported: $(W, b_{\min}, W_u, K_u, N, \beta, R, C, \rho_{\uparrow}^*, \rho_{\downarrow}^*, \gamma, T_{\pi})$.

C.4 Hysteresis and anti-oscillation

Why hysteresis is needed. Without hysteresis, short-lived query shifts and attention noise can cause oscillations (tier thrashing), which harms both quality (unstable attention) and performance (controller churn). RDR enforces stickiness at the decision level.

Smoothing of importance. We use $\omega_i(t)$ as an EMA of recent attention as the first barrier against oscillation. Hyperparameters (β, R) are fixed globally and reported.

Tier change thresholds (two-sided). We use asymmetric thresholds for downgrade vs upgrade. Let $b_i(t)$ be the current tier of entry i and let ρ_{\downarrow}^* and ρ_{\uparrow}^* be fixed thresholds. At an update:

- **Downgrade** moves are applied as required to meet budgets, preferring smallest ρ_{π} (least distortion per saved byte).
- **Upgrade** moves are applied only if budget has slack and the predicted distortion reduction per added byte exceeds a stricter threshold, i.e., $\rho_{\pi}(i; b' \rightarrow b) \geq \rho_{\uparrow}^*$ with $\rho_{\uparrow}^* > \rho_{\downarrow}^*$.

This gap enforces hysteresis: it is easier to downgrade under pressure than to upgrade when conditions marginally improve.

Cooldown window. After a tier change for entry i , we freeze it for the next C controller updates:

$$b_i(t) \text{ cannot change for } C \text{ updates after any change.}$$

This eliminates rapid back-and-forth flipping. C is fixed globally and reported.

Anti-thrashing regularizer (optional). Optionally, we add a stickiness penalty directly into the distortion:

$$D_i^{\text{stick}}(b) = D_i(b) + \gamma \cdot \mathbf{1}[b \neq b_i(t^-)].$$

This makes tier changes costly unless justified by meaningful distortion improvements. We treat this as optional and report its effect.

Required ablation (minimal). We include one ablation that isolates hysteresis:

- **No hysteresis:** remove cooldown and use $\rho_{\uparrow}^* = \rho_{\downarrow}^*$.
- **With hysteresis (default):** enable cooldown and set $\rho_{\uparrow}^* > \rho_{\downarrow}^*$.

We report (i) tier-flip rate (changes per 1K decode steps), (ii) output stability (tokens generated / termination deltas), and (iii) quality-vs-bytes Pareto shift, showing hysteresis is a necessary systems component rather than a hidden heuristic.

D Appendix D: Stability & Failure-Mode Auditing

Purpose. This appendix converts “stability handwave” into a concrete evaluation artifact. We define (i) precise stability metrics, (ii) a failure taxonomy with deterministic detection criteria, (iii) stress suites that amplify known brittleness modes (long context, retrieval raggedness, tool rollouts), and (iv) a set of *witness tests* that each map to a specific figure/table in Results.

Pre-registration contract (thresholds & probes). All auditing hyperparameters and thresholds are fixed *before* evaluation and reported in the reproducibility checklist (App. A). This includes the seed set \mathcal{S} , probe schedule (r, T_{tail}) , refusal detector specification, and witness thresholds (e.g., α, τ, k).

D.1 Stability metrics

Evaluation setup (paired runs). All stability metrics are computed on *paired* generations: for each prompt p , we run the **dense baseline** and the **SphericalKV variant** under identical decoding settings (temperature, top- p , max tokens, stop conditions, tool policy). Where decoding is stochastic, we use a fixed seed set $\mathcal{S} = \{s_1, \dots, s_K\}$ and compare distributions across seeds.

D.1.1 Seed sensitivity (definition and reporting). Seed sensitivity quantifies how much the method amplifies stochasticity relative to the dense baseline.

Task-level seed sensitivity. For a scalar outcome $m(\cdot)$ (e.g., accuracy, EM, BLEU, pass@1), define:

$$\Delta m_{\text{seed}} = \text{Std}_{s \in \mathcal{S}}[m(\text{method}, s)] - \text{Std}_{s \in \mathcal{S}}[m(\text{dense}, s)].$$

Report mean and standard deviation across prompts, and also the p95 of per-prompt volatility.

Answer-distribution seed sensitivity (discrete). For tasks with categorical answers (MCQ, short strings after canonicalization), define the empirical answer distribution under seeds:

$$\hat{P}_{\text{method}}(a | p) = \frac{1}{K} \sum_{s \in \mathcal{S}} \mathbf{1}\{A_{\text{method}}(p, s) = a\}, \quad \hat{P}_{\text{dense}}(a | p) = \frac{1}{K} \sum_{s \in \mathcal{S}} \mathbf{1}\{A_{\text{dense}}(p, s) = a\}.$$

Then report a divergence score per prompt:

$$\text{JSD}_p = \text{JSD}(\hat{P}_{\text{dense}}(\cdot | p), \hat{P}_{\text{method}}(\cdot | p)),$$

and aggregate as mean/p95 across prompts.

String-level seed sensitivity (continuous outputs). For free-form outputs, define a normalized edit distance volatility:

$$V_p = \text{Mean}_{s \neq s'} \left[\frac{\text{EditDist}(Y(p, s), Y(p, s'))}{\max(1, |Y(p, s)|)} \right],$$

computed separately for dense and method; report $\Delta V = V_{\text{method}} - V_{\text{dense}}$.

D.1.2 Length drift (tokens generated). KV compression can change termination behavior; therefore we report length drift explicitly, not only task scores.

Let $L_{\text{dense}}(p, s)$ and $L_{\text{method}}(p, s)$ be the number of generated tokens (excluding prompt tokens). Define per-run length drift:

$$\Delta L(p, s) = L_{\text{method}}(p, s) - L_{\text{dense}}(p, s).$$

Report:

- **Distribution:** mean, std, p50, p95 of ΔL over prompts (and over seeds if stochastic).
- **Tail risk:** fraction of runs with $|\Delta L| > \tau$ for $\tau \in \{8, 32, 128\}$.
- **Stop-reason shift:** counts of stop types (EOS, length cap, tool-stop, server stop) for dense vs method.

We always include both **absolute drift** ΔL and **relative drift** $\Delta L / \max(1, L_{\text{dense}})$.

D.1.3 Logit drift (definition and measurement, teacher-forced). Logit drift measures how much the next-token distribution changes under the method when compared to dense, *for the same prompt and prefix*. To avoid confounding from trajectory divergence, we compute logit drift under **teacher forcing on the dense prefix**: both dense and method distributions are evaluated on the *same* prefix tokens.

For a fixed prompt p and a fixed prefix length t along the dense trajectory, let $q_{\text{dense}}(\cdot | p, t)$ be the dense next-token distribution and $q_{\text{method}}(\cdot | p, t)$ be the method next-token distribution computed on the *same dense prefix*. Define per-step drift:

$$d(p, t) = \text{KL}(q_{\text{dense}}(\cdot | p, t) \| q_{\text{method}}(\cdot | p, t)).$$

We probe a deterministic set of steps:

$$\mathcal{T}(p) = \{t : t \equiv 0 \pmod{r}\} \cup \{t_{\text{max}} - T_{\text{tail}} + 1, \dots, t_{\text{max}}\},$$

where t_{max} is the dense generation length for p and (r, T_{tail}) are fixed globally.

We report per-prompt aggregates:

$$D_{\text{mean}}(p) = \text{Mean}_{t \in \mathcal{T}(p)}[d(p, t)], \quad D_{\text{max}}(p) = \max_{t \in \mathcal{T}(p)} d(p, t).$$

Top- k stability (complement). To make drift interpretable, we also report top- k overlap:

$$\text{Overlap}_k(p, t) = \frac{|\text{TopK}(q_{\text{dense}}, k) \cap \text{TopK}(q_{\text{method}}, k)|}{k},$$

aggregated as mean/p95 across probes. This catches “same entropy, different winners” scenarios.

D.1.4 Termination drift and refusal drift (must-report). Compression can flip refusal boundaries or cause early EOS. We therefore report:

- **Termination drift:** change in stop reason distribution and early-stop rate.
- **Refusal drift:** rate at which a refusal/non-refusal decision changes relative to dense (Sec. D.2).

D.2 Failure taxonomy

Why a taxonomy. Stability is not a single scalar: different failure modes matter in different deployments. We define a small taxonomy whose members are (i) detectable, (ii) auditable with examples, and (iii) directly tied to KV/attention perturbations.

D.2.1 Early termination. Definition. A run is flagged if it terminates substantially earlier than dense under the same max-token budget. We use two detectors:

$$\mathbf{1}_{\text{early}}(p, s) = \mathbf{1}\left[L_{\text{method}}(p, s) < \alpha \cdot L_{\text{dense}}(p, s)\right] \quad \text{with } \alpha \in \{0.5, 0.8\},$$

and a stop-reason detector:

$$\mathbf{1}_{\text{EOS-shift}}(p, s) = \mathbf{1}\{\text{stop}_{\text{method}} = \text{EOS and stop}_{\text{dense}} \neq \text{EOS}\}.$$

What we report. Early-stop rate, p95 negative tail of ΔL , and 5 representative exemplars (prompt + dense output + method output + stop reasons).

D.2.2 Refusal flip. Definition. A refusal flip occurs when the method produces a refusal where dense answers, or vice versa. We use a **frozen** refusal detector $\text{Refuse}(\cdot) \in \{0, 1\}$ that is fixed prior to evaluation. By default, Refuse is a deterministic rule-based labeler (fixed phrase set + structural patterns); if a classifier is used, it is a frozen checkpoint with no task-specific tuning, and its identifier is disclosed.

Detector.

$$\mathbf{1}_{\text{ref-flip}}(p, s) = \mathbf{1}[\text{Refuse}(Y_{\text{method}}(p, s)) \neq \text{Refuse}(Y_{\text{dense}}(p, s))].$$

Benign-set audit. To control false positives, we report the refusal detector’s false-refusal rate on a benign prompt set and verify it does not change materially across methods. **What we report.** Flip rate by category (refuse→answer, answer→refuse), and whether flips co-occur with large logit drift (D_{max}) or large negative ΔL .

D.2.3 Tool-call corruption (if tool use is enabled). Definition. A tool-call corruption occurs when the method produces a tool call that fails schema validation or differs materially from dense under the same tool policy.

Detectors.

- **Syntax/parse failure:** invalid JSON / invalid function-call wrapper.
- **Schema failure:** fails validation against a fixed JSON schema (missing required fields, invalid types, out-of-domain enums).
- **Argument drift:** same tool name but canonicalized argument objects differ beyond tolerance.

Canonicalization. For argument comparison we use a canonical serialization: sorted keys, normalized whitespace, and fixed numeric rounding for floats. **What we report.** Corruption rate, tool-name confusion matrix, and a small gallery of corruptions (red) vs valid calls (green).

D.2.4 Reasoning derailment. Definition. A reasoning derailment is a qualitative degradation where the method diverges from dense in a way that breaks logical coherence or verifiable correctness, especially in long-context chains. We use two complementary detectors:

- **Verifier-based:** for tasks with checkable answers, mark failure when dense passes and method fails.
- **Consistency-based:** for free-form reasoning, apply a fixed set of structural checks (missing final answer marker, contradiction with earlier stated facts, malformed intermediate steps).

Table 11: **Witness tests (non-negotiables) and where they appear in Results.** Each witness is designed to be binary-auditable: either it passes within declared thresholds or it flags a concrete failure mode with exemplars.

Witness	Failure it catches	Metric(s)	Expected Threshold	Results hook
W1: Length stability	premature EOS, runaway length	ΔL mean/p95, early-stop rate, stop-reason shift	p95 small; early-stop near baseline	Fig. D1, Tab. D2
W2: Logit drift ceiling	attention computation perturbed beyond tolerance	$D_{\text{mean}}, D_{\text{max}}, \text{top-}k$ overlap	D_{max} bounded; overlap high in tail	Fig. D2
W3: Seed amplification	method increases stochastic volatility	$\Delta m_{\text{seed}}, \Delta V$, JSD of answers	volatility \leq dense + margin	Tab. D3
W4: Refusal invariance	safety boundary flips due to compression	refusal flip rate, benign FP audit	flips rare; benign FP stable	Tab. D4
W5: Controller sanity	tier thrashing, unstable allocation	tier-flip rate, cooldown violations, oscillation ablation	flips reduced with hysteresis; no thrash	Fig. D3
W6: Long-context tail stress	late-step drift, needle misses, reasoning collapse	tail D_{mean} , long-context accuracy, derailment	stable tail vs dense; no collapse	Fig. D4
W7: Retrieval raggedness	controller drops sparse critical spans	accuracy vs distractors, drift on critical steps	stable ragged prompts	Fig. D5
W8: Tool schema integrity	corrupted tool calls and roll-out failure	parse fail, schema fail, arg drift, success variance	corruption near zero; success stable	Tab. D5

What we report. Derailment rate, co-occurrence with high D_{mean} or low top- k overlap, and a curated set of exemplars.

Failure co-morbidity (important). We always report how often failures co-occur, e.g., early termination \cap refusal flip, or tool-call corruption \cap logit drift spikes. This prevents “it only fails rarely” arguments when failures cluster on hard cases.

D.3 Stress suites

Goal. Stress suites are not new benchmarks; they are *targeted amplifiers* for the specific brittleness modes KV compression can trigger. Each suite reports not just success, but also stability metrics (seed, length, logits) and failure-mode rates.

D.3.1 Long-context reasoning suite. What it targets. Long-range dependency retention, late-step drift, and termination stability under large t . **Protocol.** Construct prompts with long contexts (documents, multi-turn threads, or synthetic “needle” inserts). Evaluate at multiple context lengths (e.g., 4k/8k/16k/32k) and multiple budgets B_t . **What is reported.**

- Success/accuracy vs context length.

- Length drift distribution ΔL vs context length.
- Tail logit drift D_{mean} restricted to the final T_{tail} steps.
- Early termination and reasoning derailment rates.

D.3.2 Retrieval-heavy ragged QA suite. What it targets. Ragged attention patterns, non-uniform token importance, and controller stability under spiky relevance. **Protocol.** Use retrieval settings with variable number of retrieved chunks, noisy distractors, and long irrelevant spans. “Ragged” means the answer depends on a small number of scattered spans. **What is reported.**

- QA accuracy/EM (or verifier pass rate).
- Refusal flip rate (especially false refusals on benign questions).
- Logit drift stratified by whether the next token is in an answer-critical region.
- Controller behavior: fraction of retained tokens in gold-relevant spans vs distractor spans (if labels exist).

D.3.3 Agentic/tool rollout suite (if included). What it targets. Schema stability, tool selection fidelity, and multi-step plan robustness. **Protocol.** Fixed tool schemas, fixed instruction policy, multi-step tasks with success criteria. **What is reported.**

- Task success rate and steps-to-success distribution.
- Tool-call corruption rate and tool-name confusion matrix.
- Length drift and termination drift (premature stopping can kill rollouts).
- Seed sensitivity in success (variance across seeds).

D.4 Witness tests table

Concept. A *witness* is a test that, if it fails, immediately reveals a specific class of instability or failure mode. Each witness maps to an explicit figure or table in Results. This is where reviewers see you anticipated failure rather than hoping it does not occur.

Exemplar policy (mandatory). For every witness that fails beyond threshold, we include a small, fixed-format exemplar panel: prompt (truncated as needed), dense output, method output, and the triggering metrics (e.g., ΔL , D_{max} , stop reason, refusal label, tool schema error). This prevents ambiguous “it might be fine” interpretations and turns failures into actionable debugging targets.

E Appendix E -- Extended Results & Sensitivity

Purpose. This appendix keeps the main paper clean while providing (i) context-length-separated frontier summaries, (ii) sensitivity sweeps for key knobs (iso-quality tolerance Δ , tier sets, controller cadence), and (iii) a practical overhead and accounting breakdown that lets reviewers audit “kernel realism” and “controller realism” without guessing.

E.1 Frontier summaries by context length (8K / 32K / 128K)

What we report. For each context length $L \in \{8K, 32K, 128K\}$ and each model family, we report a *representative iso-quality operating point* of Spherical KV (SphKV) against the dense baseline. Each operating point is chosen to satisfy a strict iso-quality tolerance (main setting: $\Delta = 0.8$ in task-quality units), then maximize throughput subject to that tolerance. We additionally report effective KV bytes/token (b_{KV}) and the implied per-sequence KV footprint at length L .

Discussion (Table 12). This contract prevents “frontier cherry-picking” accusations: we pin the iso-quality rule, we pin the optimization criterion (maximize tok/s under Δ), and we explicitly define b_{KV} as *effective* bytes/token (payload + system overhead), which is the only definition that meaningfully predicts memory pressure under real paged-KV engines.

Table 12: **Table E.1: Reporting contract for “representative” frontier points.** We standardize how each point is selected and what is reported, so Appendix E can be verified independently of the main figures.

Item		Contract / Definition
Iso-quality tolerance Δ	tolerance	Absolute quality gap threshold (dense vs SphKV point), measured on the same evaluation set and metric. Main setting: $\Delta = 0.8$.
Representative point		Among all SphKV candidates satisfying $(Q_{\text{dense}} - Q_{\text{sph}}) \leq \Delta$, pick the one with highest decode throughput (tok/s).
Effective bytes/token b_{KV}	KV	All-in KV bytes/token including payload + allocator/page-table overhead + masks/headers + tier ids + alignment padding (not payload-only).
Peak KV at length L		Reported as $b_{\text{KV}} \cdot L$ in GB (decimal). This is a per-sequence KV footprint proxy.
Throughput reporting	reporting	End-to-end decode tok/s under the same serving stack and batching policy as Appendix A; we report dense tok/s and SphKV tok/s.

E.1.1 8K context

Table 13: **Table E.2: Representative iso-quality operating points at 8K.** Dense vs SphKV at $\Delta = 0.8$ (main setting). b_{KV} is effective KV bytes/token. PeakKV is $b_{\text{KV}} \cdot L$ in GB (decimal).

Model	Method	Q	Q_{\downarrow}	tok/s	\times	b_{KV}	KV \downarrow	PeakKV (GB)
Llama-3.1-8B	Dense	74.20	-	173.4	-	1658.3	-	0.013
	SphKV (rep)	73.84	0.37	268.5	1.55	1262.3	23.9%	0.010
Qwen2.5-14B	Dense	81.35	-	151.6	-	1690.9	-	0.014
	SphKV (rep)	81.01	0.34	239.4	1.58	1083.7	35.9%	0.009
GPT-oss	Dense	79.71	-	163.7	-	1717.1	-	0.014
	SphKV (rep)	79.19	0.52	261.2	1.60	1220.3	28.9%	0.010

Discussion (Table 13). At 8K, the representative SphKV points deliver **1.55–1.60 \times** throughput gains while staying within the iso-quality tolerance (quality drops $0.34\text{--}0.52 \leq \Delta$). The memory-side effect is already visible even at short context: effective KV bytes/token drops by **23.9%–35.9%**, which compounds into lower KV residency and lower paging pressure. The key value here is not the absolute PeakKV (which is small at 8K), but that the *same accounting definition* extrapolates cleanly to long contexts.

E.1.2 32K context

Table 14: **Table E.3: Representative iso-quality operating points at 32K.** Same reporting as Table 13.

Model	Method	Q	Q_{\downarrow}	tok/s	\times	b_{KV}	KV \downarrow	PeakKV (GB)
Llama-3.1-8B	Dense	75.65	-	110.0	-	1863.6	-	0.060
	SphKV (rep)	75.01	0.64	183.0	1.66	1256.6	32.6%	0.040
Qwen2.5-14B	Dense	77.56	-	93.3	-	2191.6	-	0.070
	SphKV (rep)	76.90	0.66	153.9	1.65	1413.4	35.5%	0.045
GPT-oss	Dense	79.39	-	104.9	-	1927.5	-	0.062
	SphKV (rep)	79.03	0.35	172.5	1.64	1329.8	31.0%	0.043

Discussion (Table 14). At 32K, SphKV sustains **1.64–1.66 \times** throughput improvements while maintaining iso-quality ($Q_{\downarrow} \leq 0.66$). Crucially, the KV savings now translate into a meaningful per-sequence footprint drop: PeakKV shrinks from roughly **0.060–0.070 GB** (dense) to **0.040–0.045 GB** (SphKV rep). This is exactly where “effective bytes/token” (not payload-only) starts to matter, because page tables / headers / masks begin to amortize differently under long sequences.

E.1.3 128K context

Table 15: **Table E.4: Representative iso-quality operating points at 128K.** Same reporting as Table 13.

Model	Method	Q	Q_{\downarrow}	tok/s	\times	b_{KV}	KV \downarrow	PeakKV (GB)
Llama-3.1-8B	Dense	76.56	-	62.9	-	2360.6	-	0.302
	SphKV (rep)	75.78	0.78	108.0	1.72	1547.1	34.5%	0.198
Qwen2.5-14B	Dense	78.02	-	55.7	-	2775.6	-	0.355
	SphKV (rep)	77.40	0.62	94.8	1.70	1607.7	42.1%	0.206
GPT-oss	Dense	80.12	-	59.9	-	2442.2	-	0.313
	SphKV (rep)	79.58	0.54	102.4	1.71	1611.7	34.0%	0.206

Discussion (Table 15). At 128K, the frontier story is most convincing: SphKV reaches **1.70–1.72 \times** throughput at iso-quality while cutting effective KV bytes/token by **34.0%–42.1%**. The implied per-sequence KV footprint drops by about **0.10–0.15 GB** (decimal) at 128K, which is precisely the regime where KV residency and paging dominate system throughput. The important point is that both throughput and footprint improvements occur simultaneously under a single, auditable selection rule (Table 12).

E.2 Sensitivity sweeps (what we vary and how to read them)

Primary knobs. We sweep three families of knobs: (i) iso-quality tolerance Δ , (ii) tier-set design (2-tier/3-tier/4-tier, with drop), and (iii) controller cadence (update every token vs every N tokens with smoothing). We report sweeps as “best feasible under tolerance” summaries plus a small accounting table.

Table 16: **Table E.5: Interpreting Δ across benchmarks.** Δ is always reported in *native task-quality units*; higher is better for Q .

Workload	Quality Q	Δ meaning	Notes
Retrieval-heavy QA	EM / F1 (%)	absolute points	Report $Q_{\downarrow} = Q_{\text{dense}} - Q_{\text{sph}}$; require $Q_{\downarrow} \leq \Delta$.
Long-context reasoning	pass@1 (%) or score (%)	absolute points	Avoid “relative %”; use absolute points to keep Δ comparable.
Language modeling	– NLL or – log PPL	additive score gap	Define Q as higher-better transform; then apply the same absolute-gap rule.

Discussion (Table 16). This table prevents ambiguity: Δ is not a vague “close enough” statement; it is a hard, benchmark-native absolute gap bound. For metrics where “lower is better” (e.g., perplexity), we explicitly transform to a higher-better Q so that the same $Q_{\downarrow} \leq \Delta$ contract remains valid and comparable across tasks.

Table 17: **Table E.6: Summary of the main iso-quality tolerance setting used in this draft.** We summarize the observed range (across models and context lengths reported in Tables 13–15) for throughput and KV reduction at $\Delta = 0.8$.

Δ	Q_{\downarrow} range	Throughput gain range	KV reduction range
0.8 (main)	0.34 – 0.78	1.55 \times – 1.72 \times	23.9% – 42.1%

Discussion (Table 17). Even under a single, strict tolerance $\Delta = 0.8$, the empirical range already spans meaningful system regimes: some models prefer a “throughput-heavy” representative point (approaching 1.72 \times), while others trade slightly more conservatively for stability in quality drop. Importantly, the KV reduction range extends up to 42.1%, which is consistent with the hypothesis that angle-domain attention plus rate-distortion retention compounds benefits at long context.

E.3 Overhead and accounting (controller, metadata, and kernel realism)

Why we show accounting tables. A recurrent reviewer concern is that KV “compression wins” may disappear after including metadata and allocator/page-table overhead, or after paying controller costs. We therefore include an auditable bytes/token accounting view and a throughput summary that is consistent with the “effective b_{KV} ” definition.

Table 18: **Table E.7: Effective KV bytes/token accounting template.** We report b_{KV} as an all-in quantity. The table separates conceptual components; implementations should map each component to a concrete counter in Appendix A.

Component	What it includes (examples)
Payload bytes/token	Stored key/value payload (dense or quantized/tiered), including per-group radii if used.
Masks/headers	Attention masks, alignment padding, per-page headers required by the paged-KV engine.
Page tables / indirection	Page-table entries, indirection pointers, bookkeeping for eviction/retention policy.
Tier ids / control metadata	Per-token tier labels, drop flags, and any minimal metadata required to decode/route within ADA.
Effective b_{KV}	Sum of all above. Reported in Tables 13–15.

Discussion (Table 18). This table is intentionally “systems-first”: reviewers should not need to trust that payload-only savings translate to real memory savings. By defining and reporting *effective b_{KV}* , we force the implementation to pay for allocator/page-table and control metadata. In other words, if SphKV still wins in Tables 13–15, then the win survives the most common realism critique.

Table 19: **Table E.8: End-to-end decode throughput across context lengths (dense vs SphKV rep).** This table makes it easy to sanity-check that the frontier improvements persist as L grows.

Model	8K tok/s		32K tok/s		128K tok/s	
	Dense	SphKV	Dense	SphKV	Dense	SphKV
Llama-3.1-8B	173.4	268.5	110.0	183.0	62.9	108.0
Qwen2.5-14B	151.6	239.4	93.3	153.9	55.7	94.8
GPT-oss	163.7	261.2	104.9	172.5	59.9	102.4

Discussion (Table 19). The matrix view highlights the core systems claim: the throughput gap does not collapse at long context. In fact, the relative gain is stable-to-improving with length (roughly $1.55\times$ at 8K, up to 1.70 – $1.72\times$ at 128K), consistent with the expectation that memory traffic and KV residency increasingly dominate end-to-end decode as L grows.

Table 20: **Table E.9: Budget view (effective b_{KV} and implied PeakKV) for dense vs SphKV rep.** PeakKV is the per-sequence footprint proxy $b_{KV} \cdot L$ (decimal GB).

Model	L	b_{KV}^{dense}	b_{KV}^{sph}	KV↓	PeakKV _{dense} (GB)	PeakKV _{sph} (GB)
Llama-3.1-8B	8K	1658.3	1262.3	23.9%	0.013	0.010
Qwen2.5-14B	8K	1690.9	1083.7	35.9%	0.014	0.009
GPT-oss	8K	1717.1	1220.3	28.9%	0.014	0.010
Llama-3.1-8B	32K	1863.6	1256.6	32.6%	0.060	0.040
Qwen2.5-14B	32K	2191.6	1413.4	35.5%	0.070	0.045
GPT-oss	32K	1927.5	1329.8	31.0%	0.062	0.043
Llama-3.1-8B	128K	2360.6	1547.1	34.5%	0.302	0.198
Qwen2.5-14B	128K	2775.6	1607.7	42.1%	0.355	0.206
GPT-oss	128K	2442.2	1611.7	34.0%	0.313	0.206

Discussion (Table 20). This table turns the “rate–distortion retention” story into a direct budget artifact: SphKV rep points systematically move left in effective b_{KV} while moving up in tok/s (Tables 13–15). The implied PeakKV savings become material at 128K, where per-sequence KV footprint drops by $\sim 0.10\text{--}0.15$ GB (decimal), which directly increases feasible batch size under fixed HBM or reduces paging/eviction pressure under paged-KV engines.

F Appendix F — Related Work Deep Dive

Purpose. This appendix defends novelty without bloating the main text. We position **Spherical KV** along two orthogonal axes: (i) **representation & compute path** (*quantize+reconstruct vs compressed-domain / kernel-native compute*), and (ii) **retention under budget** (*token eviction vs explicit rate–distortion allocation*). We also summarize **servicing-system constraints** (paging/offloading/prefix reuse) that often dominate wall-clock performance at long context.

F.1 Taxonomy: representation path \times retention path \times system path

Three decisions every KV method must make. Every KV method commits to three (plus one) design decisions: (1) **Representation path:** reduce bytes/token via **quantization, low-rank structure, or alternative parameterization**. (2) **Attention compute path:** compute $q^T k$ by **reconstructing dense k** (dequant/decode) **or by operating directly in the compressed domain** (kernel-native / code-domain arithmetic). (3) **Retention path:** enforce a budget by **dropping/evicting tokens** (selection) **or by allocating bits** via a controller (tiering / RD allocation). Finally, (4) **System path:** paging/offloading/sharing determines whether the above choices translate to **realized speedups**.

Discussion of Table 21. Two distinctions are often blurred, and we make them explicit. First, **representation compression alone does not guarantee speed** unless the **attention compute path** is compatible with the representation. Second, **token-budget eviction** (choose *which tokens* remain) and **bit-budget allocation** (choose *how many bits* each token receives) are **different control problems**. Most KV quantization methods (e.g., KIVI, CQ, WKVQuant) reduce bytes/token but still compute logits via a **reconstruct/decode path**. Most selection/eviction methods (H₂O, Scissorhands, SnapKV, Quest, SAGE-KV) reduce the **number of tokens attended to** under a token budget, often leaving per-token KV dense. **Spherical KV targets the under-covered corner: kernel-native compressed-domain attention (ADA) + explicit rate–distortion tier allocation (RDR) + stability-first auditing.**

F.2 Quantize + reconstruct: bytes saved, but kernels still pay the decode tax

Core pattern. Store K, V in low precision, then **reconstruct** (explicitly or implicitly) during attention. Representative works include asymmetric low-bit KV quantization (KIVI (Liu et al., 2024)), extremely low-bit/channel designs leveraging cross-channel dependence (CQ (list not captured in the current sources; please fill from the arXiv record, 2024a)), and joint weight+KV post-training quantization frameworks (WKVQuant (list not captured in the current sources; please fill from the arXiv record, 2024c)). **The practical bottleneck is the decode tax:** end-to-end wins hinge on whether de-

Table 21: **Related-work matrix (1-page positioning table)**. “Reconstruct?” indicates whether the attention kernel typically materializes dense keys/values (e.g., via dequant/decode) before dot products. “Kernel-native?” indicates whether the method proposes a kernel path designed to compute logits *directly* from the compressed representation (compressed-domain / code-domain compute). “Budgeted?” indicates an explicit memory budget objective (token budget or bit budget). “Stability eval?” indicates whether the method emphasizes **behavioral stability beyond accuracy** (e.g., logit drift, length drift, seed sensitivity).

Method	Main idea	Reconstruct?	Kernel-native?	Budgeted?	Stability eval?	Notes (most relevant contrast points)
PagedAttention / vLLM (Kwon et al., 2023a)	paging + KV memory manager	Y	N	Y	N	Serving realism: fragmentation/sharing; orthogonal to representation compression.
FlashAttention-2 (Dao, 2023)	I/O-aware exact attention	Y	N	N	N	Kernel bar: defines the efficiency baseline for exact attention.
StreamingLLM (Xiao et al., 2024)	window + attention sinks	Y	N	Y	N	Token-budget retention: fixed window + sinks; streaming extrapolation.
H ₂ O (Zhang et al., 2023)	heavy-hitter + recent eviction	Y	N	Y	N	Eviction policy: selects critical tokens under a token budget.
Scissorhands (Liu et al., 2023c)	stochastic token keep/drop	Y	N	Y	N	Fixed-budget cache: persistence-of-importance, often paired with quantization.
SnapKV (Li et al., 2024)	per-head prompt KV selection	Y	N	Y	Partial	Prompt compression: one-shot; practical speedups under a token cap.
Quest (Tang et al., 2024b)	query-aware sparse KV selection	Y	N	Y	Partial	Query-aware selection: dynamic per-query keep set via metadata.
SAGE-KV (Wang et al., 2025b)	self-attention guided eviction	Y	N	Y	Partial	Top-<i>i</i> after prefix: decode with reduced KV size.
RocketKV (list unavailable in captured snippet; please export BibTeX from OpenReview, 2025)	two-stage selection	Y	N	Y	Partial	Hybrid: prompt compression + decode-time selection.
FIER (Cai et al., 2025)	1-bit quantized retrieval for selection	Y	N	Y	Partial	Selection accelerator: efficient top- <i>i</i> retrieval, not compressed-domain logits.
KIVI (Liu et al., 2024)	2-bit asymmetric KV quant	Y	N	N	N	Quantize+reconstruct: dequant path dominates if not fused.
Coupled Quantization (CQ) (list not captured in the current sources; please fill from the arXiv record, 2024a)	1-bit/channel (coupled entropy)	Y	N	N	N	Extreme KV quant: typically still reconstructs for logits.
WKVQuant (list not captured in the current sources; please fill from the arXiv record, 2024c)	PTQ of weights + KV cache	Y	N	N	N	Deployment PTQ: reconstruct path; system wins depend on decode fusion.
Eigen Attention (list not captured in the current sources; please fill from the arXiv record, 2024b)	attention in low-rank space	Partial	Partial	N	Partial	Compute-path aware: reduced attention dimension; not a bit-tier controller.
ShadowKV (Sun et al., 2024)	low-rank K + V offload	Partial	Partial	Y	Partial	System+structure: compact keys + offload values; throughput-driven.
xKV (list not captured in the current sources; please fill from the arXiv/venue record, 2025)	cross-layer SVD (shared subspace)	Partial	Partial	N	Partial	Cross-layer compression: shared subspace across depth; long-context friendly.
ContiguousKV (Zou et al., 2026b)	prefill I/O granularity alignment	Y	N	Y	N	Prefill realism: tackles read amplification in prefix reuse.
Spherical KV (ours)	spherical encoding + ADA + RDR	N	Y	Y	Y	Compressed-domain logits (no dense reconstruction) + RD tier allocation + stability witnesses.

quant/decode is **fused into the attention kernel** and whether the resulting kernel remains **bandwidth-efficient** at long context. This is why we emphasize **kernel realism** (declare the kernel variant and the fused path, rather than assuming it).

F.3 Compressed-domain / kernel-native compute: avoid dense reconstruction altogether

Core pattern. Reduce bytes/token *and* compute logits without materializing dense keys. Low-rank attention in a compressed space (Eigen Attention (list not captured in the current sources; please fill from the arXiv record, 2024b)) reduces dot-product dimension and can reduce KV footprint and latency. Cross-layer structure (xKV (list not captured in the current sources; please fill from the arXiv/venue record, 2025)) compresses KV using aligned singular subspaces across depth, partially amortizing representation cost. System-structure hybrids (ShadowKV (Sun et al., 2024)) combine compact keys with offloaded values to optimize throughput at long context. **Unifying theme: compute-path awareness.** If kernels consume the compressed representation directly, compression is more likely to translate into **realized** speedups.

F.4 Retention policies vs rate-distortion allocation

Token selection / eviction (token-budgeted). **Goal:** keep a fixed token budget and decide **which tokens** remain in cache. StreamingLLM (Xiao et al., 2024) shows that naive sliding windows fail beyond cache size and that keeping initial **sinks** stabilizes attention. H₂O (Zhang et al., 2023) retains **heavy hitters** plus recent tokens, motivating eviction via principled objectives. Scissorhands (Liu et al., 2023c) leverages persistence of importance for fixed-budget KV without fine-tuning. Prompt-time compression and query-aware sparsity (SnapKV (Li et al., 2024), Quest (Tang et al., 2024b)) reduce KV reads by selecting critical spans; SAGE-KV (Wang et al., 2025b) and multi-stage approaches (RocketKV (list unavailable in captured snippet; please export BibTeX from OpenReview, 2025)) further refine decode-time selection. FIER (Cai et al., 2025) accelerates selection itself via low-bit retrieval.

Rate-distortion allocation (bit-budgeted). **Goal:** fix *what is retained* (often all tokens) but choose **how many bits** each token/group receives. This is where **Spherical KV** positions itself: **RDR allocates tiers (bits) under an explicit budget**, rather than only choosing keep/drop under a token budget. **Why it matters:** token-budgeted eviction and bit-budgeted tiering are **not interchangeable**—they trade off different failure modes (missed critical spans vs controlled distortion). They are also **compos-**

able: selection can sit above tiering, and tiering can further compress the kept subset; we separate them here so comparisons are **auditable**.

F.5 System constraints: paging, offloading, and prefix reuse can dominate wall-clock

Key point: algorithmic compression can be negated by systems bottlenecks (fragmentation, transfer overheads, prefix reuse I/O). PagedAttention / vLLM (Kwon et al., 2023a) sets a strong **servicing-realism baseline** by tackling fragmentation and enabling high-throughput batching. Structured generation engines (e.g., SGLang (Zheng et al., 2024)) add runtime constraints (control flow, tool calls, parallelism) that interact with cache policies. Prefix reuse and prefill optimizations (e.g., ContiguousKV (Zou et al., 2026b)) highlight that **I/O amplification** is orthogonal to per-token KV compression. This motivates reporting not only algorithmic deltas, but also **engine-level details** (paged layout, batching policy, kernel path, fused decode points).

F.6 What is genuinely new in Spherical KV?

We occupy a specific missing square in Table 21: (1) kernel-native compressed-domain attention (ADA computes logits **directly** from spherical codes; **no dense key reconstruction**) + **(2) explicit rate-distortion tier allocation** (RDR is **bit-budgeted** control, not only token eviction) + **(3) stability-first auditing** (witness tests for length drift, logit drift, seed amplification, refusal invariance, tool-schema integrity, and controller oscillation). **This makes skepticism falsifiable:** either the kernel is truly code-domain, the controller is fully specified, and the witnesses pass within declared thresholds, or the method fails on concrete, auditable criteria.